

# Oncogenic KRAS G12D Mutation Promotes Dimerization through a Second, Phosphatidylserine-Dependent Interface: A Model for KRAS oligomerization

Ki-Young Lee,<sup>a</sup> Masahiro Enomoto,<sup>a</sup> Teklab Gebregiworgis,<sup>a</sup> Geneviève M.C. Gasmi-Seabrook,<sup>a</sup> Mitsuhiro Ikura,<sup>\*a,b</sup> and Christopher B. Marshall,<sup>\*a</sup>

<sup>a</sup> Princess Margaret Cancer Centre, University Health Network, <sup>b</sup> Department of Medical Biophysics, University of Toronto, Toronto, Ontario M5G 1L7.

## Table of Contents

1. Material and Methods .....	2
2. Supplementary Figures .....	7
3. Supplementary Tables .....	34
4. References .....	66

## 1. Material and Methods

### 1.1. Expression and Purification of KRAS

Human KRAS-G12D protein (residues 1-185 of isoform 4B) bearing a C118S mutation was expressed in a post-translationally unprocessed form in *Escherichia coli* BL21 (DE3) using a pET28 vector encoding the protein with a N-terminal hexa-histidine tag followed by a thrombin cleavage site. The cells were grown at 37°C in M9 media containing 4 g/L glucose and 1 g/L NH<sub>4</sub>Cl to an optical density (OD<sub>600</sub>) of 0.3-0.4, at which point the media was supplemented with 60 mg/mL 2-ketobutyric acid-4-<sup>13</sup>C and 100 mg/mL of 2-keto-3-(methyl-<sup>13</sup>C)-butyric acid to <sup>13</sup>C label the methyl groups of the Ile-C $\delta$ 1, and Leu-C $\delta$  and Val-C $\gamma$ , respectively. Expression was induced with 0.25 mM isopropyl β-D-1-thiogalactopyranoside (IPTG) at an OD<sub>600</sub> of 0.6 for 16 h at 15°C. For selective labeling of Lys <sup>15</sup>N-amides, the cells were grown 37°C in M9 media containing 4 g/L glucose, 1 g/L NH<sub>4</sub>Cl and 100 mg/L of each of the other 19 unlabeled amino acids to an optical density (OD<sub>600</sub>) of 0.6-0.8, at which time the media was supplemented with 100 mg/L U-<sup>15</sup>N-Lys and 500 mg/L of each of 19 unlabeled amino acids. After 15 min, expression was induced with 1 mM IPTG, and the culture was incubated at 37°C for 2 h to minimize isotope scrambling. The protein was purified initially using a Ni<sup>2+</sup>-NTA column, followed by thrombin digestion overnight at room temperature to remove the histidine tag, and the product was further purified using size exclusion chromatography (Superdex 75; GE Healthcare, running buffer 50 mM HEPES pH 7.4, 100 mM NaCl, and 5 mM MgCl<sub>2</sub>). Fully processed KRAS-G12D (FP-KRAS-G12D), in which the C-terminal Cys185 is farnesylated and methylated, was expressed using a baculovirus-insect cell (Hi5) expression system, as described previously<sup>1</sup>. To isotopically label FP-KRAS-G12D with U-<sup>13</sup>C-[Ile, Leu, Val, Thr], Hi5 insect cells were grown in complete insect cell medium (ESF 921, Expression Systems Inc.) to a cell density of 1.5 x 10<sup>6</sup> cells/mL. The culture was then harvested and resuspended in customized ESF921 medium lacking Ile, Leu, Val, and Thr. The resuspended cells were infected with baculovirus containing the KRAS gene, grown for 16 h, then supplemented with 150 mg/L <sup>13</sup>C-Ile, 100 mg/L <sup>13</sup>C-Leu, 50 mg/L <sup>13</sup>C-Val and 75 mg/L <sup>13</sup>C-Thr. Three single-cysteine mutants (M1C, S39C, and K169C) were introduced into KRAS G12D/C118S using a standard PCR mutagenesis protocol. Likewise, two single charge-reversal mutants (D38K and E168R) were introduced into the baculoviral plasmid encoding KRAS-G12D, as well as the pET28 vector encoding KRAS-G12D/C118S.

### 1.2. Preparation of Nanodisc-tethered KRAS-G12D

Lipid bilayer nanodiscs encircled by two copies of membrane scaffold protein 1D1 (MSP1D1) were prepared using a 1:40 MSP1D1:lipid molar ratio according to the published protocol<sup>2, 3</sup>.

These nanodiscs have a leaflet diameter of  $\sim$  10 nm and a molecular weight of  $\sim$  120 kDa<sup>4</sup>. All lipids were purchased from Avanti Polar Lipids, Inc., including 1,2-dioleoyl-sn-glycero-3-phosphocholine (DOPC), 1,2-dioleoyl-sn-glycero-3-phospho-L-serine (DOPS), 1,2-dioleoyl-sn-glycero-3-phosphoethanolamine-N-[4-(p-maleimidomethyl)cyclohexane-carboxamide] (PE-MCC), and 1,2-distearoyl-sn-glycero-3-phosphoethanolamine-N-diethylenetriaminepentaacetic acid (PE-DTPA). These four lipids were mixed at a molar ratio of 72.5:20:5:2.5 to produce nanodiscs containing 20% phosphatidylserine (PS) to mimic the inner leaflet of the plasma membrane. To produce nanodiscs lacking PS, DOPS lipids were replaced with DOPC lipids. MSP1D1 was expressed in *Escherichia coli* BL21 (DE3) from the pGBHPS-MSP vector in 2 $\times$  yeast extract tryptone media using a LEX bioreactor system. Expression was induced at 37 °C with 1 mM IPTG at an OD<sub>600</sub> of 2.5 for 1 h, followed by further incubation at 28 °C for 2.5 h. The protein was purified using a Ni<sup>2+</sup>-NTA column, followed by cleavage of the His<sub>6</sub>-GB1 tag with HRV3C protease, and final purification by size exclusion chromatography (Superdex 75; GE Healthcare, running buffer 50 mM HEPES pH 7.4, 100 mM NaCl, and 5 mM MgCl<sub>2</sub>). Nanodisc maleimide-conjugated KRAS-G12D (MC-KRAS-G12D) was prepared by conjugation of the C-terminal cysteine (Cys185) to PE-MCC for 16 h at room temperature. Free KRAS-G12D was separated from nanodisc-tethered MC-KRAS-G12D by size exclusion chromatography (Superdex 200; GE Healthcare, running buffer 50 mM HEPES pH 7.4, 100 mM NaCl, and 5 mM MgCl<sub>2</sub>). For nucleotide exchange, GDP-loaded KRAS-G12D was incubated overnight at 4°C with a 10-fold molar excess of GTP $\gamma$ S and 10 mM EDTA.

### 1.3. NMR Experiments

NMR measurements were carried out at 288 K on Bruker AVANCE III HD 700 MHz and AVANCE III HD 800 MHz spectrometers equipped with a 5-mm TCI CryoProbe. All NMR samples were prepared in 50 mM HEPES pH 7.4, 100 mM NaCl, 5 mM MgCl<sub>2</sub>, 10% (vol/vol) D<sub>2</sub>O, and excess GTP $\gamma$ S. For PRE experiments, two-dimensional (2D) <sup>1</sup>H-<sup>13</sup>C TROSY<sup>5</sup> or <sup>1</sup>H-<sup>15</sup>N HSQC spectra were collected from 80  $\mu$ M samples of nanodisc-tethered MC-KRAS-G12D in the presence and absence of FP-KRAS-G12D. The spin labels employed include: (i) TEMPO (Toronto Research Chemicals) attached to the thiol group of one of four single free cysteines (Cys1, Cys39, Cys118, or Cys169) of FP-KRAS-G12D, (ii) Gd<sup>3+</sup>- or Cu<sup>2+</sup>-chelated PE-DTPA (5% of the nanodisc lipid composition), and (iii) 2 mM Gd-DTPA-BMA in the bulk solvent. A concentrated stock of TEMPO in acetonitrile was added at a 5:1 TEMPO:KRAS-G12D molar ratio, and the mixture was incubated at 4°C for 16 h, then dialyzed at 4°C for 8 h into NMR buffer to remove the residual TEMPO reagent. For diamagnetic control experiments, the TEMPO spin label (80  $\mu$ M) was reduced with 0.8 mM ascorbic acid at 15°C for at least 2 h to ensure complete reduction. Lu<sup>3+</sup>-chelated PE-DTPA was

used as the diamagnetic control for paramagnetic Gd<sup>3+</sup>- or Cu<sup>2+</sup>-chelated PE-DTPA. The cross-peaks were assigned based on our previous assignment of wild-type KRAS in the GTPγS-bound state (BMRB entry number: 30734).

#### 1.4. PRE Analysis

NMR data were processed and analyzed using NMRPipe<sup>6</sup> and NMRView<sup>7</sup>. The intensities of the cross-peaks were measured with Lorentzian line shape fitting using the program nlinLS in the NMRPipe software package<sup>6</sup>. The transverse relaxation rate in the diamagnetic state, R<sub>2</sub>, was estimated from the half-height line width of each peak as described by Wagner and co-workers<sup>8</sup>. Overlapped cross-peaks in the spectra were excluded from the analysis. In TEMPO-PRE experiments, peak intensities were referenced to the <sup>1</sup>H peak intensity of 4,4-dimethyl-4-silapentane-1-sulfonic acid (DSS) although paired spectra were obtained using identical sample concentrations and NMR acquisition parameters. PRE effects on individual probes of KRAS-G12D were assessed by the ratio of their peak intensities in the paramagnetic versus diamagnetic samples (I<sub>para</sub>/I<sub>dia</sub>). These values were converted to <sup>1</sup>H transverse PRE rates (<sup>1</sup>H-Γ<sub>2</sub>) using equation 1

$$\frac{I_{\text{para}}}{I_{\text{dia}}} = \frac{R_2 \times \exp(-\Gamma_2 \times t)}{R_2 + \Gamma_2} \quad (\text{equation 1})$$

where t is the total INEPT evolution time in the NMR pulse sequence. The PRE effect on <sup>1</sup>H longitudinal relaxation rate (<sup>1</sup>H-R<sub>1</sub>) is typically negligible because it is much smaller than <sup>1</sup>H-Γ<sub>2</sub>. The paramagnetic relaxations of <sup>15</sup>N and <sup>13</sup>C nuclei were ignored in the analysis because they have much lower gyromagnetic ratios than <sup>1</sup>H nucleus. The <sup>1</sup>H-Γ<sub>2</sub> values were converted into distances (r) between observed protons and the paramagnetic spin label using equation 2

$$r = \sqrt[6]{\frac{\gamma_H^2 g_e^2 \beta^2 \mu_0^2 (S+1) S}{240 \pi^2} \left( 4\tau_c + \frac{3\tau_c}{1+\omega_H^2 \tau_c^2} \right)} \quad (\text{equation 2})$$

where γ<sub>H</sub> is the proton nuclear gyromagnetic ratio, g<sub>e</sub> is the electronic g factor, β is the Bohr magneton, μ<sub>0</sub> is the vacuum permeability, S is the spin quantum number for free electrons, ω<sub>H</sub> is the proton Larmor frequency, and τ<sub>c</sub> is the rotational correlation time of the electron-nucleus

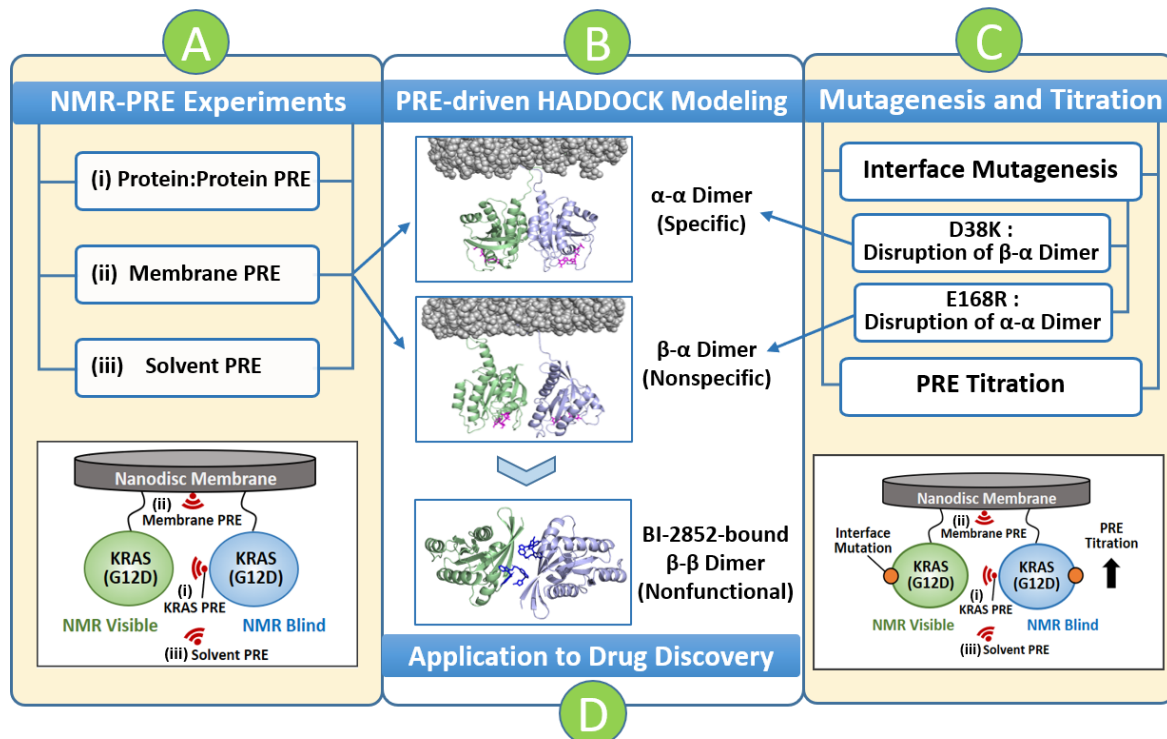
vector.  $\tau_c$  was assumed to be equal to the global correlation time of the complex.

### 1.5. Building Structures of KRAS-G12D Dimers

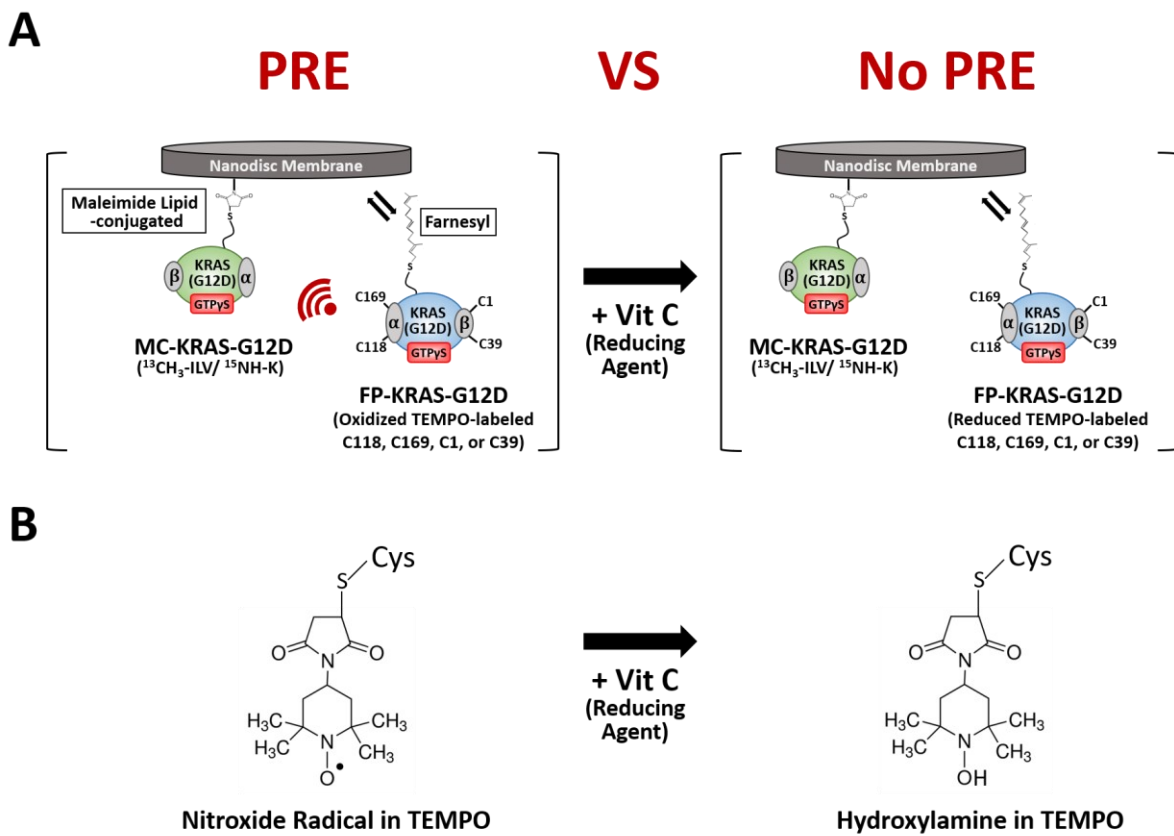
The standard protocol embedded in the HADDOCK 2.2 program<sup>9</sup> was used to generate structural clusters of the KRAS-G12D dimer. Probes that exhibit measurable TEMPO-PRE rates ( $> 10$  Hz) were set to have ‘ambiguous’ distance restraints of 2 – 5 Å from the spin label. The mutagenesis data was translated into sets of ambiguous distance restraints between two KRAS protomers, which were used as additional restraints to refine the KRAS-G12D dimer model that was initially generated from ambiguous PRE restraints from TEMPO-labeled cysteines. Specifically, for the  $\alpha$ - $\alpha$  dimer model, five probes (V44 $\gamma$ , V45 $\gamma$ , I46 $\delta$ , I142 $\delta$ , and V160 $\gamma$ ) in the  $\alpha$  interface that exhibit similar patterns of reduced PRE due to the E168R mutation (Figure 2) were set to have ambiguous restraints to the  $\alpha$  interface of the opposing protomer. For the  $\alpha$ - $\beta$  dimer model, the  $\beta$  interface was set to have ambiguous restraints for the five probes in the  $\alpha$  interface. The standard multi-body docking protocol embedded in the HADDOCK 2.2 program was used to generate the structural models of the KRAS-G12D dimer on the membrane surface. Distance restraints between the KRAS dimer and lipid headgroups on one leaflet of the nanodisc were derived from the membrane PRE data for each dimer configuration of KRAS-G12D, which was favored by interface mutants. Probes that exhibit measurable changes in the membrane PRE upon addition of FP-KRAS-G12D, with  $\Delta^{1\text{H}}\Gamma_{2,\text{di-mono}}/^{1\text{H}}\Gamma_{2,\text{mono}}$  of  $< -0.3$  or  $> 0.3$ , were set to have only the lower and upper limits, respectively, of distance restraints. These distance limits were calculated from equation 2 using the  $^{1\text{H}}\Gamma_{2,\text{mono}}$  rate of the corresponding probe. To maintain membrane association of the C-termini of the two KRAS protomers, an upper limit of 2 Å was set as an ambiguous restraint for Lys184. To construct the starting KRAS-G12D model, the crystal structure of KRAS-G12D (residues 1-180, PDB ID: 4DSO) was modified by incorporating residues 181-184, and then they were subjected to energy minimization using CNS<sup>10</sup>. The C-terminal residues 172-184 were designated fully flexible while the C-terminal helix 5 extended to residue 171 based on the crystal structure (4DSO). The starting nanodisc model was generated by incorporating a lipid bilayer containing 80% DOPC and 20% DOPS, computed via CHARMM-GUI<sup>11</sup>, into an MSP1D1 nanodisc model<sup>4</sup>. To build the HADDOCK structure of the BI-2852-stabilized KRAS-G12D dimer, unambiguous distance restraints defining the dimer interface between BI-2852-bound KRAS-G12D protomers were derived from equation 2 using  $^{1\text{H}}\Gamma_2$  PRE rates of MC-KRAS-G12D induced by TEMPO-labeled Cys1 of FP-KRAS-G12D, at a 1:1:2 MC-KRAS-G12D:FP-KRAS-G12D:BI-2852 molar ratio. The crystal structure of BI-2852-bound KRAS-G12D monomer (PDB ID: 6GJ8) was used as the starting structure in the HADDOCK calculation.

According to the sampling protocol, 3000 complex structures were generated in the first step of the rigid body docking, 400 structures were selected in the semi-flexible docking, and 200 structures were finally submitted to the water refinement steps.

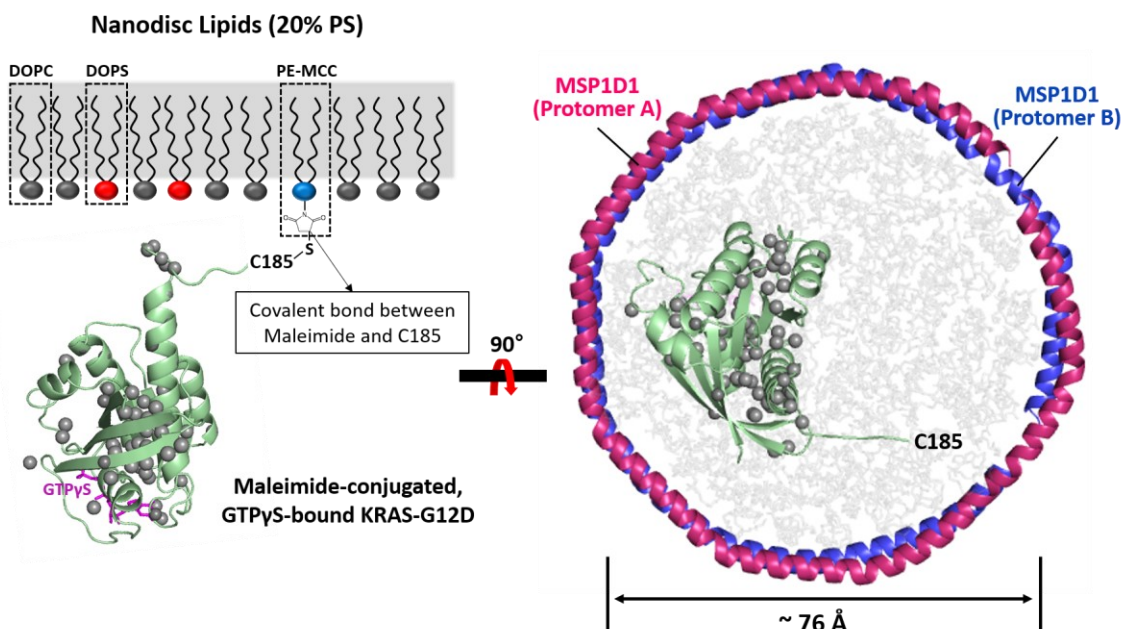
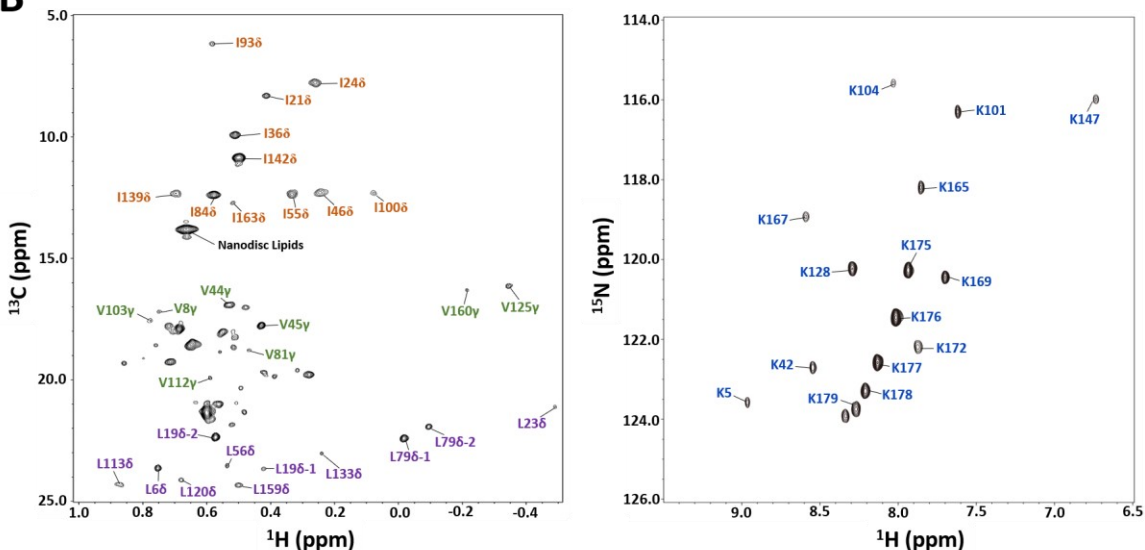
## 2. Supplementary Figures



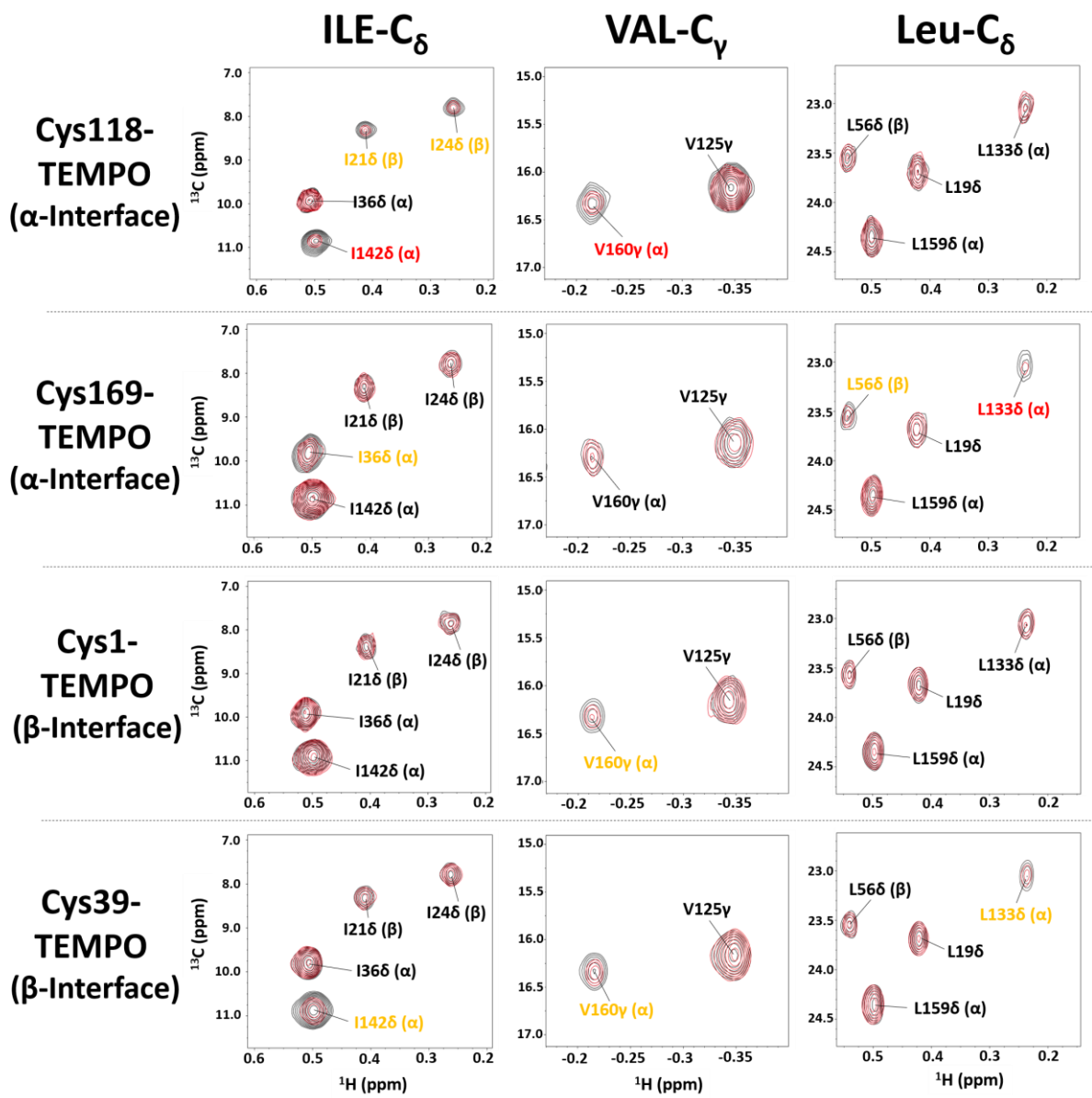
**Figure S1.** Experimental approaches used for structural studies of membrane-dependent dimerization of the KRAS G12D mutant on nanodiscs. (A) Paramagnetic relaxation enhancement (PRE) NMR experiments were used to obtain restraints for the structure determination of KRAS-G12D dimers on nanodiscs. Isotopically labeled, NMR-visible KRAS-G12D (MC-KRAS-G12D) was irreversibly attached to the lipid bilayer of a nanodisc, where it can dimerize with farnesylated and fully processed KRAS-G12D (FP-KRAS-G12D), which is not isotopically labeled. Spin labels were used to map protein:protein and protein:membrane interfaces as well as solvent exposed surfaces. These PRE experiments included (i) TEMPO nitroxide tags attached to four specific Cys residues of FP-KRAS-G12D, (ii)  $\text{Gd}^{3+}/\text{Cu}^{2+}$  ions chelated by a DTPA-modified lipid head group, and (iii) Gd-DTPA-BMA in the bulk solvent, to identify the KRAS-G12D dimerization interface, the KRAS-G12D dimer-membrane interface, and the solvent-exposed regions of the KRAS-G12D dimer, respectively. (B) PRE-derived distance restraints were used to generate two distinct structural models of KRAS-G12D dimers on the membrane using HADDOCK. (C) Interface mutagenesis and paramagnetic NMR titrations were performed to deconvolute the overall PRE observed, and identify two distinct modes of dimerization for KRAS-G12D on the membrane. Mutations were engineered to disrupt each dimer interface: D38K and E168R selectively disrupt ‘ $\beta$ - $\alpha$ ’ (same as ‘ $\alpha$ - $\beta$ ’) and ‘ $\alpha$ - $\alpha$ ’ dimers, respectively, without affecting ‘ $\alpha$ - $\alpha$ ’ and ‘ $\beta$ - $\alpha$ ’ dimers. (D) Application of the nanodisc-based NMR system to drug discovery is exemplified by the small molecule BI2852. This compound binds at a ‘ $\beta$ - $\beta$ ’ interface of KRAS-G12D on nanodiscs, and stabilizes a new dimer configuration that outcompetes the native ‘ $\alpha$ - $\alpha$ ’ and ‘ $\beta$ - $\alpha$ ’ modes of dimerization, and results in occlusion of the effector-binding site on the  $\beta$  interface.



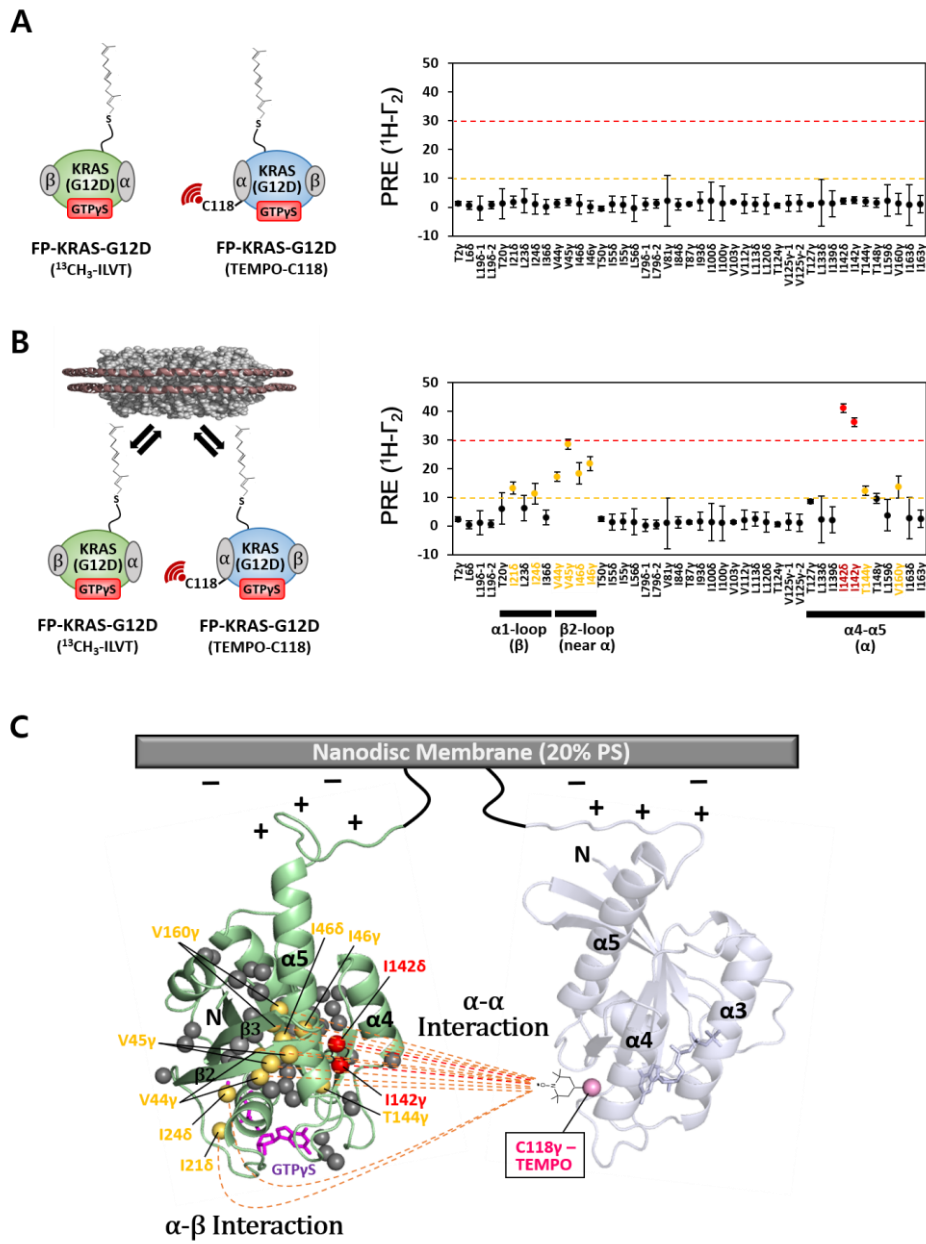
**Figure S2.** Intermolecular TEMPO-PRE experiments of KRAS-G12D on nanodiscs. (A) Illustration of the experimental design with [ILV-<sup>13</sup>C methyl/K-<sup>15</sup>N amide]-labeled MC-KRAS-G12D and FP-KRAS-G12D bearing a TEMPO spin at Cys118, Cys169, Cys1, or Cys39. Vitamin C (Vit C, i.e., ascorbic acid) is used as a reducing agent to terminate the PRE effect from the TEMPO tag on FP-KRAS-G12D. (B) Schematic of the Vit C-induced reduction of the nitroxide radical in TEMPO.

**A****B**

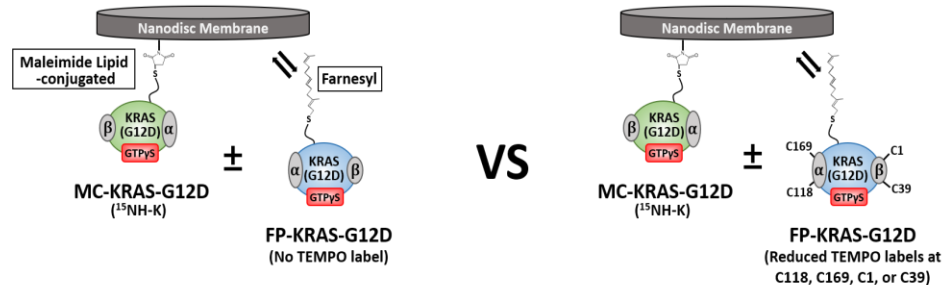
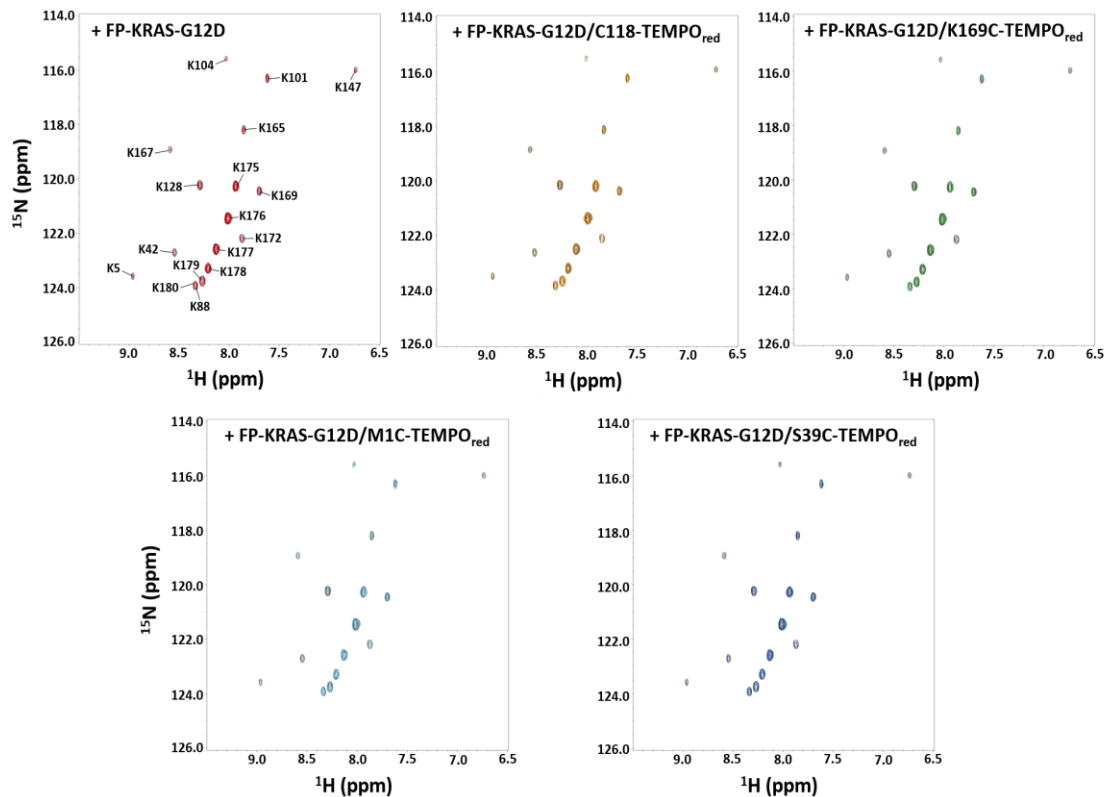
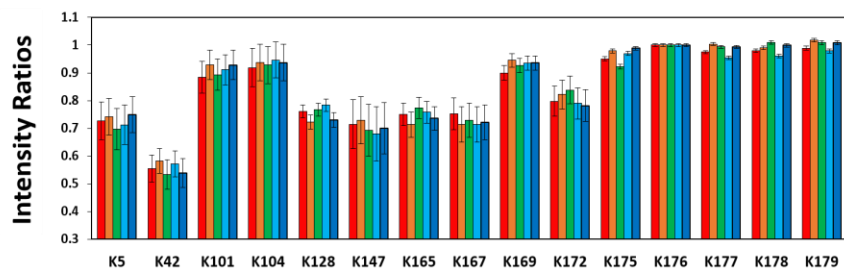
**Figure S3.** (A) Schematic of nanodisc system for NMR studies of membrane-associated KRAS. The C-terminal Cysteine (C185) of KRAS-G12D in the activated, GTP $\gamma$ S-bound state is covalently conjugated to a reactive maleimide moiety on the head group of a PE-MCC lipid pre-assembled in nanodiscs containing 20% phosphatidylserine (PS). NMR-visible probes are shown as gray spheres in KRAS-G12D. (B) Two-dimensional (2D)  $^1\text{H}$ - $^{13}\text{C}$  TROSY (left) and  $^1\text{H}$ - $^{15}\text{N}$  HSQC (right) spectra of nanodisc maleimide-conjugated KRAS-G12D isotopically  $^{13}\text{C}$ -labeled at single methyl groups of Ile, Leu, and Val (ILV, C81, C $\delta$  and C $\gamma$ , respectively) and  $^{15}\text{N}$ -labeled at amides of Lys. Assignments for individual cross-peaks analyzed in our PRE studies are indicated. The peaks that are unassigned, overlapped, or severely broadened upon dimerization are excluded from our analyses.



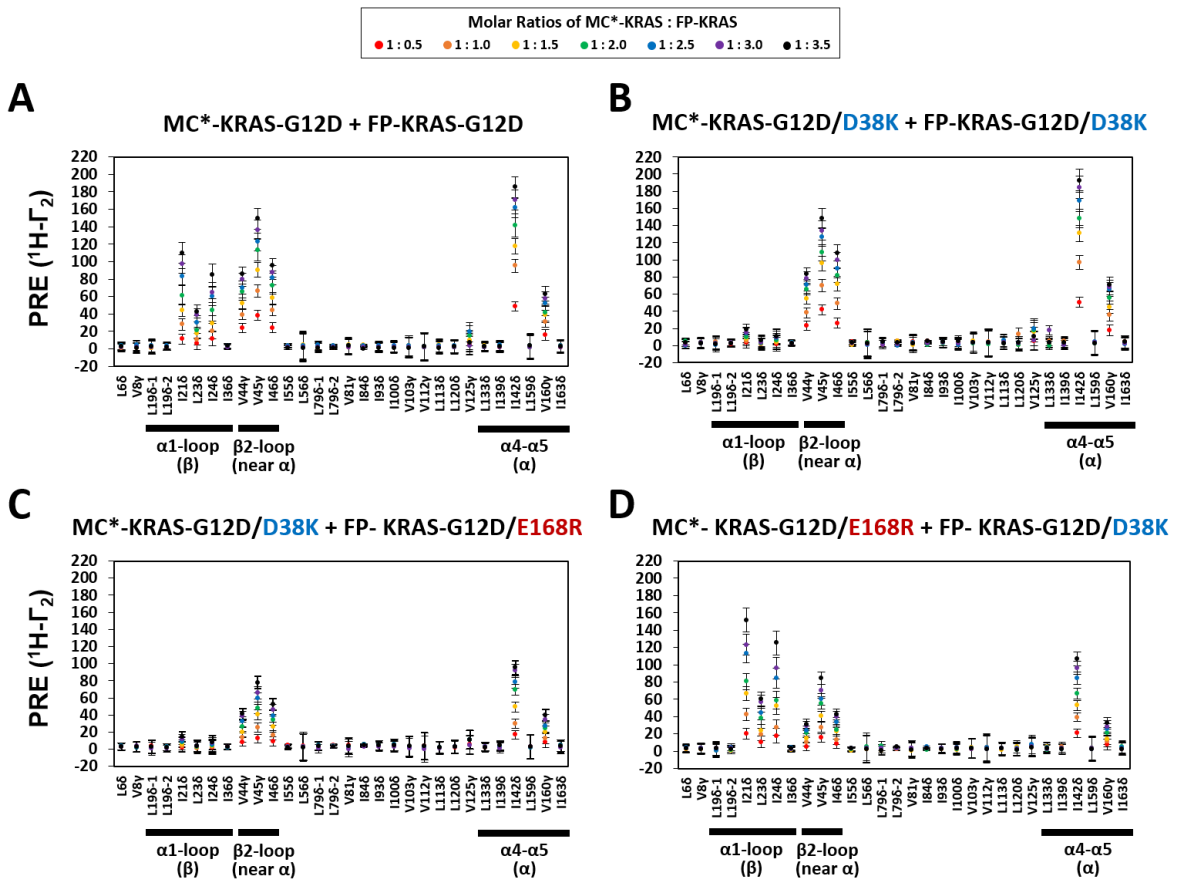
**Figure S4.** Expanded spectra showing representative peaks for ILV  $^{13}\text{C}$ -methyl probes that exhibit the PRE effects upon KRAS-G12D dimerization. Three representative spectral regions with MC-KRAS-G12D ILV  $^{13}\text{C}$ -methyl resonances are shown in the presence of FP-KRAS-G12D bearing a TEMPO label at Cys118, Cys169, Cys1, or Cys39, as indicated. The cross-peaks in the diamagnetic (black) and paramagnetic (red) states are obtained in the presence of the TEMPO label in the reduced and oxidized states, respectively, as described in Figure S2. Assignment labels are coloured according to the PRE exhibited;  $^1\text{H}-\Gamma_2$  values  $> 10 \text{ s}^{-1}$  are moderate (yellow) and  $> 30 \text{ s}^{-1}$  are strong (red), as in Figure 1. Probes that are not substantially affected by PRE are labeled in black. The interfaces where each probe is located are indicated as “ $\alpha$ ” and “ $\beta$ ” in parentheses.



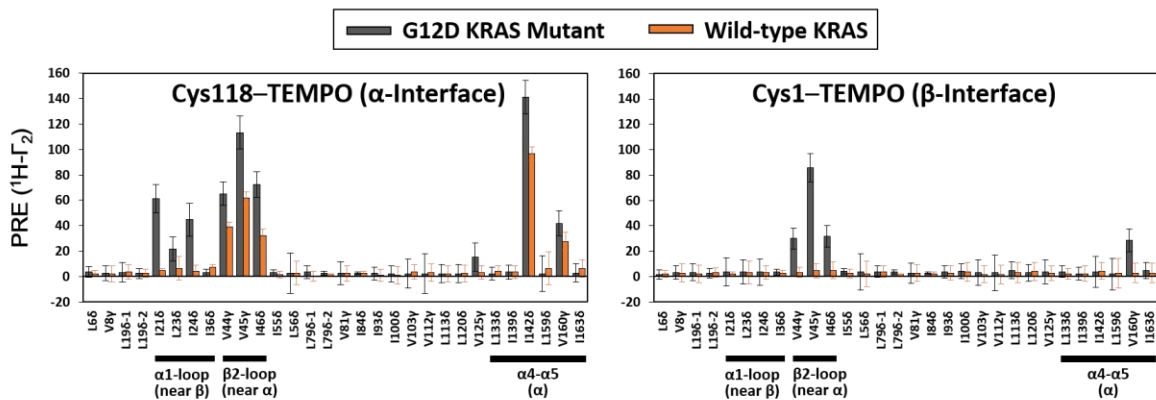
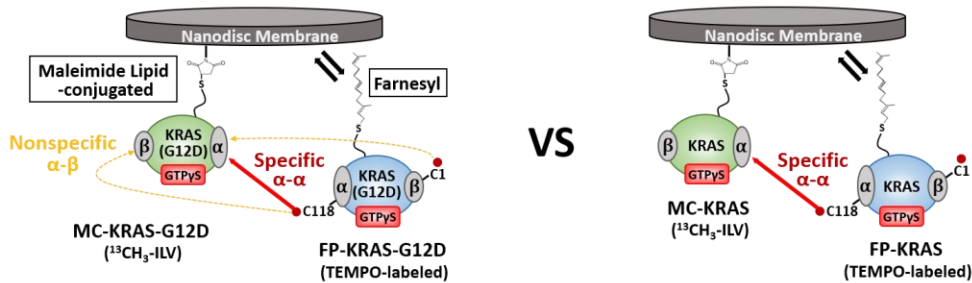
**Figure S5.** Intermolecular PRE effects between GTPyS-bound FP-KRAS-G12D molecules in the absence (A) and presence (B) of a lipid bilayer nanodisc. Left panels illustrate the experimental design with [ $^{13}\text{C}$  methyl]-labeled FP-KRAS-G12D and FP-KRAS-G12D bearing a TEMPO spin label at Cys118. The molar ratio of FP-KRAS-G12D per nanodisc leaflet was optimized as 10:1. Right panels exhibit the plots of the intermolecular PRE rates ( $^1\text{H}-\Gamma_2$ ) with regard to ILVT methyl probes of FP-KRAS-G12D.  $^1\text{H}-\Gamma_2$  threshold values  $> 10$  Hz and  $> 30$  Hz are designated moderate (yellow) and strong (red), respectively, and represented by horizontal dashed lines. (C) Mapping PRE-affected probes onto the crystal structure of GTPyS-bound KRAS-G12D (PDB ID: 4DSO) in an arbitrary dimerization model including a membrane containing 20 % phosphatidylserine (PS) lipid. PRE-affected probes are colored in the same way as in panel B. Dotted lines represent the intermolecular PRE effect from TEMPO conjugated to the Sy atom of Cys118 in the opposing protomer (arbitrarily positioned).

**A****B****C**

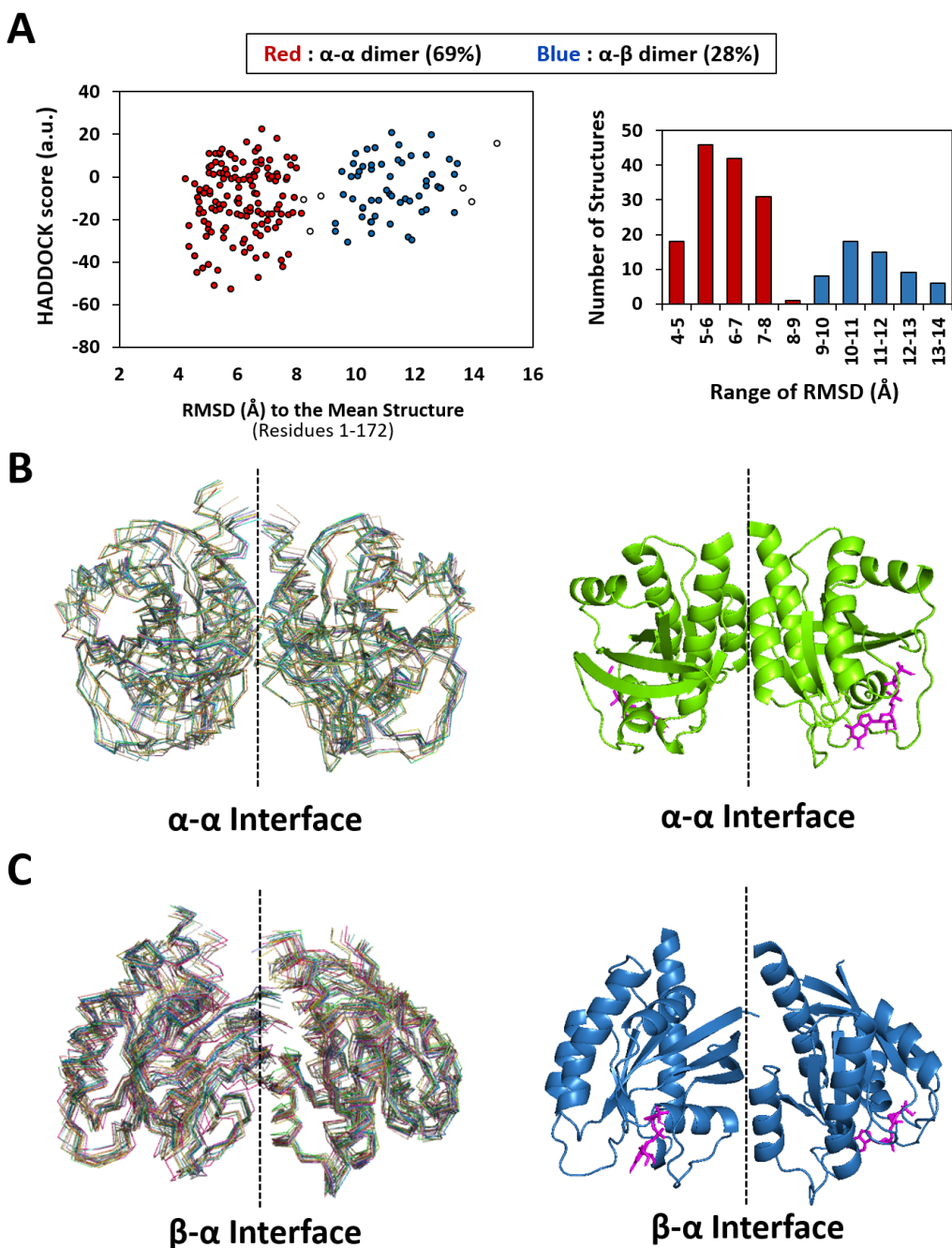
**Figure S6.** Dimerization-induced spectral perturbations for lysine  $^{15}\text{N}$ -amide probes of KRAS-G12D on the membrane suggest dimerization is not impacted by TEMPO tags. (A) Illustration of the experimental design comparing the perturbations on [ $\text{Lys}^{15}\text{N}$  amide]-labeled MC-KRAS-G12D upon addition of unlabeled FP-KRAS-G12D versus labeled with VitC-reduced diamagnetic TEMPO at Cys118, Cys169, Cys1, or Cys39 (FP-KRAS-G12D/C118-TEMPO<sub>red</sub>, FP-KRAS-G12D/K169C-TEMPO<sub>red</sub>, FP-KRAS-G12D/M1C-TEMPO<sub>red</sub>, and FP-KRAS-G12D/S39C-TEMPO<sub>red</sub>, respectively). (B) Overlay of  $^1\text{H}$ - $^{15}\text{N}$  HSQC spectra for the Lys probes of MC-KRAS-G12D in the absence (black) versus the presence of the same amounts of unlabeled FP-KRAS-G12D (red), FP-KRAS-G12D/C118-TEMPO<sub>red</sub> (orange), FP-KRAS-G12D/K169C-TEMPO<sub>red</sub> (green), FP-KRAS-G12D/M1C-TEMPO<sub>red</sub> (cyan), or FP-KRAS-G12D/S39C-TEMPO<sub>red</sub> (blue). Possibly overlapped peaks for K88 and K180 are excluded in the analysis. (C) Ratios of the peak intensities between MC-KRAS-G12D alone and with FP-KRAS-G12D (red), FP-KRAS-G12D/C118S-TEMPO<sub>red</sub> (orange), FP-KRAS-G12D/K169C-TEMPO<sub>red</sub> (green), FP-KRAS-G12D/M1C-TEMPO<sub>red</sub> (cyan), or FP-KRAS-G12D/S39C-TEMPO<sub>red</sub> (blue). These ratios are normalized to the value of 1 for K176.



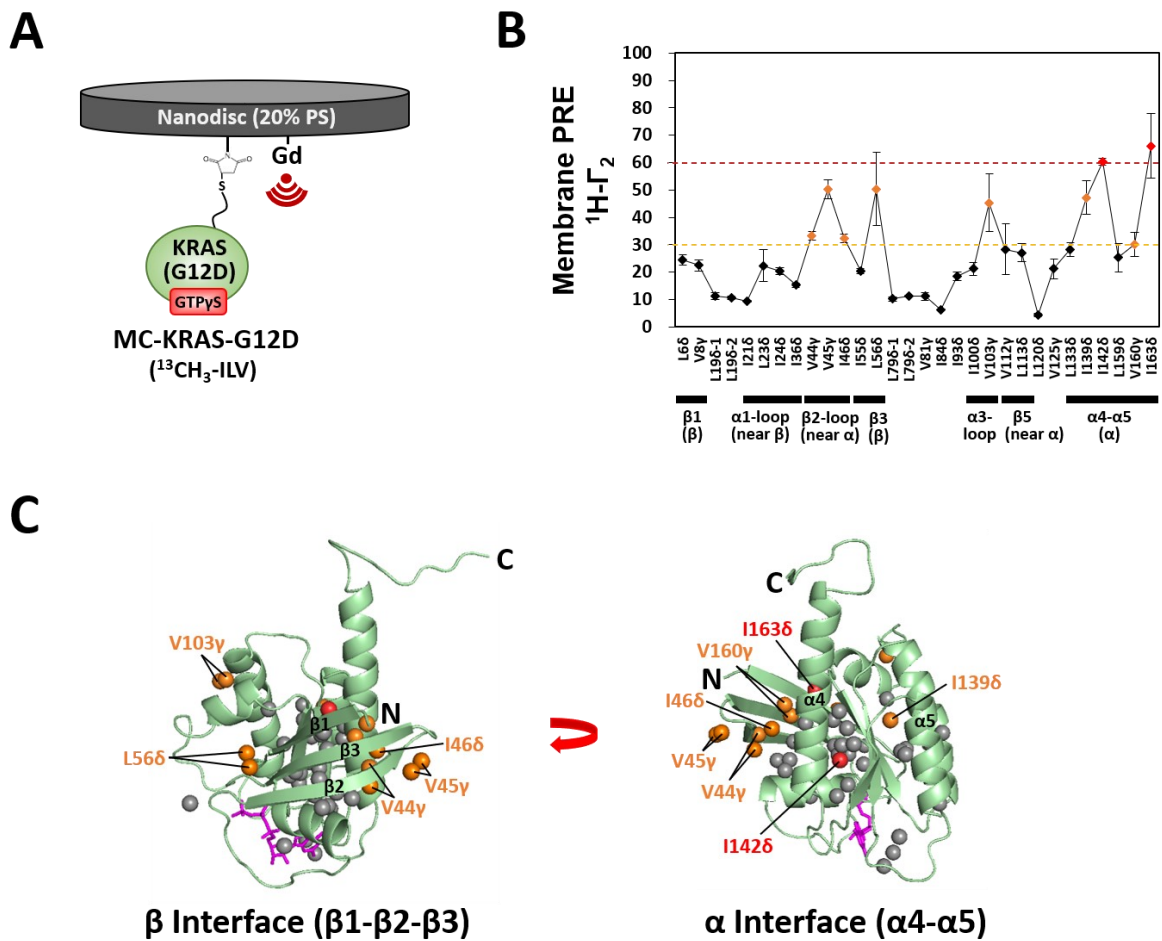
**Figure S7.** Concentration dependence of KRAS G12D PRE effects and effects of interface mutagenesis. (A) Overall  $^1\text{H}-\Gamma_2$  PRE rates of ILV  $^{13}\text{C}$ -methyl probes of MC-KRAS-G12D in the presence of increasing amounts of FP-KRAS-G12D tagged with a TEMPO spin label at Cys118. (B-D) PRE rates obtained (as in A) with three combinations of the interface-specific mutants, including (B) MC\*-KRAS-G12D/D38K and FP-KRAS-G12D/D38K, (C) MC\*-KRAS-G12D/D38K and FP-KRAS-G12D/E168R, and (D) MC\*-KRAS-G12D/D38K and FP-KRAS-G12D/E168R. The superscript “\*” represents the isotopically labeled, PRE-visible MC-KRAS-G12D protomer.

**A****B**

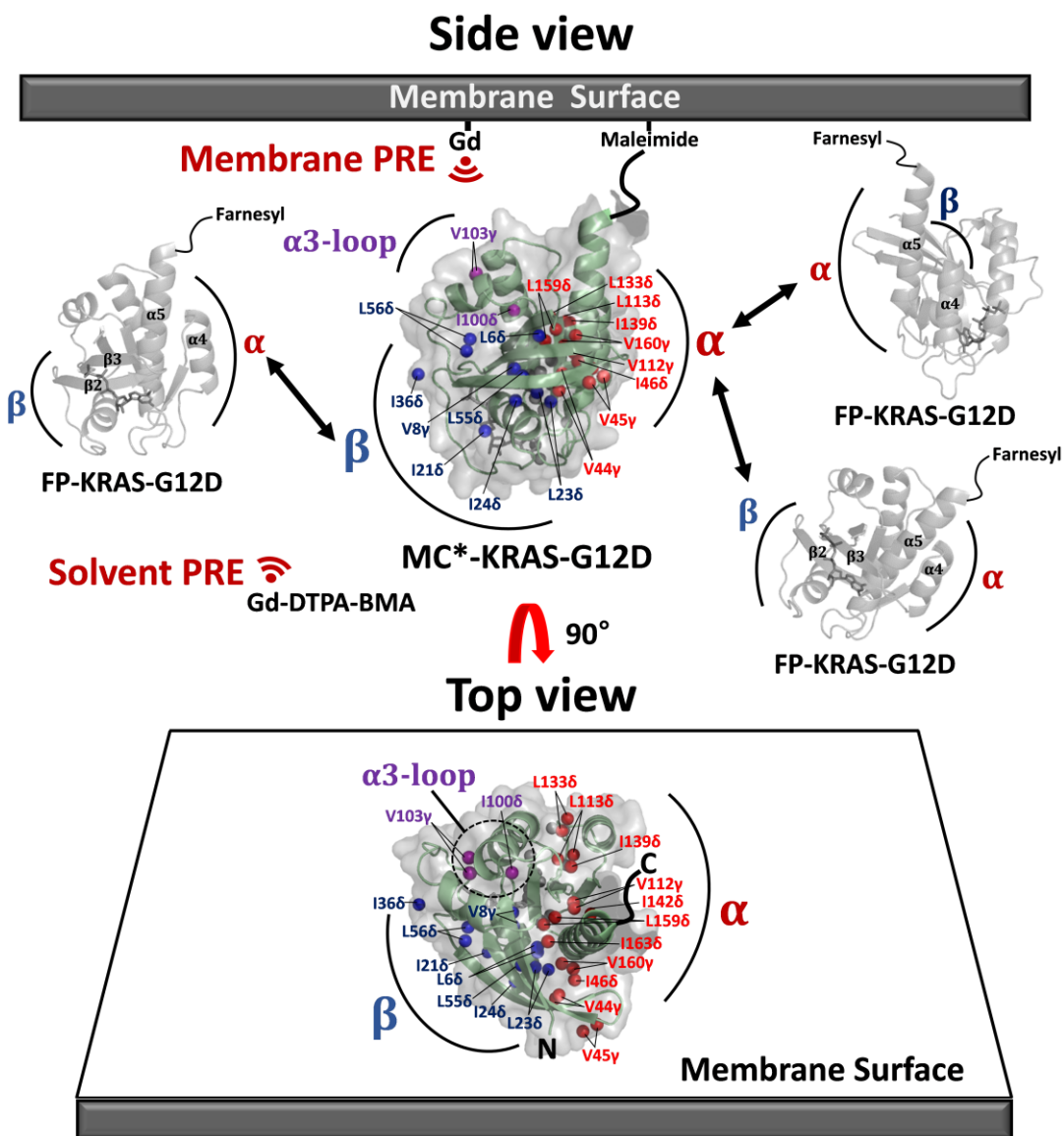
**Figure S8.** Intermolecular PRE of wild-type KRAS versus the G12D mutant on a nanodisc membrane. (A)  $^1\text{H}$  transverse PRE rates ( $^1\text{H}-\Gamma_2$ ) of ILV  $^{13}\text{C}$ -methyl probes of MC-KRAS induced by a TEMPO spin label at Cys118 in the  $\alpha$  interface (Left) or Cys1 in the  $\beta$  interface (Right) of FP-KRAS. The PRE profiles for the G12D mutant and wild-type KRAS are colored in gray and orange, respectively. The molar ratio of MC- to FP-KRAS was 1:2. (B) Schematic representations of the paramagnetic effects observed between KRAS-G12D molecules versus wild-type KRAS molecules. “ $\alpha$ ” and “ $\beta$ ” represent the  $\alpha$  interface ( $\alpha 4-\alpha 5$  site) and the  $\beta$  interface ( $\beta$ -sheet effector binding site), respectively. Wild-type KRAS dimerizes only through a specific  $\alpha$ - $\alpha$  interface as determined previously, whereas KRAS-G12D exhibits two different modes of dimerization through a specific  $\alpha$ - $\alpha$  as well as a nonspecific  $\alpha$ - $\beta$  interface, determined by PRE titration experiments (Figure 2).



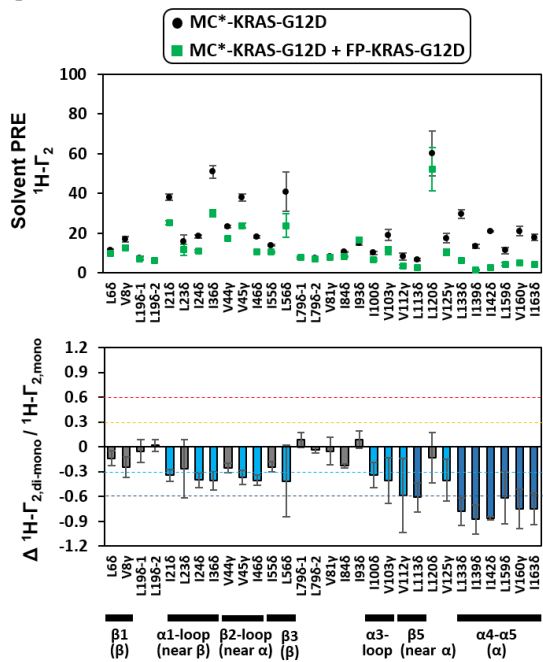
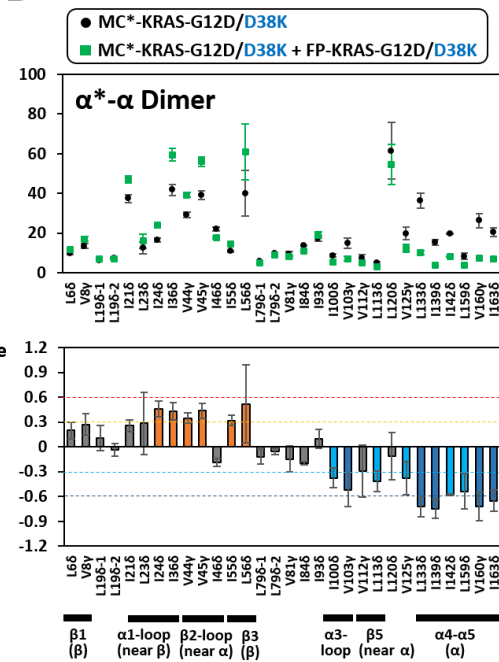
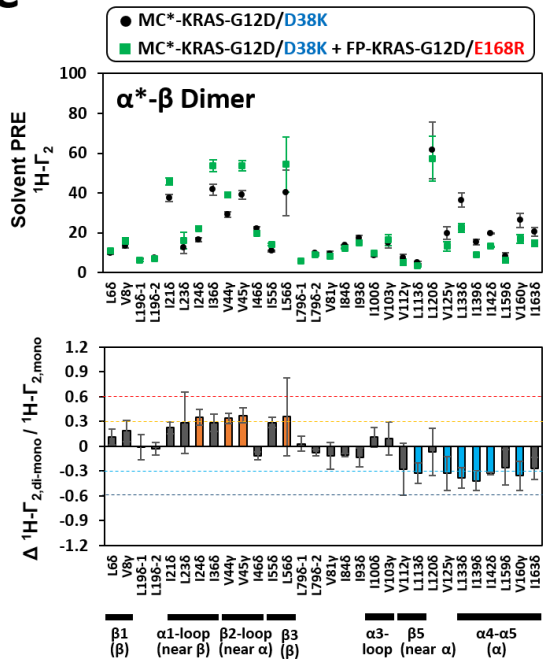
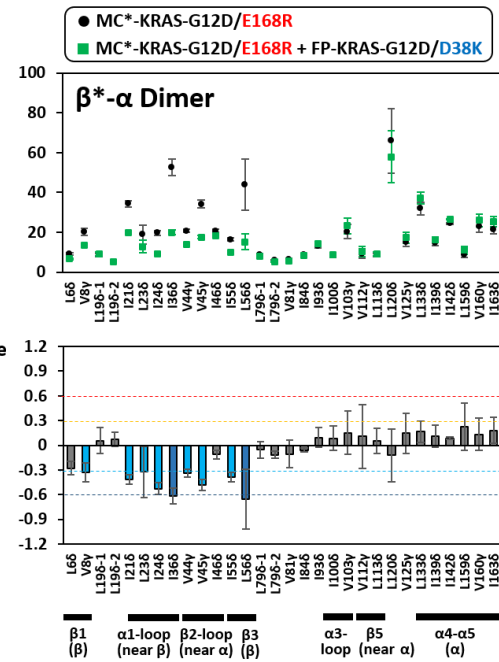
**Figure S9.** Cluster analysis of the 200 lowest HADDOCK-score structures of the KRAS-G12D dimer generated from all ambiguous PRE restraints. (A) Plot of HADDOCK scores of the 200 final structures of the  $\alpha$ - $\alpha$  and  $\alpha$ - $\beta$  dimers of KRAS-G12D (residues 1-172) versus RMSD values to the mean structure (left) and plot of number of the structures of the  $\alpha$ - $\alpha$  and  $\alpha$ - $\beta$  dimers versus the RMSD range (right). The  $\alpha$ - $\alpha$  and  $\alpha$ - $\beta$  dimer structures of KRAS-G12D are represented by red and blue circles, respectively. (B) Overlay of the 20 lowest HADDOCK-score structures of the KRAS-G12D  $\alpha$ - $\alpha$  dimer (left) and their average structure (right). (C) Overlay of the 20 lowest HADDOCK-score structures of the KRAS-G12D  $\alpha$ - $\beta$  dimer (left) and their average structure (right).



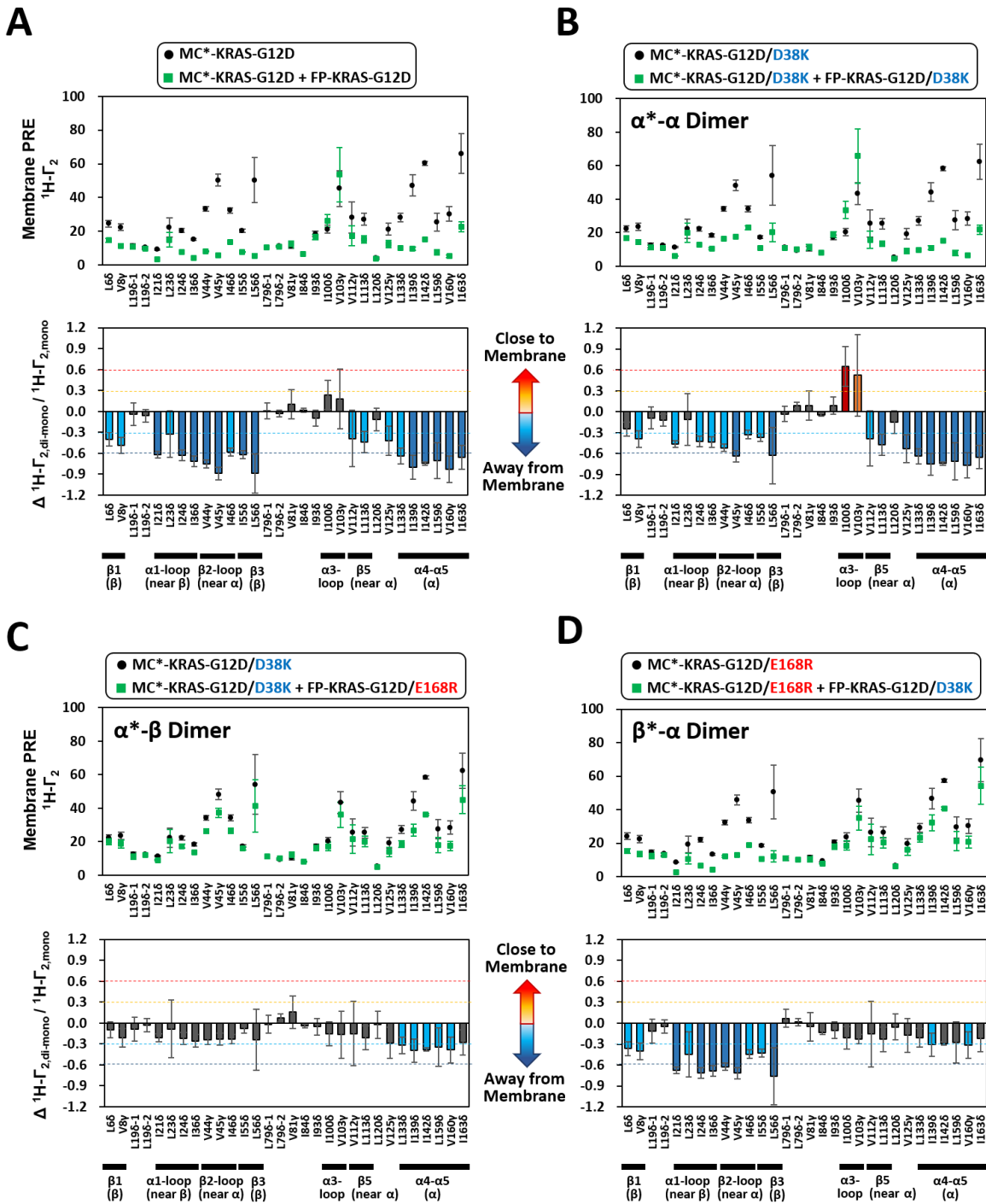
**Figure S10.** Membrane PRE effects on the KRAS-G12D monomer on a nanodisc membrane containing 20% phosphatidylserine (PS) lipids. (A) Experimental design for probing membrane PRE effects on  $^{13}\text{C}$ -labeled MC-KRAS-G12D. Membrane PRE effects are induced by  $\text{Gd}^{3+}$  ion chelated by a DTPA-modified lipid head group in nanodiscs. (B)  $^1\text{H}-\Gamma_2$  PRE rates of ILV  $^{13}\text{C}$ -methyl probes of MC-KRAS-G12D. Probes are coloured according to the PRE exhibited;  $^1\text{H}-\Gamma_2$  values  $> 30 \text{ s}^{-1}$  are moderate (yellow) and  $> 60 \text{ s}^{-1}$  are strong (red). (C) Mapping the membrane PRE effects onto the crystal structure of GTP $\gamma$ S-bound KRAS-G12D (PDB ID: 4DSO). ILV  $^{13}\text{C}$ -methyl probes that exhibit moderate and strong PRE effects are colored as in panel B.



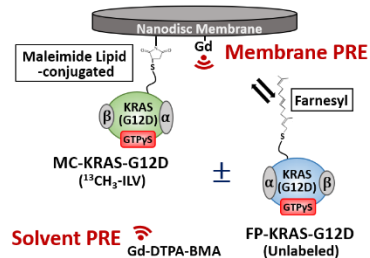
**Figure S11.** Schematic overview of 'solvent' or 'membrane' PRE experiments for  $^{13}\text{C}$  ILV-labeled MC-KRAS-G12D in the presence of unlabeled FP-KRAS-G12D to form  $\alpha^*$ - $\alpha$ ,  $\alpha^*$ - $\beta$ , and  $\beta^*$ - $\alpha$  dimers ("\*" represents the isotopically labeled interface). ILV  $^{13}\text{C}$ -methyl probes belonging to the  $\alpha$  and  $\beta$  interfaces and the  $\alpha$ 3-loop region are colored on the crystal structure of GTP $\gamma$ S-bound KRAS-G12D (PDB ID: 4DSO): red;  $\alpha$ , blue;  $\beta$ , purple;  $\alpha$ 3-loop. Solvent and membrane PRE effects are induced using 2 mM Gd-DTPA-BMA dissolved in the bulk solution and 5 % Gd $^{3+}$ -chelated head groups of PE-DTPA lipids in nanodiscs, respectively.

**A****B****C****D**

**Figure S12.** Dimerization-induced changes in solvent PRE effects on membrane-bound KRAS-G12D. Changes in solvent PRE effects on MC-KRAS-G12D induced by (A) addition of FP-KRAS-G12D and those obtained with three combinations of the interface-specific mutants, including (B) MC\*-KRAS-G12D/D38K and FP-KRAS-G12D/D38K, (C) MC\*-KRAS-G12D/D38K and FP-KRAS-G12D/E168R, and (D) MC\*-KRAS-G12D/E168R and FP-KRAS-G12D/D38K. The superscript “\*” represents the isotopically labeled, PRE-visible MC-KRAS-G12D protomer.  $^1\text{H}-\Gamma_2$  PRE rates of ILV  $^{13}\text{C}$ -methyl probes of MC-KRAS-G12D induced by 2 mM Gd-DTPA-BMA in solution were measured in the presence and absence of an equal amount of unlabeled FP-KRAS-G12D, and relative changes in  $^1\text{H}-\Gamma_2$  rates ( $\Delta^1\text{H}-\Gamma_{2,\text{di-mono}}/{}^1\text{H}-\Gamma_{2,\text{mono}}$ ) upon addition of FP-KRAS-G12D were calculated. Positive and negative values of  $\Delta^1\text{H}-\Gamma_{2,\text{di-mono}}/{}^1\text{H}-\Gamma_{2,\text{mono}}$  represent gain and loss, respectively, of the solvent PRE effect upon dimerization. Probes that exhibit dimerization-induced changes in the solvent PRE are categorized according to the threshold values of  $\Delta^1\text{H}-\Gamma_{2,\text{di-mono}}/{}^1\text{H}-\Gamma_{2,\text{mono}}$ : > 0.6 (red), > 0.3 (orange), < -0.3 (cyan), and <-0.6 (blue).



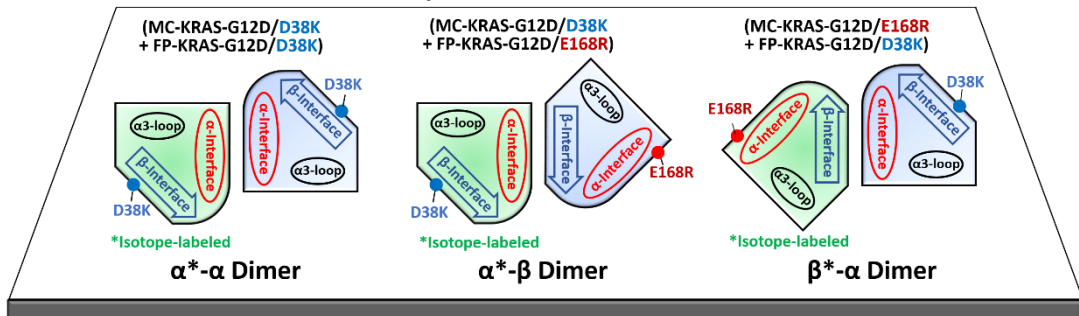
**Figure S13.** Dimerization-induced changes in membrane PRE effects on membrane-bound KRAS-G12D. Changes in membrane PRE effects on MC-KRAS-G12D induced by (A) addition of FP-KRAS-G12D and those obtained with three combinations of the interface-specific mutants, including (B) MC\*-KRAS-G12D/D38K and FP-KRAS-G12D/D38K, (C) MC\*-KRAS-G12D/D38K and FP-KRAS-G12D/E168R, and (D) MC\*-KRAS-G12D/E168R and FP-KRAS-G12D/D38K. Top panels show PRE from Gd<sup>3+</sup>-chelated head groups of PE-DTPA lipids the in the presence (green) and absence (black) of FP-KRAS-G12D, whereas the lower panels show the differential PRE between the two samples. The superscript “\*” represents the isotopically labeled, PRE-visible MC-KRAS-G12D protomer. <sup>1</sup>H- $\Gamma_2$  PRE rates of ILV <sup>13</sup>C-methyl probes of MC-KRAS-G12D induced by membrane-associated Gd<sup>3+</sup> were measured in the presence and absence of an equal amount of unlabeled FP-KRAS-G12D, and relative changes in <sup>1</sup>H- $\Gamma_2$  rates ( $\Delta^{1\text{H}}\text{-}\Gamma_{2,\text{di-mono}}/^{1\text{H}}\text{-}\Gamma_{2,\text{mono}}$ ) upon addition of FP-KRAS-G12D were calculated. Positive and negative values of  $\Delta^{1\text{H}}\text{-}\Gamma_{2,\text{di-mono}}/^{1\text{H}}\text{-}\Gamma_{2,\text{mono}}$  represent gain and loss, respectively, of the membrane PRE effect upon dimerization. Probes that exhibit dimerization-induced changes in the membrane PRE are categorized according to the threshold values of  $\Delta^{1\text{H}}\text{-}\Gamma_{2,\text{di-mono}}/^{1\text{H}}\text{-}\Gamma_{2,\text{mono}}$ : > 0.6 (red), > 0.3 (orange), < -0.3 (cyan), and <-0.6 (blue).

**A****B**

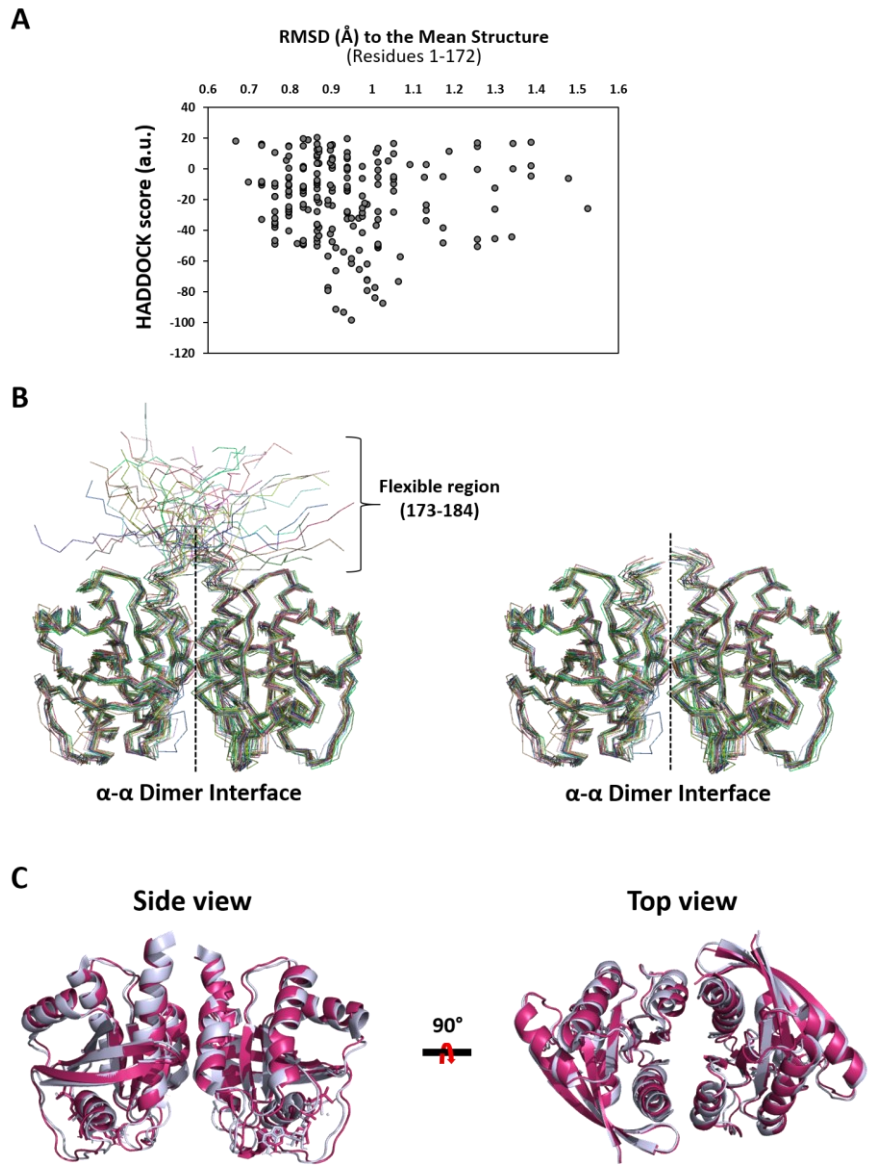
	α-Interface		β-Interface		α3-loop	
	Solvent PRE	Membrane PRE	Solvent PRE	Membrane PRE	Solvent PRE	Membrane PRE
MC-KRAS-G12D + FP-KRAS-G12D	↓ (-0.77)	↓ (-0.73)	↓ (-0.31)	↓ (-0.61)	↓ (-0.37)	↑ (+0.21)
MC-KRAS-G12D/D38K + FP-KRAS-G12D/D38K	↓ (-0.66)	↓ (-0.71)	↑ (+0.34)	↓ (-0.39)	↓ (-0.45)	↑ (+0.59)
MC-KRAS-G12D/D38K + FP-KRAS-G12D/E168R	↓ (-0.34)	↓ (-0.35)	↑ (+0.26)	↓ (-0.18)	↑ (+0.10)	↓ (-0.16)
MC-KRAS-G12D/E168R + FP-KRAS-G12D/D38K	↑ (+0.15)	↓ (-0.27)	↓ (-0.44)	↓ (-0.56)	↑ (+0.12)	↓ (-0.22)

**C**

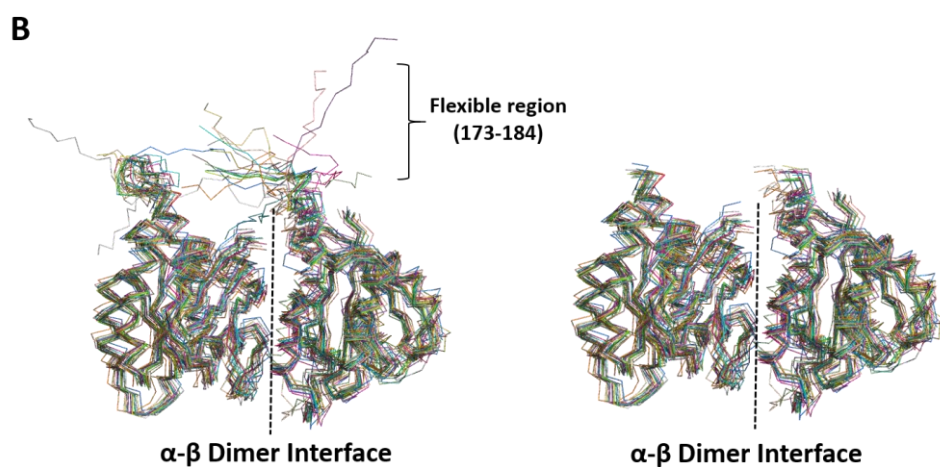
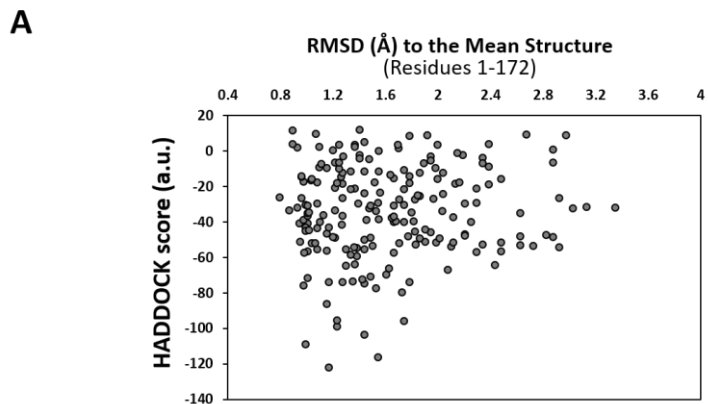
### Top View of Membrane



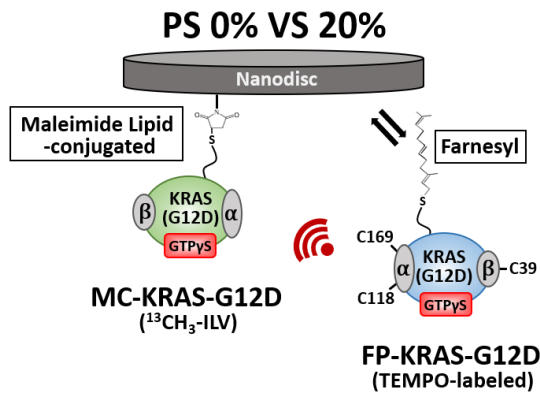
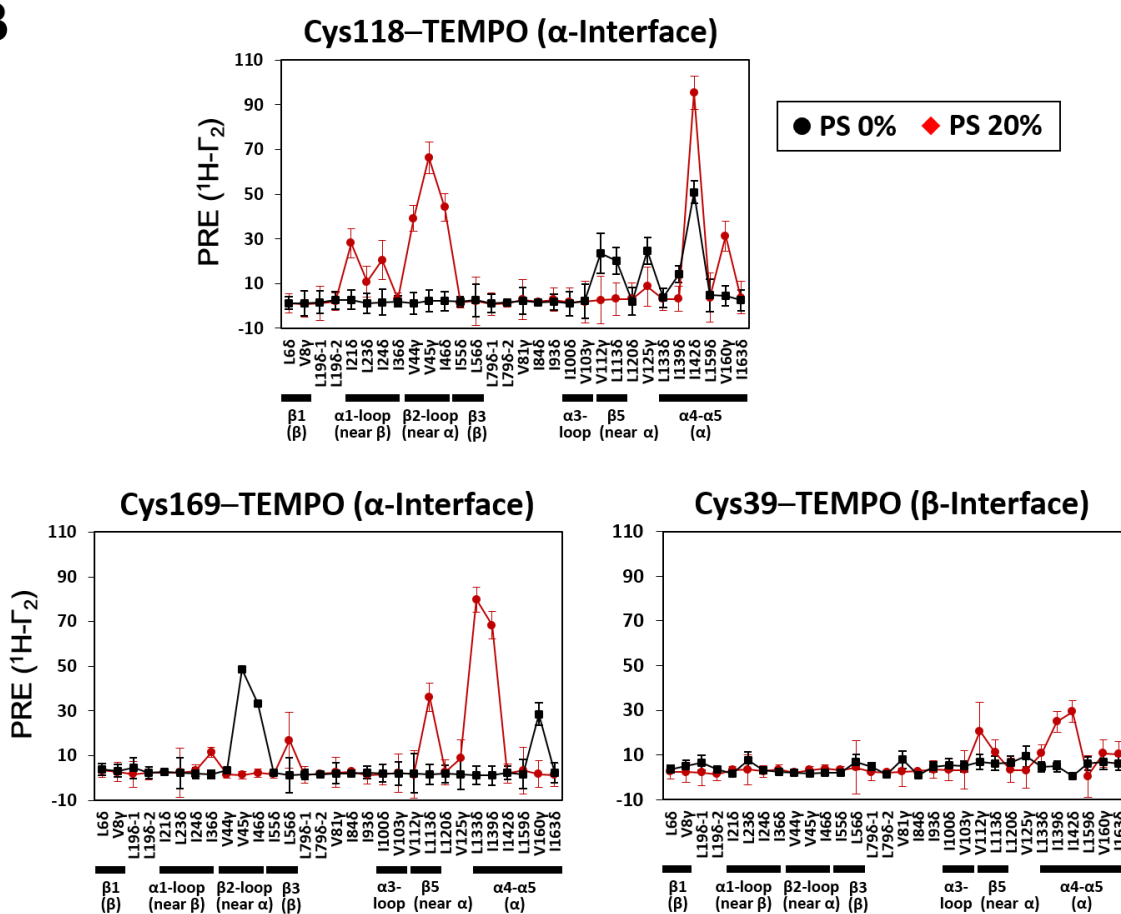
**Figure S14.** Solvent and membrane PRE probes combined with KRAS-G12D interface mutants define the orientation of each dimer configuration ( $\alpha^*$ - $\alpha$ ,  $\alpha^*$ - $\beta$ , or  $\beta^*$ - $\alpha$ ) on the membrane. (A) Experimental design for probing solvent and membrane PRE effects on <sup>13</sup>C-labeled MC-KRAS-G12D in the presence and absence of unlabeled FP-KRAS-G12D. Solvent and membrane PRE effects are induced by Gd-DTPA-BMA in the bulk solvent and Gd<sup>3+</sup> ion chelated by a DTPA-modified lipid head group, respectively. (B) Changes in solvent and membrane PRE effects on the  $\alpha$  and  $\beta$  interfaces and the  $\alpha$ 3-loop region of MC-KRAS-G12D upon addition of FP-KRAS-G12D, as well as those obtained with the interface mutants D38K or E168R introduced into both MC- and FP-KRAS-G12D. Values in parenthesis are the averages of  $\Delta^1\text{H}-\Gamma_{2,\text{di-mono}}/\Gamma_{2,\text{mono}}$  for probes in the  $\alpha$  interface, the  $\beta$  interface, or the  $\alpha$ 3-loop region of MC-KRAS-G12D. (C) Top view of three dimer configurations ( $\alpha^*$ - $\alpha$ ,  $\alpha^*$ - $\beta$ , and  $\beta^*$ - $\alpha$ ) of membrane-bound KRAS-G12D. The isotopically labeled, PRE-visible interface is marked with an asterisk. The  $\alpha$  and  $\beta$  interfaces and the  $\alpha$ 3-loop region as well as the interface mutations D38K and E168R are indicated in each dimer state.



**Figure S15.** The lowest HADDOCK-score models of the  $\alpha\text{-}\alpha$  dimer of KRAS-G12D on the membrane. (A) Plot of HADDOCK scores of the 200 final structures of the  $\alpha\text{-}\alpha$  dimer (residues 1-172) versus RMSD values to the mean structure. These structures were generated by distance restraints derived from the TEMPO-PRE data and the membrane Gd<sup>3+</sup>-PRE data for the  $\alpha\text{-}\alpha$  dimer state observed with the interface mutants MC-KRAS-G12D/D38K and FP-KRAS-G12D/D38K (see details in the Material and Methods section). (B) Overlay of the 20 lowest HADDOCK-score structures of the  $\alpha\text{-}\alpha$  dimer with (left) and without (right) the C-terminal flexible region (residues 173-184). Average backbone RMSDs for the GTPase domain (residues 1-172) in the 200 and 20 lowest HADDOCK-score structures are  $0.94 \pm 0.18 \text{ \AA}$  and  $0.82 \pm 0.15 \text{ \AA}$ , respectively, to the mean structures. (C) Comparison between reference structures of the  $\alpha\text{-}\alpha$  dimer (residues 1-172) of the G12D mutant (pink) and wild-type KRAS (blue white) in the active GTP $\gamma$ S-bound state. An average backbone RMSD for these structures is  $0.79 \text{ \AA}$ .



**Figure S16.** The lowest HADDOCK-score models of the  $\alpha\beta$  dimer of KRAS-G12D on the membrane. (A) Plot of HADDOCK scores of the 200 final structures of the  $\alpha\beta$  dimer (residues 1-172) versus RMSD values to the mean structure. These structures were generated by distance restraints derived from the TEMPO-PRE data and the membrane Gd<sup>3+</sup>-PRE data for the  $\alpha\beta$  dimer state observed with the interface mutants MC-KRAS-G12D/D38K and FP-KRAS-G12D/E168R (or MC-KRAS-G12D/E168R and FP-KRAS-G12D/D38K) (see details in the Material and Methods section). (B) Overlay of the 20 lowest HADDOCK-score structures of the  $\alpha\beta$  dimer with (left) and without (right) the C-terminal flexible region (residues 173-184). Average backbone RMSDs for the GTPase domain (residues 1-172) in the 200 and 20 lowest HADDOCK-score structures are  $1.62 \pm 0.55 \text{ \AA}$  and  $1.34 \pm 0.47 \text{ \AA}$ , respectively, to the mean structures.

**A****B**

C

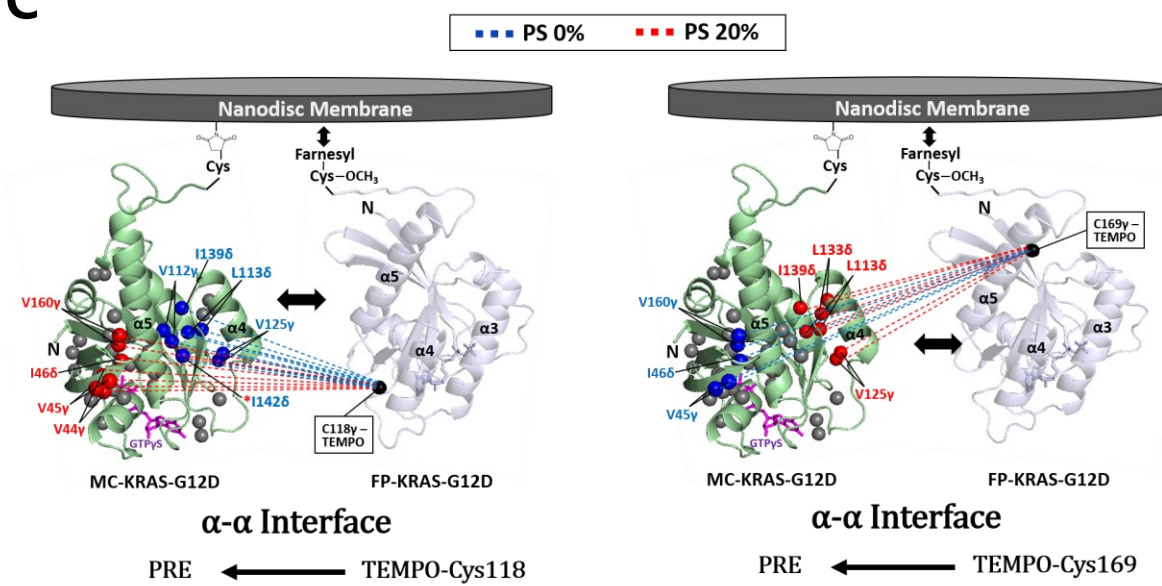


**Figure S17.** Impact of phosphatidylserine (PS) on the intermolecular protein-protein PRE between KRAS-G12D molecules on the membrane (0% versus 20% PS). (A) Experimental design with [ILV-<sup>13</sup>C methyl]-labeled MC-KRAS-G12D and FP-KRAS-G12D bearing a TEMPO spin label at Cys118, Cys169, or Cys39. (B) <sup>1</sup>H- $\Gamma_2$  PRE rates for ILV <sup>13</sup>C-methyls of MC-KRAS-G12D in the presence of FP-KRAS-G12D tagged with TEMPO at Cys118, Cys169, or Cys39. These data were obtained in the absence (100% DOPC, black) or presence (red) of 20% phosphatidylserine lipids. (C) Mapping KRAS-G12D protein:protein PRE effects at the  $\alpha$ - $\alpha$  dimer interface. These effects are mapped onto the crystal structure of GTPyS-bound KRAS-G12D (PDB ID: 4DSO) in an arbitrary dimerization model including a nanodisc membrane. ILV <sup>13</sup>C-methyls that exhibit <sup>1</sup>H- $\Gamma_2$  values  $> 10 \text{ s}^{-1}$  in the presence and absence of 20% PS lipids are colored in red and blue, respectively. Dotted lines represent the PRE effects that arise from TEMPO conjugated to the Sy atom of Cys118 (left) and Cys169 (right) in the opposing protomer (arbitrarily positioned).

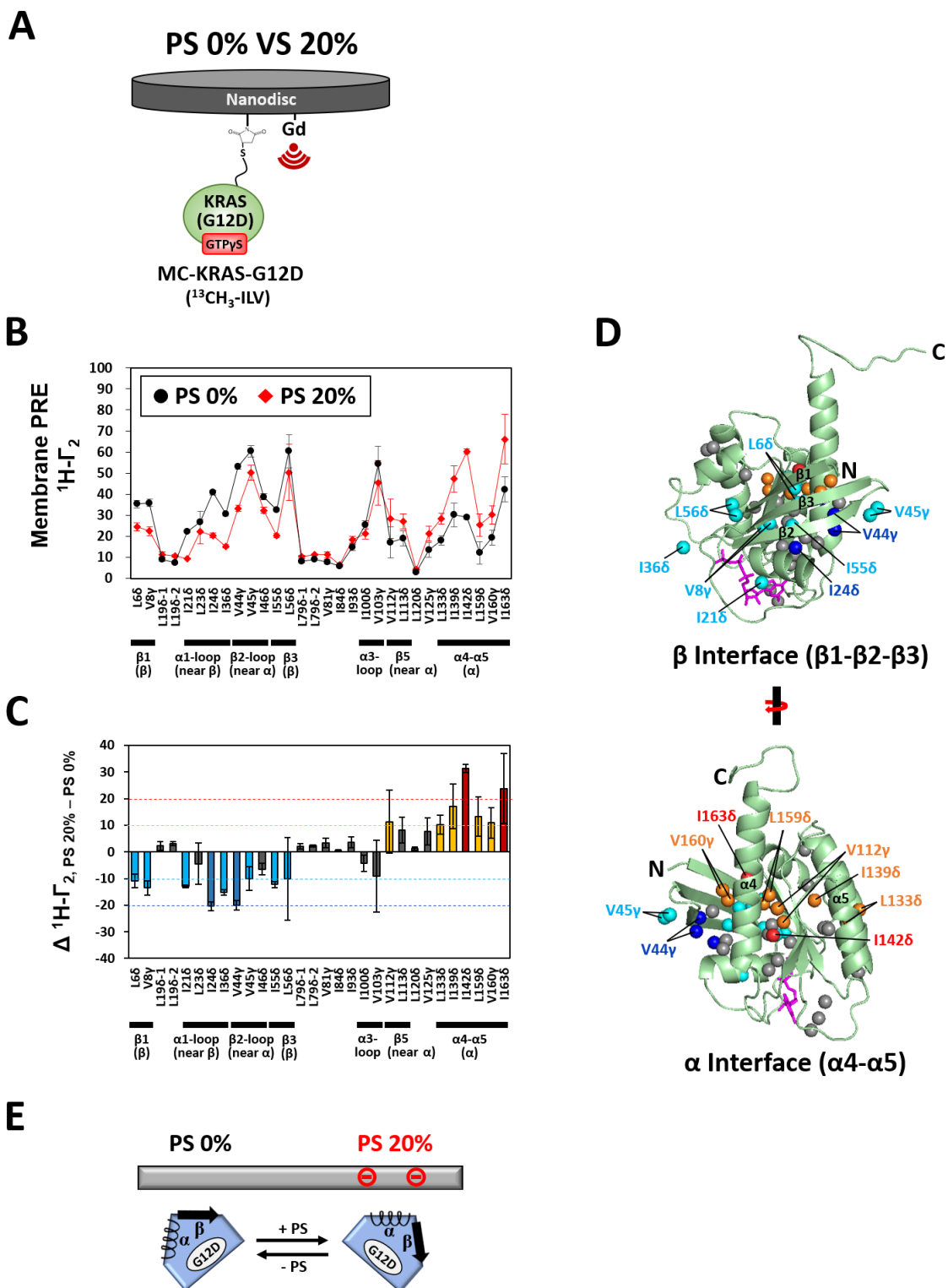


**Figure S18.** Impact of phosphatidylserine (PS) on membrane PRE on the KRAS-G12D monomer on a nanodisc membrane. (A) Experimental design for probing membrane PRE effects on  $^{13}\text{C}$ -labeled MC-KRAS-G12D. Membrane PRE effects are induced by  $\text{Gd}^{3+}$  ion chelated by a DTPA-modified lipid head group in nanodiscs. (B)  $^1\text{H}-\Gamma_2$  PRE rates of ILV  $^{13}\text{C}$ -methyl probes of MC-KRAS-G12D in the absence (100% DOPC, black) or presence (red) of 20% PS lipids. (C) Changes in  $^1\text{H}-\Gamma_2$  PRE rates ( $\Delta^1\text{H}-\Gamma_2, \text{PS } 20\% - \text{PS } 0\%$ ) for MC-KRAS-G12D probes upon incorporation of 20% PS lipids into nanodiscs. Positive and negative values of  $\Delta^1\text{H}-\Gamma_2, \text{PS } 20\% - \text{PS } 0\%$  represent gain and loss, respectively, of the membrane PRE effect upon incorporation of 20% PS lipids into nanodiscs. Probes that exhibit PS-induced changes in the membrane PRE are categorized according to the threshold values of  $\Delta^1\text{H}-\Gamma_2, \text{PS } 20\% - \text{PS } 0\% : > 0.6$  (red),  $> 0.3$  (orange),  $< -0.3$  (cyan), and  $<-0.6$  (blue). (D) Mapping PS-induced changes in the membrane PRE effect onto the crystal structure of GTP $\gamma$ S-bound KRAS-G12D (PDB ID: 4DSO). ILV  $^{13}\text{C}$ -methyl probes that exhibit PS-induced changes in the membrane PRE effect are colored as in panel C. (E) Schematic representation of major orientations of the KRAS-G12D monomer with respect to the membrane containing 0% versus 20% PS lipids.

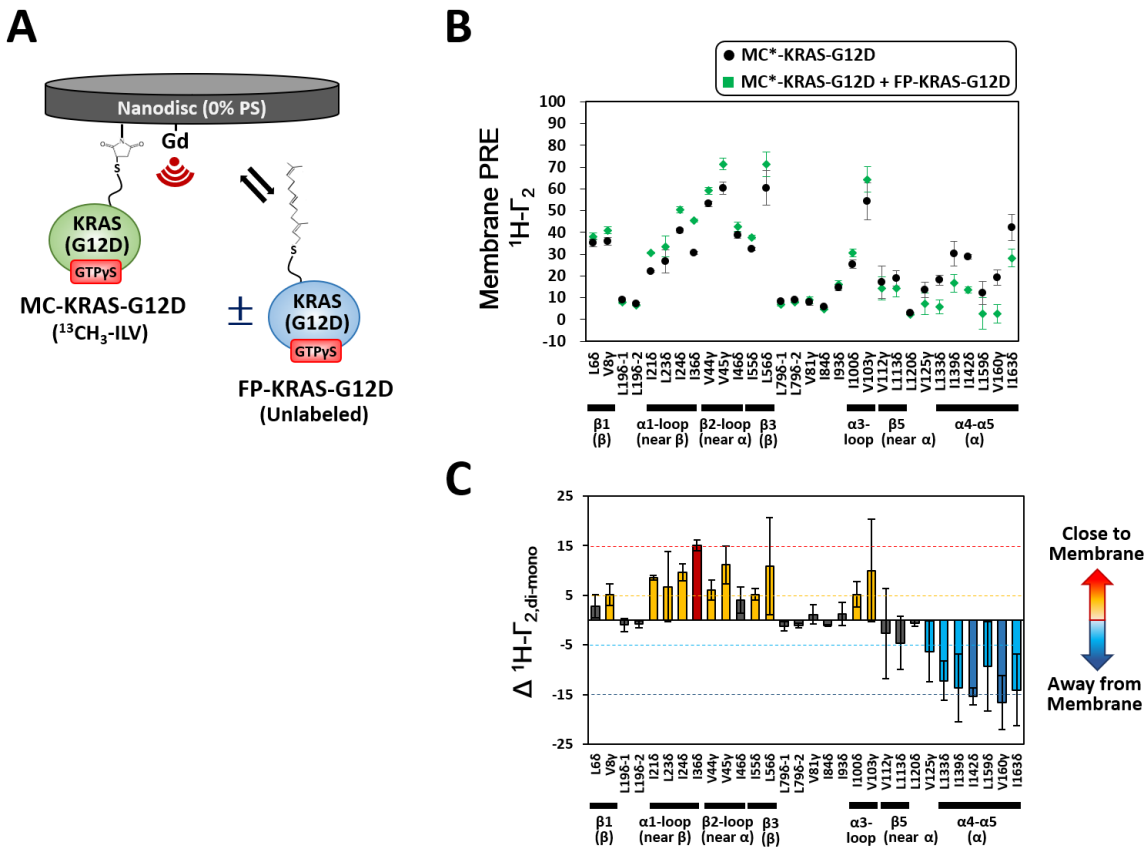


**Figure S19.** Dimerization-induced changes in membrane PRE effects on KRAS-G12D on a membrane lacking phosphatidylserine (PS) lipids. (A) Experimental design for probing membrane PRE effects on <sup>13</sup>C-labeled MC-KRAS-G12D in the presence and absence of unlabeled FP-KRAS-G12D. Membrane PRE effects are induced by Gd<sup>3+</sup> ion chelated by a DTPA-modified lipid head group in nanodiscs. (B) Membrane PRE effects on MC-KRAS-G12D from Gd<sup>3+</sup>-chelated head groups of PE-DTPA lipids in the presence (green) and absence (black) of FP-KRAS-G12D. (C) Differential PRE between the two samples in panel C. <sup>1</sup>H- $\Gamma_2$  PRE rates of ILV <sup>13</sup>C-methyl probes of MC-KRAS-G12D induced by membrane-associated Gd<sup>3+</sup> were measured in the presence and absence of an equal amount of unlabeled FP-KRAS-G12D, and changes in <sup>1</sup>H- $\Gamma_2$  rates ( $\Delta$ <sup>1</sup>H- $\Gamma_{2,\text{di-mono}}$ ) upon addition of FP-KRAS-G12D were calculated. Positive and negative values of  $\Delta$ <sup>1</sup>H- $\Gamma_{2,\text{di-mono}}$  represent gain and loss, respectively, of the membrane PRE effect upon dimerization. Probes that exhibit dimerization-induced changes in the membrane PRE are categorized according to the threshold values of  $\Delta$ <sup>1</sup>H- $\Gamma_{2,\text{di-mono}}/\text{<sup>1</sup>H-}\Gamma_{2,\text{mono}}$ : > 0.6 (red), > 0.3 (orange), < -0.3 (cyan), and < -0.6 (blue).

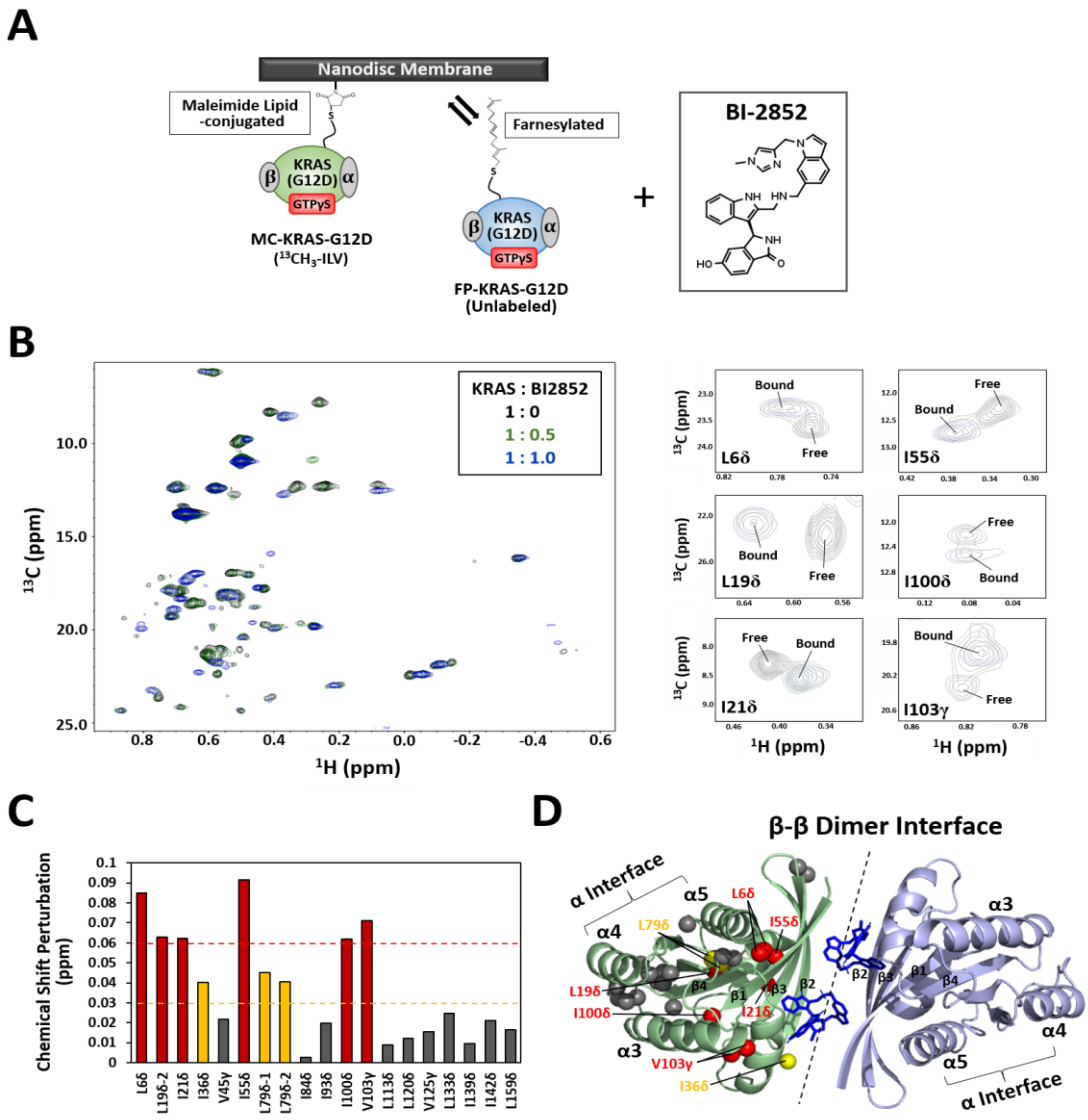


**Figure S20.** Chemical shift perturbations of membrane-bound KRAS-G12D upon addition of BI-2852. (A) Schematic of nanodisc-based system for NMR studies of KRAS dimerization in the presence of BI-2852.  $^{13}\text{C}$  ILV-labeled KRAS-G12D (MC-KRAS-G12D) irreversibly conjugated via its C-terminus to a maleimide moiety on the head group of a PE-MCC lipid in nanodiscs is mixed with fully processed, farnesylated KRAS-G12D (FP-KRAS-G12D) and the BI-2852 compound. (B) Overlay of  $^1\text{H}$ - $^{13}\text{C}$  TROSY spectra of MC-KRAS-G12D obtained with the KRAS-G12D:BI-2852 molar ratios of 1:0 (black), 1:0.5 (green), and 1:1 (blue). Expanded views of split peaks that correspond to the free and BI-2852-bound states are shown at the right. (C) Plot of BI-2852-induced chemical shift perturbations (CSPs) versus each probe in MC-KRAS-G12D. Probes are categorized according to the extent of CSP (threshold values > 0.06, strong, red, > 0.03, moderate, yellow, < 0.03, low, gray). CSP values were calculated from the equation  $\sqrt{(0.184 \times \Delta\delta_{\text{C}})^2 + (\Delta\delta_{\text{H}})^2}$ , where  $\Delta\delta_{\text{C}}$  and  $\Delta\delta_{\text{H}}$  are chemical shift changes for  $^{13}\text{C}$  and  $^1\text{H}$ , respectively, upon binding to BI-2852. (D) CSP-affected probes mapped onto the reference HADDOCK structure of the BI-2852-stabilized KRAS-G12D dimer. Probes are colored in the same way as in panel C.

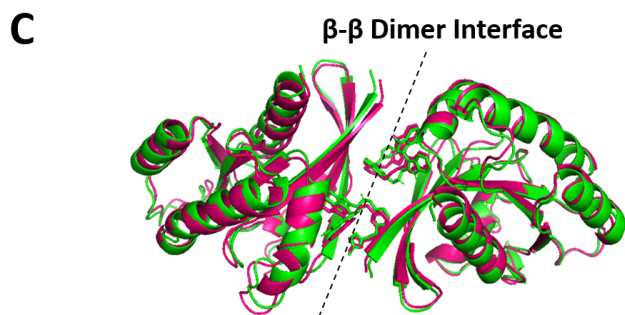
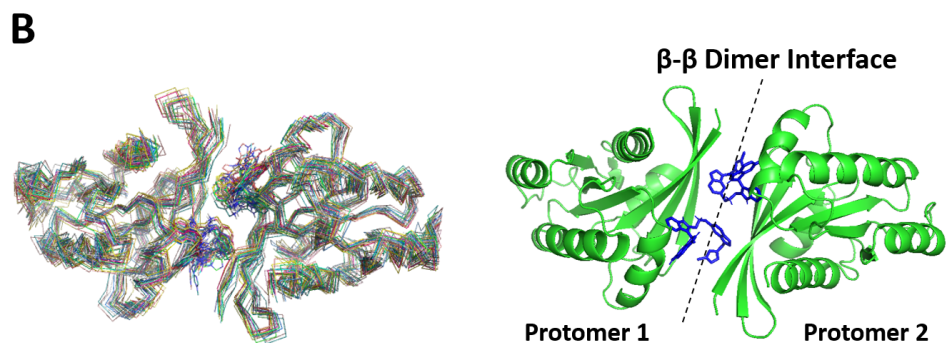
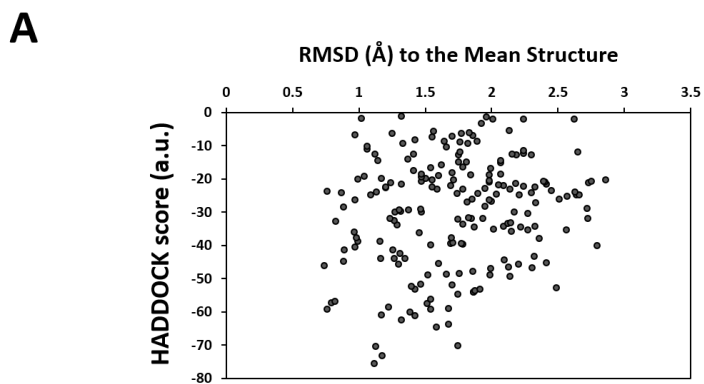


**Figure S21.** HADDOCK models of the BI-2852-stabilized  $\beta$ - $\beta$  dimer of KRAS-G12D. (A) Plot of HADDOCK scores of the 200 lowest HADDOCK-score structures of the BI-2852-stabilized  $\beta$ - $\beta$  dimer (residues 1-168) versus RMSD values to the mean structure. (B) Overlay of the 20 best HADDOCK structures of the BI-2852-stabilized  $\beta$ - $\beta$  dimer (left) and their average structure (right). Average backbone RMSDs for the 200 and 20 lowest HADDOCK-score structures are  $1.73 \pm 0.49$   $\text{\AA}$  and  $1.36 \pm 0.32$   $\text{\AA}$ , respectively, to the mean structures. (C) Overlay of the HADDOCK (green) and crystal (pink, PDB ID: 6GJ8) structures of the BI-2852-stabilized  $\beta$ - $\beta$  dimer of KRAS-G12D. An average backbone RMSD for these structures is  $1.01$   $\text{\AA}$ .

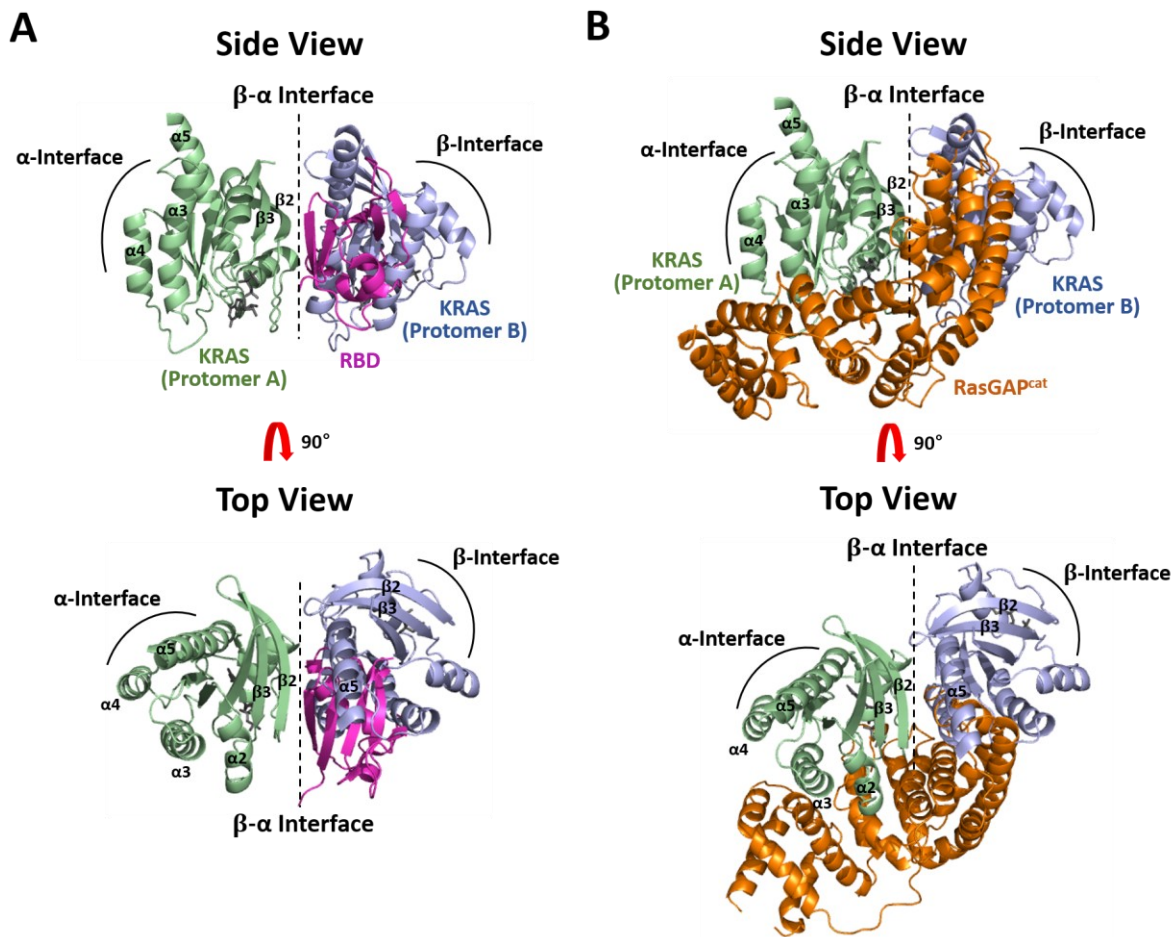


**Figure S22.** Overlay of NMR-driven structure of the KRAS-G12D  $\alpha$ - $\beta$  dimer with crystal structures of KRAS in complex with interacting proteins: (A) the CRAF-RAS binding domain (CRAF-RBD), and (B) the catalytic domain of P120 RasGAP (RasGAP<sup>cat</sup>). These complex models are reconstituted based on the crystal structures of the HRAS-RBD complex (PDB ID: 4G0N) and the HRAS-RasGAP complex (PDB ID: 1WQ1), respectively. Binding of RAF-RBD or RasGAP<sup>cat</sup> to KRAS-G12D is incompatible with the structure of the KRAS-G12D  $\alpha$ - $\beta$  dimer.

### 3. Supplementary Tables

**Table S1.** Distances between each TEMPO-labeled cysteine and each probe in the reference HADDOCK structures of both the  $\alpha$ - $\alpha$  and  $\alpha$ - $\beta$  dimers of KRAS-G12D generated using all ambiguous PRE restraints.

$\alpha$ -interface Spin	PRE-affected Probes	Distance ( $\text{\AA}$ ) Observed In $\alpha$ - $\alpha$ dimer	Distance ( $\text{\AA}$ ) Observed In $\alpha$ - $\beta$ dimer	PRE-competent Dimer State <sup>#</sup>
Cys118 $\gamma$ -TEMPO	21 $\delta$	31.9	16.1	$\alpha$ - $\beta$
	23 $\delta$	22.5	17.8	$\alpha$ - $\beta$
	24 $\delta$	27.0	16.4	$\alpha$ - $\beta$
	42	27.7	15.7	$\alpha$ - $\beta$
	44 $\gamma$	19.7	25.4	$\alpha$ - $\alpha$
	45 $\gamma$	18.5	25.8	$\alpha$ - $\alpha$
	46 $\delta$	19.0	27.2	$\alpha$ - $\alpha$
	142 $\delta$	16.7	29.6	$\alpha$ - $\alpha$
	160 $\gamma$	20.6	26.5	$\alpha$ - $\alpha$
Cys169 $\gamma$ -TEMPO	5	26.5	15.4	$\alpha$ - $\beta$
	36 $\delta$	38.4	20.8	$\alpha$ - $\beta$
	42	33.9	17.9	$\alpha$ - $\beta$
	56 $\delta$	31.9	14.8	$\alpha$ - $\beta$
	113 $\delta$	17.2	33.1	$\alpha$ - $\alpha$
	128	19.8	41.9	$\alpha$ - $\alpha$
	133 $\delta$	16.0	37.1	$\alpha$ - $\alpha$
	139 $\delta$	14.8	33.27	$\alpha$ - $\alpha$
	169	15.4	29.7	$\alpha$ - $\alpha$

	172	17.2	30.0	α-α
	175	17.1	34.2	α-α
	176	18.4	35.7	α-α
	177	19.9	34.7	α-α
	178	19.7	33.5	α-α
	179	19.8	33.9	α-α
β-interface Spin	PRE-affected Probes	Distance (Å) Observed In α-β dimer	Distance (Å) Observed In α-α dimer	PRE-competent Dimer State <sup>#</sup>
Cys1γ -TEMPO	44γ	42.7	14.1	α-β
	45γ	44.8	10.4	α-β
	46δ	38.3	11.7	α-β
	160γ	37.7	13.7	α-β
	165	34.9	15.3	α-β
Cys39γ -TEMPO	112γ	33.2	14.7	α-β
	113δ	33.1	15.5	α-β
	128	28.2	16.8	α-β
	133δ	32.8	15.0	α-β
	139δ	32.2	12.7	α-β
	142δ	29.6	16.1	α-β
	160γ	38.0	19.6	α-β
	163δ	39.6	19.7	α-β
	165	34.2	15.3	α-β
	167	37.1	17.3	α-β
	169	35.8	16.1	α-β

# These dimer states were selected considering that nitroxide spin in TEMPO can induce the PRE effect within  $\sim 22 \text{ \AA}$ .

**Table S2.** Statistics for the 20 lowest HADDOCK-score structures of the  $\alpha$ - $\alpha$  and  $\alpha$ - $\beta$  dimers of KRAS-G12D on the membrane.

**$\alpha$ - $\alpha$  Dimer of KRAS-G12D**

**PRE-derived Distance Restraints**

Number of TEMPO-PRE restraints	32
Number of Mutant PRE restraints	10
Number of Membrane PRE restraints	42

**Energy Statistics**

HADDOCK score (a.u.)	$-74 \pm 14$
Van der Waals energy (kcal/mol)	$-49 \pm 12$
Electrostatic energy (kcal/mol)	$-377 \pm 89$
Desolvation energy (kcal/mol)	$49 \pm 15$
Restraints violation energy (kcal/mol)	$21 \pm 16$

**$\alpha$ - $\beta$  Dimer of KRAS-G12D**

**PRE-derived Distance Restraints**

Number of TEMPO-PRE restraints	24
Number of Mutant PRE restraints	8
Number of Membrane PRE restraints	20

**Energy Statistics**

HADDOCK score (a.u.)	$-89 \pm 19$
Van der Waals energy (kcal/mol)	$-38 \pm 9$
Electrostatic energy (kcal/mol)	$-557 \pm 130$
Desolvation energy (kcal/mol)	$56 \pm 17$
Restraints violation energy (kcal/mol)	$50 \pm 6$

**Table S3.** Intermolecular interactions within the KRAS-lipid interface in the 20 lowest HADDOCK-score structures for both the  $\alpha$ - $\alpha$  and  $\alpha$ - $\beta$  dimers of KRAS-G12D on the membrane.

α-α Dimer Model of KRAS-G12D									
Model	Chain <sup>#</sup>	Residue Number	Residue Name	Atom Name	Chain	Residue Number	Residue Name	Atom Name <sup>£</sup>	Distance <sup>*</sup> (Å)
1	A	178	LYS	HZ1	C	16	PS	O13B	3.30
1	A	178	LYS	HZ2	C	1	PC	O14	3.97
1	A	178	LYS	HZ2	C	16	PS	O13A	2.76
1	A	178	LYS	HZ2	C	16	PS	O13B	4.00
1	A	178	LYS	HZ3	C	16	PS	O13A	2.13
1	A	178	LYS	HZ3	C	16	PS	O13B	3.08
1	A	180	LYS	O	C	16	PS	HAA	3.48
1	A	180	LYS	HZ1	C	9	PS	O12	3.38
1	A	180	LYS	HZ1	C	9	PS	O13B	3.12
1	A	180	LYS	HZ1	C	29	PC	O14	3.80
1	A	180	LYS	HZ2	C	9	PS	O12	2.12
1	A	180	LYS	HZ2	C	9	PS	O13A	3.45
1	A	180	LYS	HZ2	C	9	PS	O13B	1.66
1	A	180	LYS	HZ2	C	9	PS	O14	3.68
1	A	180	LYS	HZ3	C	9	PS	O12	3.78
1	A	180	LYS	HZ3	C	9	PS	O13A	3.97
1	A	180	LYS	HZ3	C	9	PS	O13B	2.46
1	A	181	SER	O	C	16	PS	HAA	3.53
1	A	181	SER	O	C	16	PS	HAB	3.71
1	A	182	LYS	HZ1	C	16	PS	O13	3.95
1	A	182	LYS	O	C	16	PS	HAA	3.50
1	A	182	LYS	O	C	16	PS	HAB	3.08
1	A	183	THR	HN	C	16	PS	O11	3.94
1	A	183	THR	HN	C	16	PS	O12	3.70
1	A	183	THR	HN	C	16	PS	O13	1.97
1	A	183	THR	HG1	C	16	PS	O13	3.75
1	A	184	LYS	HZ1	C	29	PC	O11	2.93
1	A	184	LYS	HZ1	C	29	PC	O12	2.97
1	A	184	LYS	HZ1	C	29	PC	O13	3.39
1	A	184	LYS	HZ1	C	29	PC	O21	3.00
1	A	184	LYS	HZ3	C	29	PC	O21	3.11
1	B	180	LYS	HZ1	C	3	PC	O11	3.60
1	B	180	LYS	HZ1	C	3	PC	O13	1.97
1	B	180	LYS	HZ1	C	12	PC	O12	3.56
1	B	180	LYS	HZ1	C	12	PC	O13	2.61
1	B	180	LYS	HZ2	C	3	PC	O13	3.59
1	B	180	LYS	HZ2	C	12	PC	O12	3.64
1	B	180	LYS	HZ2	C	12	PC	O13	2.64
1	B	180	LYS	HZ2	C	12	PC	O14	3.86
1	B	180	LYS	HZ3	C	3	PC	O13	2.92
1	B	180	LYS	HZ3	C	12	PC	O13	3.88
1	B	182	LYS	HZ1	C	10	PC	O22	3.37
1	B	182	LYS	HZ2	C	10	PC	O22	3.03
1	B	182	LYS	HZ3	C	10	PC	O21	3.87
1	B	182	LYS	HZ3	C	10	PC	O22	1.68
1	B	183	THR	HG1	C	7	PC	O13	3.77
1	B	183	THR	HG1	C	7	PC	O14	3.82
1	B	183	THR	HG1	C	7	PC	O22	3.54

1	B	184	LYS	HN	C	7	PC	014	3.50
1	B	184	LYS	HZ1	C	17	PS	011	3.75
1	B	184	LYS	HZ1	C	17	PS	013B	2.96
1	B	184	LYS	HZ1	C	17	PS	022	2.63
1	B	184	LYS	HZ2	C	17	PS	011	3.45
1	B	184	LYS	HZ2	C	17	PS	012	3.27
1	B	184	LYS	HZ2	C	17	PS	013	3.31
1	B	184	LYS	HZ2	C	17	PS	013B	3.36
1	B	184	LYS	HZ2	C	17	PS	021	3.24
1	B	184	LYS	HZ2	C	17	PS	022	1.67
1	B	184	LYS	HZ3	C	17	PS	011	3.36
1	B	184	LYS	HZ3	C	17	PS	012	2.71
1	B	184	LYS	HZ3	C	17	PS	013	3.97
1	B	184	LYS	HZ3	C	17	PS	013A	2.91
1	B	184	LYS	HZ3	C	17	PS	013B	1.67
1	B	184	LYS	HZ3	C	17	PS	022	3.29
2	A	184	LYS	HZ1	C	61	PS	013A	1.92
2	A	184	LYS	HZ1	C	61	PS	013B	2.26
2	A	184	LYS	HZ2	C	61	PS	013A	3.08
2	A	184	LYS	HZ2	C	61	PS	013B	2.75
2	A	184	LYS	HZ3	C	61	PS	013A	2.94
2	A	184	LYS	HZ3	C	61	PS	013B	3.71
2	B	184	LYS	O	C	34	PC	N	3.01
3	A	177	LYS	HZ1	C	9	PS	013B	3.53
3	A	180	LYS	HZ1	C	31	PC	013	3.43
3	A	182	LYS	HN	C	31	PC	013	3.73
3	A	182	LYS	HN	C	31	PC	014	3.39
3	A	182	LYS	HZ1	C	31	PC	011	3.75
3	A	182	LYS	HZ1	C	31	PC	014	2.90
3	A	182	LYS	HZ2	C	31	PC	014	3.21
3	A	182	LYS	HZ2	C	44	PS	022	3.83
3	A	182	LYS	HZ3	C	31	PC	011	3.61
3	A	182	LYS	HZ3	C	31	PC	012	3.80
3	A	182	LYS	HZ3	C	31	PC	014	1.70
3	A	182	LYS	O	C	31	PC	N	3.56
3	A	184	LYS	O	C	55	PC	N	3.33
3	B	177	LYS	HZ1	C	1	PC	013	2.06
3	B	177	LYS	HZ1	C	1	PC	014	3.53
3	B	177	LYS	HZ2	C	1	PC	013	2.33
3	B	177	LYS	HZ3	C	1	PC	013	3.13
3	B	177	LYS	HZ3	C	3	PC	012	3.85
3	B	180	LYS	HZ1	C	7	PC	011	3.78
3	B	180	LYS	HZ1	C	7	PC	013	2.51
3	B	180	LYS	HZ1	C	7	PC	022	3.43
3	B	180	LYS	HZ3	C	7	PC	013	4.00
3	B	180	LYS	HZ3	C	7	PC	022	3.34
3	B	181	SER	HN	C	2	PC	013	3.84
3	B	183	THR	HG1	C	8	PC	011	3.59
3	B	183	THR	HG1	C	8	PC	031	3.50
3	B	183	THR	HG1	C	8	PC	032	3.80
3	B	184	LYS	O	C	8	PC	N	3.22
3	B	184	LYS	HZ1	C	20	PC	011	3.11
3	B	184	LYS	HZ1	C	20	PC	013	3.57
3	B	184	LYS	HZ1	C	20	PC	014	1.72
3	B	184	LYS	HZ2	C	20	PC	022	3.05
3	B	184	LYS	HZ2	C	20	PC	011	3.78

3	B	184	LYS	HZ2	C	20	PC	014	3.15
3	B	184	LYS	HZ2	C	20	PC	022	2.65
3	B	184	LYS	HZ3	C	20	PC	011	3.76
3	B	184	LYS	HZ3	C	20	PC	014	3.26
3	B	184	LYS	HZ3	C	20	PC	021	3.58
3	B	184	LYS	HZ3	C	20	PC	022	1.80
4	A	179	LYS	HZ1	C	7	PC	012	3.44
4	A	179	LYS	HZ1	C	7	PC	014	2.88
4	A	179	LYS	HZ2	C	7	PC	011	3.98
4	A	179	LYS	HZ2	C	7	PC	012	3.53
4	A	179	LYS	HZ2	C	7	PC	014	1.74
4	A	179	LYS	HZ3	C	7	PC	014	3.39
4	A	180	LYS	HZ1	C	10	PC	012	3.96
4	A	180	LYS	HZ2	C	8	PC	013	3.98
4	A	180	LYS	HZ2	C	8	PC	014	3.48
4	A	180	LYS	HZ2	C	10	PC	012	3.47
4	A	181	SER	HG	C	10	PC	013	3.13
4	A	181	SER	HG	C	10	PC	014	3.62
4	A	182	LYS	HN	C	10	PC	013	1.84
4	A	182	LYS	HZ1	C	10	PC	021	3.84
4	A	182	LYS	HZ1	C	10	PC	022	1.68
4	A	182	LYS	HZ2	C	10	PC	022	3.36
4	A	182	LYS	HZ3	C	10	PC	022	3.05
4	A	183	THR	HN	C	10	PC	013	3.94
4	A	183	THR	HG1	C	10	PC	022	3.83
4	A	184	LYS	HZ1	C	17	PS	013A	3.05
4	A	184	LYS	HZ1	C	17	PS	013B	3.53
4	A	184	LYS	HZ2	C	17	PS	013A	1.72
4	A	184	LYS	HZ2	C	17	PS	013B	2.76
4	A	184	LYS	HZ3	C	17	PS	013A	2.61
4	A	184	LYS	HZ3	C	17	PS	013B	2.09
4	B	176	LYS	HZ3	C	2	PC	014	3.69
5	A	182	LYS	HZ1	C	9	PS	014	2.94
5	A	182	LYS	HZ2	C	9	PS	014	3.27
5	A	182	LYS	HZ3	C	9	PS	012	3.82
5	A	182	LYS	HZ3	C	9	PS	014	1.87
5	A	184	LYS	HN	C	9	PS	012	3.75
5	A	184	LYS	HN	C	9	PS	013A	2.36
5	B	181	SER	HN	C	10	PC	013	3.08
5	B	182	LYS	HN	C	2	PC	014	2.66
5	B	182	LYS	HZ3	C	8	PC	012	3.42
5	B	182	LYS	O	C	2	PC	N	3.94
6	A	184	LYS	HZ3	C	15	PC	013	3.60
6	A	184	LYS	HZ3	C	15	PC	014	4.00
6	B	178	LYS	HZ1	C	16	PS	013A	3.20
6	B	178	LYS	HZ2	C	16	PS	013A	1.80
6	B	178	LYS	HZ2	C	16	PS	013B	3.42
6	B	178	LYS	HZ3	C	16	PS	013A	3.24
6	B	179	LYS	HZ1	C	2	PC	022	3.27
6	B	179	LYS	HZ1	C	4	PC	012	3.98
6	B	179	LYS	HZ1	C	4	PC	013	2.92
6	B	179	LYS	HZ2	C	2	PC	021	3.33
6	B	179	LYS	HZ2	C	2	PC	022	1.68
6	B	179	LYS	HZ2	C	4	PC	012	3.16
6	B	179	LYS	HZ2	C	4	PC	013	2.80
6	B	179	LYS	HZ3	C	2	PC	021	3.30

6	B	179	LYS	HZ3	C	2	PC	022	2.80
6	B	181	SER	HG	C	6	PC	013	3.83
6	B	181	SER	HG	C	6	PC	022	2.98
6	B	182	LYS	HZ1	C	13	PC	014	3.93
6	B	182	LYS	HZ2	C	13	PC	013	3.91
6	B	182	LYS	HZ2	C	13	PC	014	2.54
6	B	182	LYS	HZ3	C	13	PC	013	3.93
6	B	182	LYS	HZ3	C	13	PC	014	2.74
6	B	183	THR	HG1	C	30	PC	012	3.92
6	B	184	LYS	HN	C	25	PC	012	3.66
6	B	184	LYS	HN	C	25	PC	014	3.26
7	B	184	LYS	O	C	25	PC	N	3.49
7	A	180	LYS	HZ3	C	3	PC	013	3.92
7	A	182	LYS	HZ1	C	7	PC	021	3.94
7	A	182	LYS	HZ1	C	7	PC	022	1.76
7	A	182	LYS	HZ2	C	7	PC	022	3.36
7	A	182	LYS	HZ3	C	7	PC	022	3.30
7	A	184	LYS	HZ1	C	3	PC	021	3.45
7	A	184	LYS	HZ1	C	3	PC	022	1.72
7	A	184	LYS	HZ2	C	3	PC	021	3.54
7	A	184	LYS	HZ2	C	3	PC	022	2.75
7	A	184	LYS	HZ2	C	3	PC	031	3.97
7	A	184	LYS	HZ3	C	3	PC	022	3.10
7	A	184	LYS	HZ3	C	11	PC	022	2.81
7	B	183	THR	HN	C	9	PS	013B	3.91
7	B	183	THR	HG1	C	9	PS	012	3.37
7	B	183	THR	HG1	C	9	PS	013A	3.23
7	B	183	THR	HG1	C	9	PS	013B	1.72
7	B	184	LYS	HN	C	9	PS	013A	3.32
7	B	184	LYS	HN	C	9	PS	013B	1.80
7	B	184	LYS	HZ1	C	9	PS	013A	2.79
7	B	184	LYS	HZ1	C	23	PS	012	3.92
7	B	184	LYS	HZ1	C	23	PS	013	2.97
7	B	184	LYS	HZ1	C	23	PS	014	1.88
7	B	184	LYS	HZ2	C	9	PS	013A	1.66
7	B	184	LYS	HZ2	C	9	PS	013B	3.58
7	B	184	LYS	HZ2	C	23	PS	013	3.69
7	B	184	LYS	HZ2	C	23	PS	014	3.25
7	B	184	LYS	HZ3	C	9	PS	013A	3.22
7	B	184	LYS	HZ3	C	14	PC	032	3.81
7	B	184	LYS	HZ3	C	23	PS	014	3.45
8	A	184	LYS	HZ1	C	51	PC	014	3.46
8	A	184	LYS	HZ2	C	51	PC	012	3.47
8	A	184	LYS	HZ2	C	51	PC	013	3.51
8	A	184	LYS	HZ2	C	51	PC	014	1.87
8	A	184	LYS	HZ3	C	51	PC	012	3.11
8	A	184	LYS	HZ3	C	51	PC	013	3.60
8	A	184	LYS	HZ3	C	51	PC	014	2.88
8	A	184	LYS	HZ3	C	66	PS	013A	3.78
8	B	177	LYS	HZ1	C	5	PC	011	3.97
8	B	177	LYS	HZ1	C	5	PC	012	3.80
8	B	177	LYS	HZ1	C	5	PC	013	1.75
8	B	177	LYS	HZ1	C	5	PC	014	2.99
8	B	177	LYS	HZ2	C	5	PC	013	3.39
8	B	177	LYS	HZ2	C	5	PC	014	3.79
8	B	177	LYS	HZ3	C	5	PC	013	2.87

8	B	177	LYS	HZ3	C	5	PC	014	3.65
8	B	180	LYS	HZ1	C	24	PS	013A	2.63
8	B	180	LYS	HZ2	C	24	PS	013A	1.75
8	B	180	LYS	HZ2	C	24	PS	013B	3.97
8	B	180	LYS	HZ3	C	24	PS	013A	3.37
8	B	182	LYS	HZ2	C	27	PC	022	3.62
8	B	182	LYS	HZ2	C	27	PC	031	3.59
8	B	183	THR	HG1	C	52	PC	014	2.80
10	A	176	LYS	HZ1	C	1	PC	013	1.79
10	A	176	LYS	HZ1	C	1	PC	014	3.74
10	A	176	LYS	HZ2	C	1	PC	013	3.43
10	A	176	LYS	HZ3	C	1	PC	013	2.69
10	A	176	LYS	HZ3	C	1	PC	014	3.41
10	A	179	LYS	HZ1	C	14	PC	013	3.43
10	A	179	LYS	HZ2	C	14	PC	012	3.77
10	A	179	LYS	HZ2	C	14	PC	013	1.74
10	A	179	LYS	HZ2	C	14	PC	014	3.83
10	A	179	LYS	HZ2	C	14	PC	021	3.56
10	A	179	LYS	HZ3	C	14	PC	013	2.91
10	A	179	LYS	HZ3	C	14	PC	021	3.54
10	A	181	SER	HG	C	11	PC	012	3.47
10	A	181	SER	HG	C	11	PC	014	1.82
10	A	183	THR	HN	C	27	PC	011	3.27
10	A	184	LYS	O	C	40	PC	N	3.15
10	A	184	LYS	HZ2	C	73	PC	013	3.76
10	A	184	LYS	HZ3	C	73	PC	014	3.61
10	B	180	LYS	HZ1	C	13	PC	014	2.83
10	B	180	LYS	HZ2	C	13	PC	014	3.44
10	B	180	LYS	HZ3	C	13	PC	012	3.75
10	B	180	LYS	HZ3	C	13	PC	013	3.86
10	B	180	LYS	HZ3	C	13	PC	014	2.18
10	B	184	LYS	HN	C	30	PC	014	3.90
10	B	184	LYS	HZ1	C	30	PC	013	2.78
10	B	184	LYS	HZ1	C	30	PC	022	3.52
10	B	184	LYS	HZ2	C	30	PC	013	3.81
10	B	184	LYS	HZ3	C	30	PC	013	2.39
11	A	184	LYS	HN	C	46	PS	013A	3.39
11	A	184	LYS	HN	C	46	PS	013B	1.74
11	A	184	LYS	HZ1	C	25	PC	013	2.93
11	A	184	LYS	HZ3	C	25	PC	013	3.44
11	A	184	LYS	HZ3	C	25	PC	014	3.68
11	A	184	LYS	HZ3	C	46	PS	013	3.84
11	A	184	LYS	HZ3	C	46	PS	014	3.83
11	B	176	LYS	HZ2	C	3	PC	013	3.94
11	B	180	LYS	HZ1	C	24	PS	013A	3.24
11	B	180	LYS	HZ1	C	24	PS	013B	3.40
11	B	180	LYS	HZ2	C	24	PS	013A	2.30
11	B	180	LYS	HZ2	C	24	PS	013B	1.72
11	B	180	LYS	HZ3	C	24	PS	013A	3.95
11	B	180	LYS	HZ3	C	24	PS	013B	3.05
11	B	181	SER	HG	C	24	PS	012	3.25
11	B	181	SER	HG	C	24	PS	013	1.92
11	B	181	SER	HG	C	24	PS	014	2.81
11	B	182	LYS	HN	C	24	PS	014	3.19
11	B	184	LYS	O	C	41	PC	N	3.40
12	A	178	LYS	HZ1	C	24	PS	013A	3.55

12	A	178	LYS	HZ1	C	24	PS	013B	3.21
12	A	178	LYS	HZ2	C	24	PS	013A	3.01
12	A	178	LYS	HZ2	C	24	PS	013B	3.51
12	A	178	LYS	HZ3	C	24	PS	013A	1.86
12	A	178	LYS	HZ3	C	24	PS	013B	2.04
12	A	181	SER	HN	C	27	PC	011	2.95
12	A	181	SER	HG	C	27	PC	011	3.79
12	B	184	LYS	O	C	72	PC	N	3.04
13	A	181	SER	HN	C	15	PC	011	3.93
13	A	181	SER	HN	C	15	PC	014	2.53
13	A	181	SER	HG	C	15	PC	011	3.70
13	A	182	LYS	HN	C	15	PC	014	2.71
13	A	184	LYS	HN	C	13	PC	014	3.98
13	A	184	LYS	O	C	30	PC	N	3.82
13	B	180	LYS	HZ1	C	10	PC	013	3.65
13	B	180	LYS	HZ1	C	10	PC	022	2.97
13	B	180	LYS	HZ2	C	10	PC	011	3.83
13	B	180	LYS	HZ2	C	10	PC	013	3.28
13	B	180	LYS	HZ2	C	10	PC	022	2.00
13	B	180	LYS	HZ3	C	10	PC	011	3.09
13	B	180	LYS	HZ3	C	10	PC	013	1.97
13	B	180	LYS	HZ3	C	10	PC	022	3.05
13	B	184	LYS	HZ1	C	33	PC	022	3.12
13	B	184	LYS	HZ2	C	33	PC	022	3.56
13	B	184	LYS	HZ3	C	33	PC	022	2.71
13	B	184	LYS	O	C	7	PC	N	3.08
14	A	178	LYS	HZ1	C	1	PC	014	3.31
14	A	178	LYS	HZ2	C	1	PC	014	3.22
14	A	178	LYS	HZ3	C	1	PC	012	3.88
14	A	178	LYS	HZ3	C	1	PC	013	3.97
14	A	178	LYS	HZ3	C	1	PC	014	1.70
14	A	184	LYS	HZ3	C	27	PC	013	3.97
14	B	184	LYS	HZ1	C	8	PC	012	3.48
14	B	184	LYS	HZ1	C	8	PC	013	3.21
14	B	184	LYS	HZ1	C	8	PC	014	3.17
14	B	184	LYS	HZ2	C	8	PC	012	3.43
14	B	184	LYS	HZ2	C	8	PC	013	3.69
14	B	184	LYS	HZ3	C	8	PC	012	3.40
14	B	184	LYS	HZ3	C	8	PC	013	2.46
14	B	184	LYS	HZ3	C	8	PC	014	3.74
15	A	184	LYS	O	C	10	PC	N	3.64
15	A	184	LYS	O	C	22	PC	N	3.73
16	B	184	LYS	HZ1	C	21	PC	013	1.90
16	B	184	LYS	HZ2	C	21	PC	013	3.55
16	B	184	LYS	HZ3	C	21	PC	013	2.89
17	B	180	LYS	HZ1	C	16	PS	013A	3.23
17	B	180	LYS	HZ1	C	16	PS	013B	2.31
17	B	180	LYS	HZ2	C	16	PS	013A	3.03
17	B	180	LYS	HZ2	C	16	PS	013B	2.93
17	B	180	LYS	HZ3	C	16	PS	013A	3.28
17	B	180	LYS	HZ3	C	16	PS	013B	2.03
17	B	182	LYS	HZ1	C	30	PC	013	3.59
18	A	179	LYS	HZ1	C	14	PC	013	3.42
18	A	179	LYS	HZ1	C	14	PC	021	3.94
18	A	179	LYS	HZ2	C	14	PC	012	3.99
18	A	179	LYS	HZ2	C	14	PC	013	2.86

18	A	179	LYS	HZ2	C	14	PC	014	2.84
18	A	179	LYS	HZ2	C	14	PC	021	4.00
18	A	179	LYS	HZ3	C	14	PC	012	3.82
18	A	179	LYS	HZ3	C	14	PC	013	1.75
18	A	179	LYS	HZ3	C	14	PC	014	3.14
18	A	179	LYS	HZ3	C	14	PC	021	2.85
18	A	182	LYS	HZ1	C	24	PS	013A	3.61
18	A	182	LYS	HZ1	C	24	PS	013B	3.28
18	A	182	LYS	HZ2	C	24	PS	013A	2.84
18	A	182	LYS	HZ2	C	24	PS	013B	1.78
18	A	182	LYS	HZ3	C	24	PS	013A	2.01
18	A	182	LYS	HZ3	C	24	PS	013B	2.54
18	A	183	THR	HG1	C	12	PC	032	3.98
18	A	184	LYS	HZ3	C	28	PC	013	3.59
20	A	179	LYS	HZ1	C	17	PS	013A	3.94
20	A	179	LYS	HZ1	C	17	PS	013B	3.46
20	A	179	LYS	HZ2	C	7	PC	013	3.64
20	A	179	LYS	HZ2	C	7	PC	014	3.67
20	A	179	LYS	HZ3	C	7	PC	014	3.87
20	A	179	LYS	HZ3	C	17	PS	013B	3.99
20	A	182	LYS	O	C	22	PC	N	3.98
20	A	184	LYS	HZ1	C	61	PS	013A	2.75
20	A	184	LYS	HZ1	C	61	PS	013B	1.87
20	A	184	LYS	HZ2	C	61	PS	013A	1.91
20	A	184	LYS	HZ2	C	61	PS	013B	2.61
20	A	184	LYS	HZ3	C	61	PS	013A	3.21
20	A	184	LYS	HZ3	C	61	PS	013B	2.89
20	B	184	LYS	HZ1	C	46	PS	013A	3.88
20	B	184	LYS	HZ2	C	46	PS	013B	1.69
20	B	184	LYS	HZ3	C	46	PS	013B	2.84
20	B	184	LYS	HZ3	C	46	PS	013B	3.22

### $\alpha\text{-}\beta$ Dimer Model of KRAS-G12D

Model	Chain	Residue Number	Residue Name	Atom Name	Chain	Residue Number	Residue Name	Atom Name <sup>c</sup>	Distance <sup>*</sup> (Å)
1	A	176	LYS	O	C	30	PC	N	3.80
1	A	176	LYS	HZ2	C	46	PS	013A	3.99
1	A	176	LYS	HZ3	C	46	PS	013A	2.73
1	A	176	LYS	HZ3	C	46	PS	013B	3.53
1	A	184	LYS	O	C	32	PC	N	3.20
1	B	177	LYS	HZ1	C	5	PC	032	2.72
1	B	177	LYS	HZ1	C	9	PS	021	3.83
1	B	177	LYS	HZ1	C	9	PS	022	2.49
1	B	177	LYS	HZ2	C	5	PC	032	3.23
1	B	177	LYS	HZ2	C	9	PS	021	3.78
1	B	177	LYS	HZ2	C	9	PS	022	1.80
1	B	177	LYS	HZ3	C	5	PC	031	3.44
1	B	177	LYS	HZ3	C	5	PC	032	1.81
1	B	177	LYS	HZ3	C	9	PS	022	3.08
1	B	178	LYS	HZ1	C	1	PC	022	3.88
1	B	178	LYS	HZ1	C	1	PC	032	2.70
1	B	178	LYS	HZ2	C	1	PC	031	3.75
1	B	178	LYS	HZ2	C	1	PC	032	1.69
1	B	178	LYS	HZ2	C	9	PS	011	3.70
1	B	178	LYS	HZ2	C	9	PS	014	3.32
1	B	178	LYS	HZ3	C	1	PC	032	3.35

1	B	178	LYS	HZ3	C	9	PS	012	3.91
1	B	178	LYS	HZ3	C	9	PS	013A	3.46
1	B	178	LYS	HZ3	C	9	PS	013B	3.43
1	B	180	LYS	O	C	9	PS	HAA	3.94
1	B	181	SER	HG	C	6	PC	031	3.23
1	B	181	SER	HG	C	6	PC	032	1.80
1	B	182	LYS	HZ1	C	23	PS	012	3.71
1	B	182	LYS	HZ1	C	23	PS	013	3.71
1	B	182	LYS	HZ1	C	23	PS	013A	3.84
1	B	182	LYS	HZ1	C	23	PS	013B	1.72
1	B	182	LYS	HZ2	C	23	PS	013B	3.18
1	B	182	LYS	HZ3	C	23	PS	013B	2.58
1	B	183	THR	HG1	C	16	PS	013	3.91
1	B	184	LYS	HZ1	C	23	PS	013A	1.71
1	B	184	LYS	HZ1	C	23	PS	013B	2.08
1	B	184	LYS	HZ2	C	23	PS	013A	3.14
1	B	184	LYS	HZ2	C	23	PS	013B	2.89
1	B	184	LYS	HZ3	C	23	PS	013A	2.69
1	B	184	LYS	HZ3	C	23	PS	013B	3.63
2	A	175	LYS	HZ1	C	34	PC	012	3.98
2	A	175	LYS	HZ1	C	34	PC	014	1.81
2	A	175	LYS	HZ2	C	34	PC	014	3.49
2	A	175	LYS	HZ3	C	34	PC	014	3.01
2	A	176	LYS	HZ1	C	51	PC	012	3.92
2	A	176	LYS	HZ1	C	51	PC	014	2.63
2	A	176	LYS	HZ2	C	51	PC	022	3.31
2	A	176	LYS	HZ2	C	51	PC	014	3.43
2	A	176	LYS	HZ3	C	51	PC	022	3.11
2	A	176	LYS	HZ3	C	51	PC	012	3.89
2	A	176	LYS	HZ3	C	51	PC	014	3.10
2	A	176	LYS	HZ3	C	51	PC	021	3.19
2	A	176	LYS	HZ3	C	51	PC	022	1.65
2	A	177	LYS	HN	C	29	PC	013	3.38
2	A	178	LYS	HN	C	23	PS	013A	3.85
2	A	178	LYS	HZ1	C	16	PS	013A	3.53
2	A	178	LYS	HZ1	C	16	PS	013B	1.70
2	A	178	LYS	HZ1	C	23	PS	013B	3.14
2	A	178	LYS	HZ2	C	16	PS	013B	3.37
2	A	178	LYS	HZ2	C	23	PS	013A	3.10
2	A	178	LYS	HZ2	C	23	PS	013B	1.69
2	A	178	LYS	HZ3	C	16	PS	013	3.64
2	A	178	LYS	HZ3	C	16	PS	013B	2.76
2	A	178	LYS	HZ3	C	23	PS	013B	3.25
2	A	178	LYS	HZ3	C	29	PC	014	3.81
2	A	180	LYS	HZ1	C	9	PS	012	3.69
2	A	180	LYS	HZ1	C	9	PS	013A	3.50
2	A	180	LYS	HZ1	C	9	PS	013B	1.76
2	A	180	LYS	HZ1	C	23	PS	013	3.71
2	A	180	LYS	HZ1	C	23	PS	014	3.04
2	A	180	LYS	HZ2	C	9	PS	012	2.73
2	A	180	LYS	HZ2	C	9	PS	013A	3.89
2	A	180	LYS	HZ2	C	9	PS	013B	2.79
2	A	180	LYS	HZ2	C	23	PS	013	3.65
2	A	180	LYS	HZ2	C	23	PS	014	3.84
2	A	180	LYS	HZ3	C	9	PS	012	2.51
2	A	180	LYS	HZ3	C	9	PS	013A	3.08

2	A	180	LYS	HZ3	C	9	PS	013B	2.53
2	A	180	LYS	HZ3	C	9	PS	014	3.55
2	A	181	SER	O	C	6	PC	N	3.90
2	A	181	SER	HN	C	9	PS	012	3.98
2	A	181	SER	HN	C	9	PS	013	2.51
2	A	181	SER	HG	C	16	PS	013A	1.76
2	A	181	SER	HG	C	16	PS	013B	3.19
2	A	182	LYS	HZ1	C	5	PC	012	3.99
2	A	182	LYS	HZ1	C	5	PC	014	1.69
2	A	182	LYS	HZ1	C	5	PC	021	3.64
2	A	182	LYS	HZ1	C	5	PC	022	2.97
2	A	182	LYS	HZ2	C	5	PC	014	3.18
2	A	182	LYS	HZ2	C	5	PC	022	3.04
2	A	182	LYS	HZ3	C	5	PC	014	2.89
2	A	182	LYS	HZ3	C	5	PC	021	3.29
2	A	182	LYS	HZ3	C	5	PC	022	1.65
2	A	183	THR	O	C	1	PC	N	3.98
2	A	183	THR	HN	C	1	PC	022	3.21
2	A	183	THR	HG1	C	1	PC	021	3.56
2	A	183	THR	HG1	C	1	PC	022	1.73
2	A	184	LYS	O	C	1	PC	N	3.53
2	B	184	LYS	HZ1	C	44	PS	013A	1.97
2	B	184	LYS	HZ1	C	44	PS	013B	2.88
2	B	184	LYS	HZ2	C	44	PS	013A	2.39
2	B	184	LYS	HZ2	C	44	PS	013B	1.70
2	B	184	LYS	HZ3	C	44	PS	013A	3.40
2	B	184	LYS	HZ3	C	44	PS	013B	3.26
3	A	178	LYS	HZ1	C	48	PC	011	3.69
3	A	178	LYS	HZ1	C	48	PC	013	1.70
3	A	178	LYS	HZ1	C	48	PC	014	3.24
3	A	178	LYS	HZ2	C	48	PC	013	3.34
3	A	178	LYS	HZ3	C	48	PC	013	3.17
3	A	178	LYS	HZ3	C	48	PC	014	3.61
3	A	184	LYS	O	C	56	PC	N	3.11
3	B	175	LYS	HZ1	C	31	PC	013	3.43
3	B	176	LYS	O	C	31	PC	N	3.65
3	B	178	LYS	HZ1	C	44	PS	022	3.12
3	B	178	LYS	HZ1	C	44	PS	031	3.28
3	B	178	LYS	HZ1	C	44	PS	032	1.77
3	B	178	LYS	HZ1	C	55	PC	014	3.70
3	B	178	LYS	HZ2	C	44	PS	022	3.37
3	B	178	LYS	HZ2	C	44	PS	032	3.41
3	B	178	LYS	HZ2	C	55	PC	011	3.16
3	B	178	LYS	HZ2	C	55	PC	013	3.53
3	B	178	LYS	HZ2	C	55	PC	014	2.05
3	B	178	LYS	HZ3	C	44	PS	021	3.67
3	B	178	LYS	HZ3	C	44	PS	022	1.72
3	B	178	LYS	HZ3	C	44	PS	031	3.62
3	B	178	LYS	HZ3	C	44	PS	032	3.08
3	B	178	LYS	HZ3	C	55	PC	011	3.65
3	B	178	LYS	HZ3	C	55	PC	013	3.47
3	B	178	LYS	HZ3	C	55	PC	014	3.23
3	B	179	LYS	O	C	55	PC	N	3.65
3	B	180	LYS	HZ1	C	78	PC	032	2.65
3	B	180	LYS	HZ2	C	78	PC	031	3.84
3	B	180	LYS	HZ2	C	78	PC	032	1.73

3	B	180	LYS	HZ3	C	78	PC	032	3.23
3	B	182	LYS	HZ1	C	75	PC	032	3.06
3	B	182	LYS	HZ2	C	75	PC	022	3.60
3	B	182	LYS	HZ2	C	75	PC	031	3.49
3	B	182	LYS	HZ2	C	75	PC	032	1.83
3	B	182	LYS	HZ3	C	75	PC	022	3.38
3	B	182	LYS	HZ3	C	75	PC	031	3.77
3	B	182	LYS	HZ3	C	75	PC	032	2.46
4	A	175	LYS	HZ1	C	79	PS	013A	1.66
4	A	175	LYS	HZ1	C	79	PS	013B	2.99
4	A	175	LYS	HZ2	C	79	PS	013A	2.88
4	A	175	LYS	HZ2	C	79	PS	013B	3.02
4	A	175	LYS	HZ3	C	79	PS	013A	3.22
4	A	175	LYS	HZ3	C	79	PS	013B	3.89
4	A	182	LYS	HZ1	C	46	PS	022	3.38
4	A	182	LYS	HZ1	C	46	PS	031	3.32
4	A	182	LYS	HZ1	C	46	PS	032	2.62
4	A	182	LYS	HZ2	C	46	PS	022	3.20
4	A	182	LYS	HZ2	C	46	PS	032	3.04
4	A	182	LYS	HZ3	C	46	PS	021	3.16
4	A	182	LYS	HZ3	C	46	PS	022	1.85
4	A	182	LYS	HZ3	C	46	PS	031	3.18
4	A	182	LYS	HZ3	C	46	PS	032	1.83
4	A	183	THR	HN	C	72	PC	022	3.87
4	A	183	THR	HG1	C	72	PC	022	3.44
4	A	184	LYS	O	C	67	PS	HAA	3.08
4	A	184	LYS	O	C	67	PS	HAC	3.30
4	A	184	LYS	HZ1	C	67	PS	012	3.86
4	A	184	LYS	HZ1	C	67	PS	013	3.75
4	A	184	LYS	HZ1	C	67	PS	013A	3.19
4	A	184	LYS	HZ1	C	67	PS	014	3.24
4	A	184	LYS	HZ2	C	67	PS	012	3.14
4	A	184	LYS	HZ2	C	67	PS	013	3.41
4	A	184	LYS	HZ2	C	67	PS	013A	3.15
4	A	184	LYS	HZ2	C	67	PS	014	1.82
4	A	184	LYS	HZ3	C	67	PS	012	3.11
4	A	184	LYS	HZ3	C	67	PS	013A	1.65
4	A	184	LYS	HZ3	C	67	PS	013B	3.75
4	A	184	LYS	HZ3	C	67	PS	014	3.13
4	B	184	LYS	HZ1	C	23	PS	013A	2.68
4	B	184	LYS	HZ1	C	23	PS	013B	3.34
4	B	184	LYS	HZ1	C	44	PS	013A	2.02
4	B	184	LYS	HZ1	C	44	PS	013B	3.82
4	B	184	LYS	HZ2	C	23	PS	013A	3.47
4	B	184	LYS	HZ2	C	23	PS	013B	3.37
4	B	184	LYS	HZ2	C	44	PS	013A	2.12
4	B	184	LYS	HZ2	C	44	PS	013B	3.06
4	B	184	LYS	HZ3	C	23	PS	013A	1.83
4	B	184	LYS	HZ3	C	23	PS	013B	2.20
4	B	184	LYS	HZ3	C	44	PS	013A	3.28
5	A	176	LYS	O	C	14	PC	N	3.82
5	A	176	LYS	HZ3	C	21	PC	014	3.72
5	A	177	LYS	HZ1	C	9	PS	013A	2.94
5	A	177	LYS	HZ1	C	9	PS	013B	3.17
5	A	177	LYS	HZ1	C	9	PS	022	3.16
5	A	177	LYS	HZ2	C	9	PS	013A	1.78

5	A	177	LYS	HZ2	C	9	PS	013B	2.74
5	A	177	LYS	HZ2	C	9	PS	022	3.98
5	A	177	LYS	HZ3	C	9	PS	012	3.84
5	A	177	LYS	HZ3	C	9	PS	013A	2.43
5	A	177	LYS	HZ3	C	9	PS	013B	1.70
5	A	178	LYS	O	C	9	PS	HAA	3.46
5	A	179	LYS	O	C	9	PS	HAA	3.83
5	A	179	LYS	O	C	9	PS	HAB	3.74
5	A	181	SER	HG	C	23	PS	013A	3.06
5	A	181	SER	HG	C	23	PS	013B	1.83
5	A	183	THR	HG1	C	23	PS	013A	3.29
5	A	183	THR	HG1	C	23	PS	013B	2.68
5	A	184	LYS	HZ3	C	51	PC	012	3.90
5	A	184	LYS	HZ3	C	51	PC	013	3.85
5	B	178	LYS	HZ1	C	17	PS	013A	3.80
5	B	178	LYS	HZ1	C	17	PS	013B	2.64
5	B	178	LYS	HZ2	C	17	PS	013A	2.12
5	B	178	LYS	HZ2	C	17	PS	013B	1.73
5	B	178	LYS	HZ3	C	17	PS	013A	3.41
5	B	178	LYS	HZ3	C	17	PS	013B	3.18
6	A	175	LYS	HZ1	C	79	PS	013A	3.27
6	A	175	LYS	HZ1	C	79	PS	013B	3.15
6	A	175	LYS	HZ2	C	79	PS	013A	1.64
6	A	175	LYS	HZ2	C	79	PS	013B	2.19
6	A	175	LYS	HZ3	C	79	PS	013A	3.12
6	A	175	LYS	HZ3	C	79	PS	013B	3.12
6	A	176	LYS	O	C	34	PC	N	3.89
6	A	177	LYS	HZ1	C	16	PS	013B	3.39
6	A	177	LYS	HZ2	C	16	PS	013B	2.96
6	A	177	LYS	HZ3	C	16	PS	013A	3.52
6	A	177	LYS	HZ3	C	16	PS	013B	1.69
6	A	179	LYS	HZ1	C	16	PS	013A	2.28
6	A	179	LYS	HZ1	C	16	PS	013B	3.69
6	A	179	LYS	HZ2	C	16	PS	013A	3.48
6	A	179	LYS	HZ3	C	16	PS	013A	2.91
6	A	179	LYS	HZ3	C	16	PS	013B	3.59
6	A	181	SER	O	C	30	PC	N	3.96
6	A	181	SER	HG	C	46	PS	013A	3.83
6	A	183	THR	HN	C	46	PS	013B	3.76
6	A	183	THR	HG1	C	46	PS	013A	3.09
6	A	183	THR	HG1	C	46	PS	013B	1.62
6	A	184	LYS	HZ1	C	67	PS	013B	3.00
6	A	184	LYS	HZ2	C	67	PS	012	3.91
6	A	184	LYS	HZ2	C	67	PS	013A	2.54
6	A	184	LYS	HZ2	C	67	PS	013B	1.72
6	A	184	LYS	HZ3	C	67	PS	013A	3.94
6	A	184	LYS	HZ3	C	67	PS	013B	3.02
6	B	184	LYS	HZ1	C	3	PC	022	3.78
6	B	184	LYS	HZ1	C	11	PC	022	2.66
6	B	184	LYS	HZ2	C	3	PC	022	2.70
6	B	184	LYS	HZ2	C	11	PC	022	3.39
6	B	184	LYS	HZ3	C	3	PC	022	3.60
6	B	184	LYS	HZ3	C	11	PC	021	3.81
6	B	184	LYS	HZ3	C	11	PC	022	1.80
7	A	176	LYS	HZ1	C	46	PS	013B	3.57
7	A	176	LYS	HZ2	C	46	PS	013A	3.73

7	A	176	LYS	HZ2	C	46	PS	013B	1.92
7	A	176	LYS	HZ3	C	46	PS	013B	2.88
7	A	182	LYS	HZ2	C	43	PS	013A	3.92
7	A	182	LYS	HZ3	C	43	PS	013A	3.77
7	A	182	LYS	HZ3	C	43	PS	013B	3.74
7	A	183	THR	HG1	C	48	PC	013	3.37
7	B	184	LYS	HZ2	C	9	PS	012	3.94
7	B	184	LYS	HZ2	C	9	PS	014	3.90
7	B	184	LYS	HZ3	C	9	PS	012	3.87
7	B	184	LYS	HZ3	C	9	PS	013B	3.92
8	B	182	LYS	HZ2	C	46	PS	013B	3.79
8	B	184	LYS	HZ1	C	46	PS	013A	2.68
8	B	184	LYS	HZ1	C	46	PS	013B	1.84
8	B	184	LYS	HZ2	C	46	PS	013A	1.79
8	B	184	LYS	HZ2	C	46	PS	013B	2.61
8	B	184	LYS	HZ3	C	46	PS	013A	3.25
8	B	184	LYS	HZ3	C	46	PS	013B	3.33
9	A	175	LYS	HZ3	C	79	PS	013B	3.59
9	A	177	LYS	HZ1	C	16	PS	013B	3.81
9	A	177	LYS	HZ2	C	16	PS	013B	3.52
9	A	178	LYS	O	C	25	PC	N	3.78
9	A	178	LYS	HZ1	C	46	PS	013B	2.69
9	A	178	LYS	HZ2	C	46	PS	013B	3.19
9	A	178	LYS	HZ3	C	46	PS	013A	3.63
9	A	178	LYS	HZ3	C	46	PS	013B	1.68
9	A	179	LYS	HZ1	C	16	PS	013A	2.74
9	A	179	LYS	HZ1	C	16	PS	013B	1.71
9	A	179	LYS	HZ2	C	16	PS	013A	2.77
9	A	179	LYS	HZ2	C	16	PS	013B	2.77
9	A	179	LYS	HZ3	C	16	PS	013A	3.25
9	A	179	LYS	HZ3	C	16	PS	013B	3.24
9	A	181	SER	O	C	30	PC	N	3.63
9	A	182	LYS	HN	C	46	PS	013A	3.09
9	A	183	THR	HN	C	46	PS	013A	3.52
9	A	183	THR	HG1	C	46	PS	013A	1.72
9	A	183	THR	HG1	C	46	PS	013B	3.47
9	A	184	LYS	O	C	67	PS	HAA	3.19
9	A	184	LYS	O	C	67	PS	HAB	2.14
9	A	184	LYS	O	C	67	PS	HAC	2.43
9	B	184	LYS	HZ1	C	23	PS	013A	3.53
9	B	184	LYS	HZ1	C	23	PS	013B	2.75
10	A	175	LYS	HZ1	C	79	PS	013A	2.63
10	A	175	LYS	HZ1	C	79	PS	013B	2.16
10	A	175	LYS	HZ2	C	34	PC	014	3.92
10	A	175	LYS	HZ2	C	79	PS	013A	3.49
10	A	175	LYS	HZ2	C	79	PS	013B	2.40
10	A	175	LYS	HZ3	C	34	PC	014	3.99
10	A	175	LYS	HZ3	C	79	PS	013A	3.30
10	A	175	LYS	HZ3	C	79	PS	013B	3.32
10	A	176	LYS	O	C	34	PC	N	3.29
10	A	177	LYS	HZ1	C	16	PS	013A	1.67
10	A	177	LYS	HZ1	C	16	PS	013B	3.58
10	A	177	LYS	HZ1	C	16	PS	014	3.79
10	A	177	LYS	HZ2	C	16	PS	013A	2.98
10	A	177	LYS	HZ3	C	16	PS	013A	3.32
10	A	177	LYS	HZ3	C	16	PS	014	3.55

10	A	183	THR	HG1	C	46	PS	013A	3.05
10	A	183	THR	HG1	C	46	PS	013B	1.72
10	B	183	THR	O	C	18	PC	013	3.95
10	B	183	THR	O	C	18	PC	014	3.94
10	B	184	LYS	HZ1	C	33	PC	014	3.22
10	B	184	LYS	HZ2	C	33	PC	011	3.93
10	B	184	LYS	HZ2	C	33	PC	012	3.50
10	B	184	LYS	HZ2	C	33	PC	014	1.75
10	B	184	LYS	HZ3	C	33	PC	011	3.77
10	B	184	LYS	HZ3	C	33	PC	012	3.45
10	B	184	LYS	HZ3	C	33	PC	014	2.61
11	A	177	LYS	HZ2	C	46	PS	013A	3.95
11	A	178	LYS	HZ3	C	46	PS	013A	3.99
11	A	179	LYS	HZ1	C	50	PC	013	3.46
11	A	179	LYS	HZ2	C	50	PC	011	3.04
11	A	179	LYS	HZ2	C	50	PC	013	1.78
11	A	179	LYS	HZ2	C	50	PC	014	3.86
11	A	179	LYS	HZ3	C	50	PC	013	3.10
11	A	180	LYS	HN	C	77	PC	031	3.89
11	A	181	SER	HG	C	79	PS	012	2.81
11	A	181	SER	HG	C	79	PS	013A	1.77
11	A	181	SER	HG	C	79	PS	013B	3.99
11	A	182	LYS	HZ3	C	77	PC	013	3.92
11	A	184	LYS	HZ1	C	79	PS	013A	3.95
11	A	184	LYS	HZ1	C	79	PS	013B	3.13
11	A	184	LYS	HZ2	C	79	PS	013	3.37
11	A	184	LYS	HZ2	C	79	PS	013A	3.90
11	A	184	LYS	HZ2	C	79	PS	013B	3.07
11	A	184	LYS	HZ2	C	79	PS	014	3.94
11	A	184	LYS	HZ3	C	79	PS	012	3.98
11	A	184	LYS	HZ3	C	79	PS	013	3.64
11	A	184	LYS	HZ3	C	79	PS	013A	2.47
11	A	184	LYS	HZ3	C	79	PS	013B	1.67
11	B	182	LYS	HZ1	C	9	PS	013B	2.93
11	B	183	THR	O	C	23	PS	HAA	3.12
11	B	183	THR	O	C	23	PS	HAB	2.07
11	B	183	THR	O	C	23	PS	HAC	3.80
11	B	183	THR	HN	C	23	PS	012	3.35
11	B	183	THR	HG1	C	23	PS	011	3.66
11	B	183	THR	HG1	C	23	PS	012	3.42
11	B	183	THR	HG1	C	23	PS	014	3.47
11	B	184	LYS	HZ1	C	23	PS	013A	3.51
11	B	184	LYS	HZ1	C	23	PS	013B	3.50
11	B	184	LYS	HZ2	C	23	PS	013A	3.31
11	B	184	LYS	HZ2	C	23	PS	013B	2.28
11	B	184	LYS	HZ3	C	23	PS	013A	1.86
11	B	184	LYS	HZ3	C	23	PS	013B	2.16
12	A	178	LYS	HZ1	C	46	PS	013A	3.70
12	A	178	LYS	HZ1	C	46	PS	013B	1.78
12	A	178	LYS	HZ2	C	46	PS	013A	3.91
12	A	178	LYS	HZ2	C	46	PS	013B	2.84
12	A	178	LYS	HZ3	C	46	PS	013B	3.45
12	A	181	SER	O	C	30	PC	N	4.00
12	A	183	THR	HG1	C	30	PC	012	3.69
12	A	183	THR	HG1	C	30	PC	013	3.02
12	A	183	THR	HG1	C	30	PC	014	3.76

12	A	184	LYS	O	C	47	PC	N	3.04
12	B	180	LYS	HZ1	C	24	PS	013A	3.22
12	B	180	LYS	HZ1	C	24	PS	013B	1.68
12	B	180	LYS	HZ1	C	27	PC	012	3.13
12	B	180	LYS	HZ2	C	24	PS	013B	2.95
12	B	180	LYS	HZ3	C	24	PS	013B	3.22
12	B	180	LYS	HZ3	C	27	PC	012	2.84
12	B	180	LYS	HZ3	C	27	PC	013	3.78
12	B	183	THR	HN	C	21	PC	012	3.68
12	B	184	LYS	O	C	14	PC	N	3.79
13	A	175	LYS	HZ1	C	45	PS	012	3.18
13	A	175	LYS	HZ1	C	45	PS	013	3.83
13	A	175	LYS	HZ1	C	45	PS	013A	3.13
13	A	175	LYS	HZ1	C	45	PS	013B	1.70
13	A	175	LYS	HZ2	C	45	PS	012	2.72
13	A	175	LYS	HZ2	C	45	PS	013	2.38
13	A	175	LYS	HZ2	C	45	PS	013B	3.03
13	A	175	LYS	HZ2	C	45	PS	014	3.52
13	A	175	LYS	HZ3	C	28	PC	011	3.18
13	A	175	LYS	HZ3	C	45	PS	013A	3.98
13	A	175	LYS	HZ3	C	45	PS	013B	3.28
13	A	176	LYS	HN	C	24	PS	014	3.33
13	A	176	LYS	HZ1	C	12	PC	014	3.23
13	A	176	LYS	HZ1	C	17	PS	013A	3.83
13	A	176	LYS	HZ1	C	17	PS	013B	3.61
13	A	176	LYS	HZ1	C	17	PS	021	3.25
13	A	176	LYS	HZ1	C	17	PS	022	1.70
13	A	176	LYS	HZ2	C	12	PC	014	3.93
13	A	176	LYS	HZ2	C	17	PS	013A	3.65
13	A	176	LYS	HZ2	C	17	PS	022	2.81
13	A	176	LYS	HZ3	C	17	PS	013A	3.98
13	A	176	LYS	HZ3	C	17	PS	013B	3.61
13	A	176	LYS	HZ3	C	17	PS	022	3.32
13	A	178	LYS	HZ1	C	24	PS	013A	2.75
13	A	178	LYS	HZ1	C	24	PS	013B	1.90
13	A	178	LYS	HZ2	C	24	PS	013B	2.34
13	A	178	LYS	HZ3	C	24	PS	013B	3.33
13	A	181	SER	HG	C	27	PC	011	3.92
13	A	183	THR	HG1	C	41	PC	013	3.83
13	A	184	LYS	O	C	74	PC	N	3.12
14	A	176	LYS	O	C	50	PC	N	3.72
14	A	176	LYS	HN	C	50	PC	013	3.82
14	A	177	LYS	O	C	25	PC	N	3.77
14	A	178	LYS	HZ1	C	46	PS	012	3.79
14	A	178	LYS	HZ1	C	46	PS	013B	3.25
14	A	178	LYS	HZ1	C	46	PS	014	3.98
14	A	178	LYS	HZ2	C	46	PS	012	3.78
14	A	178	LYS	HZ2	C	46	PS	013B	2.82
14	A	178	LYS	HZ2	C	46	PS	014	3.24
14	A	178	LYS	HZ3	C	46	PS	013A	3.01
14	A	178	LYS	HZ3	C	46	PS	013B	1.71
14	A	179	LYS	HZ2	C	16	PS	013B	3.63
14	A	180	LYS	HZ1	C	13	PC	014	3.82
14	A	180	LYS	HZ2	C	13	PC	014	3.77
14	A	180	LYS	HZ3	C	13	PC	013	3.97
14	A	181	SER	O	C	30	PC	N	3.49

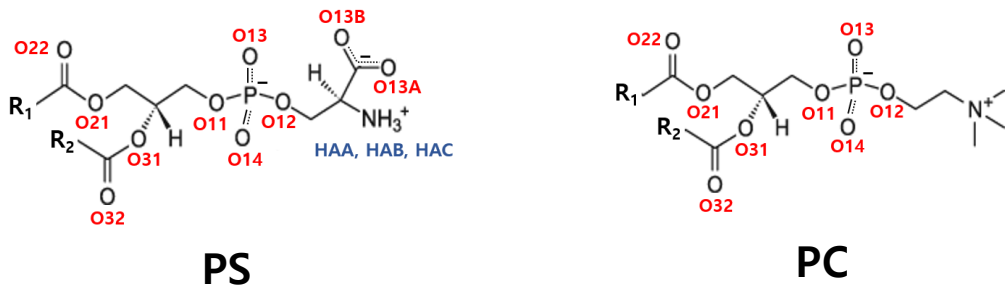
14	A	184	LYS	HZ1	C	67	PS	O13A	3.33
14	A	184	LYS	HZ2	C	67	PS	O12	3.78
14	A	184	LYS	HZ2	C	67	PS	O13A	1.64
14	A	184	LYS	HZ2	C	67	PS	O13B	2.98
14	A	184	LYS	HZ3	C	67	PS	O13A	2.98
14	A	184	LYS	HZ3	C	67	PS	O13B	3.20
14	B	184	LYS	O	C	44	PS	HAA	3.50
14	B	184	LYS	O	C	44	PS	HAB	3.34
14	B	184	LYS	O	C	44	PS	HAC	2.02
14	B	184	LYS	HN	C	44	PS	O13A	3.39
15	A	176	LYS	O	C	50	PC	N	3.70
15	A	177	LYS	O	C	25	PC	N	3.93
15	A	177	LYS	HZ2	C	16	PS	O13B	3.15
15	A	178	LYS	O	C	25	PC	N	3.24
15	A	178	LYS	HZ1	C	46	PS	O13B	2.91
15	A	178	LYS	HZ2	C	46	PS	O13B	2.98
15	A	178	LYS	HZ3	C	46	PS	O13A	3.76
15	A	178	LYS	HZ3	C	46	PS	O13B	1.75
15	A	179	LYS	HZ1	C	16	PS	O13A	3.44
15	A	179	LYS	HZ1	C	16	PS	O13B	3.27
15	A	179	LYS	HZ2	C	16	PS	O13A	2.58
15	A	179	LYS	HZ2	C	16	PS	O13B	1.76
15	A	179	LYS	HZ3	C	16	PS	O13A	1.85
15	A	179	LYS	HZ3	C	16	PS	O13B	2.61
15	A	184	LYS	O	C	47	PC	N	3.29
15	B	184	LYS	HZ2	C	23	PS	O13B	3.74
16	A	175	LYS	HZ1	C	47	PC	O14	3.29
16	A	175	LYS	HZ1	C	67	PS	O13A	2.82
16	A	175	LYS	HZ1	C	67	PS	O13B	2.87
16	A	175	LYS	HZ2	C	67	PS	O13A	1.96
16	A	175	LYS	HZ2	C	67	PS	O13B	1.78
16	A	175	LYS	HZ3	C	67	PS	O13A	3.56
16	A	175	LYS	HZ3	C	67	PS	O13B	2.60
16	A	176	LYS	O	C	47	PC	N	3.52
16	A	176	LYS	HZ1	C	46	PS	O13A	3.20
16	A	176	LYS	HZ1	C	46	PS	O13B	2.67
16	A	176	LYS	HZ2	C	46	PS	O13A	2.52
16	A	176	LYS	HZ2	C	46	PS	O13B	1.68
16	A	176	LYS	HZ3	C	46	PS	O13A	2.25
16	A	176	LYS	HZ3	C	46	PS	O13B	2.85
16	A	178	LYS	HZ1	C	26	PC	O13	4.00
16	A	178	LYS	HZ1	C	48	PC	O11	3.85
16	A	178	LYS	HZ1	C	48	PC	O13	3.05
16	A	178	LYS	HZ1	C	48	PC	O14	1.88
16	A	178	LYS	HZ2	C	48	PC	O14	3.52
16	A	178	LYS	HZ3	C	48	PC	O13	2.88
16	A	178	LYS	HZ3	C	48	PC	O14	3.15
16	A	183	THR	O	C	56	PC	N	3.28
16	A	184	LYS	O	C	56	PC	N	3.97
17	A	175	LYS	HZ1	C	50	PC	O12	3.95
17	A	175	LYS	HZ1	C	50	PC	O13	1.76
17	A	175	LYS	HZ2	C	50	PC	O13	2.89
17	A	175	LYS	HZ3	C	50	PC	O13	2.84
17	A	176	LYS	HN	C	34	PC	O14	2.85
17	A	177	LYS	O	C	25	PC	N	3.30
17	A	177	LYS	HZ1	C	16	PS	O13	3.52

17	A	177	LYS	HZ1	C	16	PS	014	1.78
17	A	177	LYS	HZ2	C	16	PS	013	3.65
17	A	177	LYS	HZ2	C	16	PS	014	2.88
17	A	177	LYS	HZ3	C	16	PS	014	3.45
17	A	177	LYS	HZ3	C	29	PC	014	3.67
17	A	184	LYS	O	C	47	PC	N	3.42
17	B	182	LYS	HZ3	C	23	PS	014	3.31
18	A	178	LYS	HZ1	C	46	PS	013B	2.36
18	A	178	LYS	HZ2	C	46	PS	013A	3.80
18	A	178	LYS	HZ2	C	46	PS	013B	1.91
18	A	178	LYS	HZ3	C	46	PS	013B	3.26
18	A	179	LYS	HZ1	C	16	PS	013B	3.06
18	A	179	LYS	HZ2	C	16	PS	013B	2.83
18	A	179	LYS	HZ3	C	16	PS	013A	3.74
18	A	179	LYS	HZ3	C	16	PS	013B	1.74
18	A	184	LYS	O	C	47	PC	N	3.46
18	B	184	LYS	HZ1	C	44	PS	013A	3.44
18	B	184	LYS	HZ1	C	44	PS	013B	2.75
18	B	184	LYS	HZ2	C	44	PS	013A	1.78
18	B	184	LYS	HZ2	C	44	PS	013B	1.85
18	B	184	LYS	HZ3	C	44	PS	013A	2.97
18	B	184	LYS	HZ3	C	44	PS	013B	3.46
19	A	175	LYS	HZ2	C	66	PS	013	2.97
19	A	176	LYS	HZ1	C	49	PC	014	2.51
19	A	176	LYS	HZ1	C	66	PS	011	3.74
19	A	176	LYS	HZ1	C	66	PS	014	3.97
19	A	176	LYS	HZ2	C	49	PC	011	3.42
19	A	176	LYS	HZ2	C	49	PC	013	3.32
19	A	176	LYS	HZ2	C	49	PC	014	1.95
19	A	176	LYS	HZ3	C	49	PC	014	3.47
19	A	178	LYS	HZ1	C	51	PC	013	3.96
19	A	179	LYS	HZ1	C	9	PS	013A	1.73
19	A	179	LYS	HZ1	C	9	PS	013B	3.91
19	A	179	LYS	HZ1	C	23	PS	012	3.92
19	A	179	LYS	HZ2	C	9	PS	013A	3.41
19	A	179	LYS	HZ2	C	23	PS	012	3.43
19	A	179	LYS	HZ2	C	23	PS	013B	3.89
19	A	179	LYS	HZ3	C	9	PS	013A	3.07
19	A	179	LYS	HZ3	C	23	PS	013B	3.44
19	A	184	LYS	HZ1	C	25	PC	013	3.31
19	A	184	LYS	HZ1	C	46	PS	013B	2.86
19	A	184	LYS	HZ2	C	25	PC	013	2.40
19	A	184	LYS	HZ2	C	25	PC	014	3.74
19	A	184	LYS	HZ2	C	46	PS	013A	3.74
19	A	184	LYS	HZ2	C	46	PS	013B	1.71
19	A	184	LYS	HZ3	C	25	PC	012	3.85
19	A	184	LYS	HZ3	C	25	PC	013	1.83
19	A	184	LYS	HZ3	C	46	PS	013B	2.93
20	A	175	LYS	HZ1	C	79	PS	013A	3.42
20	A	175	LYS	HZ1	C	79	PS	013B	3.81
20	A	175	LYS	HZ2	C	79	PS	013A	2.94
20	A	175	LYS	HZ2	C	79	PS	013B	3.68
20	A	175	LYS	HZ3	C	79	PS	013A	1.74
20	A	175	LYS	HZ3	C	79	PS	013B	2.69
20	A	176	LYS	O	C	50	PC	N	3.97
20	A	176	LYS	HZ2	C	51	PC	014	3.46

20	A	177	LYS	O	C	50	PC	N	3.98
20	A	179	LYS	HZ1	C	16	PS	O13A	3.22
20	A	179	LYS	HZ1	C	16	PS	O13B	3.43
20	A	179	LYS	HZ2	C	16	PS	O13A	3.65
20	A	179	LYS	HZ2	C	16	PS	O13B	2.88
20	A	179	LYS	HZ3	C	16	PS	O13A	2.00
20	A	179	LYS	HZ3	C	16	PS	O13B	1.79
20	A	181	SER	O	C	30	PC	N	3.86
20	A	182	LYS	HN	C	46	PS	O13A	3.62
20	A	182	LYS	HN	C	46	PS	O13B	3.77
20	A	183	THR	HN	C	46	PS	O13A	3.62
20	A	183	THR	HG1	C	46	PS	O13A	1.72
20	A	183	THR	HG1	C	46	PS	O13B	3.01
20	A	184	LYS	O	C	67	PS	HAA	3.11
20	A	184	LYS	O	C	67	PS	HAB	2.06
20	A	184	LYS	O	C	67	PS	HAC	2.22
20	A	184	LYS	HZ2	C	69	PC	O13	3.95

# Chains A and B are the protomers in the KRAS homodimer. One of the protomers is more intimately associated with the membrane surface by the disordered C-terminal polybasic region (K175-K184).

ε Lipid head group atoms involved in binding to the KRAS protomers are indicated on the chemical structures of phosphatidylserine (PS) and phosphatidylcholine (PC) below.



\* Cutoff distance to define an electrostatic interaction is 4.0 Å.

**Table S4.** Intermolecular interactions within the dimer interface of the 20 lowest HADDOCK-score structures of both the  $\alpha$ - $\alpha$  and  $\alpha$ - $\beta$  dimers of KRAS-G12D on the membrane.

<b><math>\alpha</math>-<math>\alpha</math> Dimer Model of KRAS-G12D</b>											
Model	Chain	Residue Number	Residue Name	Atom Name	Chain	Residue Number	Residue Name	Atom Name	Distance* (Å)	Ion Pair*	
1	A	47	ASP	OD1	B	132	ASP	HN	2.44		
	A	131	GLN	OE1	B	161	ARG	HH21	1.91		
	A	131	GLN	HE22	B	154	ASP	OD1	1.73		
	A	135	ARG	HH12	B	168	GLU	OE1	1.65	O	
	A	154	ASP	OD1	B	131	GLN	HE22	1.70		
	A	161	ARG	HH12	B	131	GLN	OE1	2.08		
	A	164	ARG	HH12	B	132	ASP	OD1	2.03	O	
	A	168	GLU	OE1	B	135	ARG	HH12	1.77	O	
	A	176	LYS	O	B	178	LYS	HZ3	1.74		
2	A	131	GLN	OE1	B	161	ARG	HH12	2.25		
	A	131	GLN	HE22	B	154	ASP	OD1	2.04		
	A	135	ARG	HH12	B	168	GLU	OE1	1.91	O	
	A	154	ASP	OD1	B	131	GLN	HE22	1.68		
	A	161	ARG	HH12	B	131	GLN	OE1	2.04		
	A	161	ARG	HH21	B	131	GLN	OE1	2.03		
	A	168	GLU	OE1	B	135	ARG	HH12	1.80	O	
	A	180	LYS	HZ1	B	107	GLU	OE1	1.63	O	
	A	180	LYS	HZ2	B	106	SER	O	2.01		
3	A	131	GLN	OE1	B	161	ARG	HH12	2.23		
	A	131	GLN	OE1	B	161	ARG	HH21	2.25		
	A	131	GLN	HE22	B	154	ASP	OD1	1.69		
	A	132	ASP	OD2	B	164	ARG	HH12	2.09	O	
	A	135	ARG	HH12	B	168	GLU	OE1	1.61	O	
	A	136	SER	HG	B	168	GLU	OE2	2.05		
	A	154	ASP	OD1	B	131	GLN	HE22	2.08		
	A	161	ARG	HH21	B	131	GLN	OE1	2.19		
	A	168	GLU	OE1	B	135	ARG	HH12	1.87	O	
4	A	131	GLN	OE1	B	161	ARG	HH21	1.75		
	A	131	GLN	HE22	B	154	ASP	OD1	1.76		
	A	135	ARG	HH12	B	168	GLU	OE1	1.87	O	
	A	154	ASP	OD1	B	131	GLN	HE22	2.34		
	A	154	ASP	OD2	B	131	GLN	HE22	2.21		
	A	161	ARG	HH12	B	127	THR	O	2.03		
	A	161	ARG	HH21	B	131	GLN	OE1	2.20		
	A	168	GLU	OE1	B	135	ARG	HH12	1.77	O	
	A	174	GLY	O	B	182	LYS	HZ3	1.79		
5	A	131	GLN	OE1	B	161	ARG	HH12	1.73		

	A	131	GLN	HE22	B	154	ASP	OD1	2.02	
	A	135	ARG	HH12	B	168	GLU	OE2	1.69	O
	A	154	ASP	OD1	B	131	GLN	HE22	2.23	
	A	161	ARG	HH12	B	131	GLN	OE1	2.16	
	A	161	ARG	HH21	B	131	GLN	OE1	2.47	
	A	168	GLU	OE1	B	135	ARG	HH12	1.70	O
	A	177	LYS	HZ3	B	107	GLU	OE1	1.62	
6	A	131	GLN	OE1	B	161	ARG	HH12	2.17	
	A	131	GLN	OE1	B	161	ARG	HH21	2.18	
	A	131	GLN	HE22	B	154	ASP	OD1	1.97	
	A	131	GLN	HE22	B	154	ASP	OD2	2.48	
	A	135	ARG	HH12	B	168	GLU	OE1	1.66	O
	A	154	ASP	OD1	B	131	GLN	HE22	1.74	
	A	161	ARG	HH12	B	131	GLN	OE1	2.07	
	A	168	GLU	OE1	B	135	ARG	HH12	1.87	O
	A	180	LYS	HZ2	B	107	GLU	OE1	1.83	
	A	180	LYS	HZ2	B	107	GLU	OE2	1.98	
7	A	131	GLN	OE1	B	161	ARG	HH21	2.23	
	A	131	GLN	HE22	B	154	ASP	OD1	2.11	
	A	135	ARG	HH12	B	168	GLU	OE2	1.64	O
	A	154	ASP	OD1	B	131	GLN	HE22	1.69	
	A	161	ARG	HH21	B	131	GLN	OE1	1.81	
	A	168	GLU	OE1	B	135	ARG	HH12	2.12	O
	A	168	GLU	OE2	B	135	ARG	HH11	2.10	O
8	A	131	GLN	OE1	B	161	ARG	HH12	2.09	
	A	131	GLN	HE22	B	154	ASP	OD1	1.85	
	A	135	ARG	HH12	B	168	GLU	OE2	1.67	O
	A	154	ASP	OD1	B	131	GLN	HE22	1.77	
	A	161	ARG	HH21	B	131	GLN	OE1	2.05	
	A	164	ARG	HH12	B	132	ASP	OD1	2.38	O
	A	168	GLU	OE1	B	135	ARG	HH12	2.09	
	A	168	GLU	OE2	B	135	ARG	HH11	2.03	O
	A	175	LYS	HZ3	B	107	GLU	OE2	1.61	
9	A	131	GLN	OE1	B	161	ARG	HH21	1.77	
	A	131	GLN	HE22	B	154	ASP	OD1	1.74	
	A	135	ARG	HH11	B	168	GLU	OE2	2.33	O
	A	135	ARG	HH12	B	168	GLU	OE1	1.82	O
	A	135	ARG	HH12	B	168	GLU	OE2	2.49	O
	A	154	ASP	OD1	B	131	GLN	HE22	1.72	
	A	161	ARG	HH21	B	131	GLN	OE1	1.79	
	A	168	GLU	OE2	B	135	ARG	HH12	1.78	O
	A	178	LYS	HZ3	B	107	GLU	OE1	1.65	O
	A	182	LYS	HZ2	B	105	ASP	O	2.24	
	A	182	LYS	HZ3	B	105	ASP	OD1	1.76	O

	A	183	THR	HG1	B	105	ASP	OD2	1.63	
10	A	131	GLN	OE1	B	161	ARG	HH12	1.91	
	A	131	GLN	HE22	B	154	ASP	OD1	1.67	
	A	135	ARG	HH12	B	168	GLU	OE1	1.74	O
	A	135	ARG	HH12	B	168	GLU	OE2	2.13	O
	A	154	ASP	OD1	B	131	GLN	HE22	1.68	
	A	161	ARG	HH12	B	131	GLN	OE1	1.87	
	A	168	GLU	OE1	B	135	ARG	HH12	1.76	O
11	A	131	GLN	OE1	B	161	ARG	HH12	1.97	
	A	131	GLN	HE22	B	154	ASP	OD1	2.31	
	A	131	GLN	HE22	B	154	ASP	OD2	2.25	
	A	135	ARG	HH12	B	168	GLU	OE1	2.01	O
	A	154	ASP	OD1	B	131	GLN	HE22	1.80	
	A	161	ARG	HH21	B	131	GLN	OE1	2.32	
	A	168	GLU	OE1	B	135	ARG	HH12	1.74	O
12	A	131	GLN	OE1	B	161	ARG	HH12	2.14	
	A	131	GLN	OE1	B	161	ARG	HH21	2.01	
	A	131	GLN	HE22	B	154	ASP	OD1	1.78	
	A	132	ASP	OD2	B	164	ARG	HH12	2.29	O
	A	135	ARG	HH12	B	168	GLU	OE1	1.65	O
	A	136	SER	HG	B	168	GLU	OE2	1.74	O
	A	154	ASP	OD1	B	131	GLN	HE22	1.64	
	A	161	ARG	HH12	B	131	GLN	OE1	2.48	
	A	161	ARG	HH21	B	131	GLN	OE1	1.80	
	A	168	GLU	OE2	B	135	ARG	HH12	1.74	O
13	A	131	GLN	OE1	B	161	ARG	HH12	2.10	
	A	131	GLN	HE22	B	154	ASP	OD1	2.04	
	A	135	ARG	HH12	B	168	GLU	OE2	1.66	O
	A	154	ASP	OD1	B	131	GLN	HE22	1.92	
	A	161	ARG	HH12	B	131	GLN	OE1	2.06	
	A	168	GLU	OE1	B	135	ARG	HH12	1.73	O
	A	173	ASP	OD2	B	177	LYS	HZ2	2.05	O
14	A	131	GLN	OE1	B	161	ARG	HH12	2.10	
	A	131	GLN	HE22	B	154	ASP	OD1	1.70	
	A	135	ARG	HH12	B	168	GLU	OE1	1.96	O
	A	136	SER	HG	B	168	GLU	OE1	2.03	
	A	136	SER	HG	B	168	GLU	OE2	2.18	
	A	154	ASP	OD1	B	131	GLN	HE22	1.70	
	A	161	ARG	HH12	B	131	GLN	OE1	2.42	
	A	161	ARG	HH21	B	131	GLN	OE1	1.83	
	A	164	ARG	HH12	B	132	ASP	OD2	1.93	O
	A	168	GLU	OE1	B	135	ARG	HH12	1.61	O
	A	182	LYS	HZ2	B	105	ASP	OD1	1.69	O
15	A	105	ASP	OD1	B	179	LYS	HZ3	1.61	O

15	A	105	ASP	OD2	B	178	LYS	HZ1	1.61	O
	A	131	GLN	OE1	B	161	ARG	HH12	2.08	
	A	131	GLN	OE1	B	161	ARG	HH21	1.97	
	A	131	GLN	HE22	B	154	ASP	OD1	1.81	
	A	132	ASP	OD2	B	164	ARG	HH12	2.07	O
	A	135	ARG	HH12	B	168	GLU	OE2	1.74	O
	A	136	SER	HG	B	168	GLU	OE2	1.69	O
	A	154	ASP	OD1	B	131	GLN	HE22	1.83	
	A	161	ARG	HH12	B	131	GLN	OE1	1.95	
	A	168	GLU	OE1	B	135	ARG	HH12	2.07	O
	A	168	GLU	OE2	B	135	ARG	HH11	2.38	O
16	A	107	GLU	OE1	B	177	LYS	HZ1	1.62	O
	A	131	GLN	OE1	B	161	ARG	HH12	2.23	
	A	131	GLN	OE1	B	161	ARG	HH21	2.34	
	A	131	GLN	HE22	B	154	ASP	OD1	1.79	
	A	135	ARG	HH12	B	168	GLU	OE1	1.63	O
	A	154	ASP	OD1	B	131	GLN	HE22	1.83	
	A	161	ARG	HH21	B	131	GLN	OE1	1.69	
	A	168	GLU	OE1	B	135	ARG	HH12	1.67	O
17	A	47	ASP	OD2	B	132	ASP	HN	2.32	
	A	131	GLN	OE1	B	161	ARG	HH12	2.09	
	A	131	GLN	HE22	B	154	ASP	OD1	2.06	
	A	135	ARG	HH12	B	168	GLU	OE1	1.61	O
	A	154	ASP	OD1	B	131	GLN	HE22	1.71	
	A	161	ARG	HH12	B	131	GLN	OE1	2.00	
	A	161	ARG	HH21	B	131	GLN	OE1	2.20	
	A	168	GLU	OE1	B	135	ARG	HH12	1.62	O
	A	168	GLU	OE1	B	136	SER	HG	2.25	O
	A	168	GLU	OE2	B	136	SER	HG	1.97	
18	A	182	LYS	HZ2	B	107	GLU	OE2	1.66	O
	A	105	ASP	OD2	B	182	LYS	HN	1.96	
	A	128	LYS	HZ3	B	47	ASP	O	1.77	
	A	131	GLN	OE1	B	161	ARG	HH12	2.26	
	A	131	GLN	OE1	B	161	ARG	HH21	1.93	
	A	131	GLN	HE22	B	154	ASP	OD1	1.95	
	A	135	ARG	HH12	B	168	GLU	OE1	1.72	O
	A	154	ASP	OD1	B	131	GLN	HE22	1.97	
	A	161	ARG	HH12	B	131	GLN	OE1	1.90	
19	A	168	GLU	OE1	B	135	ARG	HH12	1.90	O
	A	107	GLU	OE1	B	178	LYS	HZ3	1.64	O
	A	131	GLN	OE1	B	161	ARG	HH12	1.94	
	A	131	GLN	OE1	B	161	ARG	HH21	2.44	
	A	131	GLN	HE22	B	154	ASP	OD1	1.71	

20	A	136	SER	OG	B	172	LYS	HZ2	2.23	
	A	154	ASP	OD1	B	131	GLN	HE22	1.65	
	A	161	ARG	HH12	B	131	GLN	OE1	2.05	
	A	161	ARG	HH21	B	131	GLN	OE1	2.26	
	A	168	GLU	OE1	B	135	ARG	HH12	1.77	O
	A	179	LYS	HZ3	B	98	GLU	OE2	1.64	O
	A	131	GLN	OE1	B	161	ARG	HH12	1.93	
	A	131	GLN	OE1	B	161	ARG	HH21	2.27	
	A	131	GLN	HE22	B	154	ASP	OD1	1.81	
	A	135	ARG	HH12	B	168	GLU	OE1	1.81	O
	A	154	ASP	OD1	B	131	GLN	HE22	1.74	
	A	161	ARG	HH12	B	131	GLN	OE1	2.09	
	A	168	GLU	OE1	B	135	ARG	HH12	1.74	O

### $\alpha$ - $\beta$ Dimer Model of KRAS-G12D

Model	Chain	Residue Number	Residue Name	Atom Name	Chain	Residue Number	Residue Name	Atom Name	Distance* (Å)	Ion Pair*
1	A	25	GLN	OE1	B	143	GLU	HN	1.83	
	A	27	HIS	HE2	B	143	GLU	O	2.30	
	A	33	ASP	OD1	B	128	LYS	HZ3	1.68	O
	A	33	ASP	OD1	B	135	ARG	HH11	1.84	O
	A	33	ASP	OD1	B	135	ARG	HH21	2.42	O
	A	33	ASP	OD2	B	135	ARG	HH21	1.75	O
	A	38	ASP	OD1	B	135	ARG	HE	1.72	O
	A	38	ASP	OD2	B	135	ARG	HH22	1.58	O
2	A	3	GLU	OE1	B	182	LYS	HZ3	1.62	O
	A	33	ASP	OD2	B	128	LYS	HZ3	1.60	O
	A	34	PRO	O	B	128	LYS	HZ1	2.49	
	A	38	ASP	OD2	B	135	ARG	HE	1.85	O
	A	38	ASP	OD2	B	135	ARG	HH22	2.00	O
	A	40	TYR	OH	B	131	GLN	HE21	1.90	
3	A	25	GLN	HE2	B	127	THR	OG1	1.83	
	A	27	HIS	HE2	B	143	GLU	OE2	1.76	
	A	33	ASP	OD2	B	128	LYS	HZ3	1.60	O
	A	38	ASP	OD1	B	135	ARG	HE	2.16	O
	A	38	ASP	OD2	B	135	ARG	HH22	1.60	O
	A	41	ARG	HE	B	154	ASP	OD1	1.70	O
	A	41	ARG	HH2	B	158	THR	OG1	1.90	
4	A	33	ASP	OD2	B	128	LYS	HZ3	1.61	O
	A	38	ASP	OD2	B	135	ARG	HE	2.30	O
	A	38	ASP	OD2	B	135	ARG	HH22	1.64	O
	A	43	GLN	HN	B	154	ASP	OD1	2.02	
5	A	3	GLU	OE1	B	165	LYS	HZ3	1.63	O
	A	25	GLN	HE2	B	143	GLU	OE1	2.25	
	A	33	ASP	OD2	B	128	LYS	HZ3	1.58	O

	A	38	ASP	OD1	B	135	ARG	HH22	1.63	O
	A	38	ASP	OD2	B	135	ARG	HE	1.97	O
	A	41	ARG	HH2	B	162	GLU	OE2	1.58	O
	A	43	GLN	HN	B	154	ASP	OD2	1.69	
	A	105	ASP	O	B	184	LYS	HZ2	2.10	
	A	106	SER	OG	B	184	LYS	HZ1	1.74	
6	A	27	HIS	HE2	B	143	GLU	OE2	1.95	
	A	31	GLU	OE2	B	128	LYS	HZ2	1.74	O
	A	33	ASP	OD2	B	128	LYS	HZ3	1.63	O
	A	37	GLU	O	B	135	ARG	HE	2.40	O
	A	38	ASP	OD2	B	135	ARG	HH22	1.72	O
7	A	25	GLN	OE1	B	131	GLN	HE21	1.95	
	A	25	GLN	HE2	B	141	PHE	O	2.27	
	A	25	GLN	O	B	150	GLN	HE22	2.23	
	A	27	HIS	HE2	B	143	GLU	OE2	1.83	
	A	33	ASP	OD2	B	128	LYS	HZ3	1.65	O
	A	38	ASP	OD1	B	135	ARG	HE	1.76	O
	A	38	ASP	OD2	B	135	ARG	HH22	1.63	O
	A	43	GLN	HN	B	154	ASP	OD2	1.89	
	A	43	GLN	OE1	B	161	ARG	HH12	1.96	
8	A	25	GLN	HE2	B	141	PHE	O	2.47	
	A	33	ASP	OD1	B	128	LYS	HZ2	1.62	O
	A	33	ASP	OD1	B	135	ARG	HH21	2.19	O
	A	38	ASP	OD2	B	135	ARG	HE	1.77	O
	A	38	ASP	OD2	B	135	ARG	HH22	2.04	O
	A	40	TYR	OH	B	131	GLN	HE21	1.88	
	A	41	ARG	HE	B	162	GLU	OE2	1.94	O
	A	41	ARG	HH2	B	162	GLU	OE1	1.67	O
	A	41	ARG	HH2	B	138	GLY	O	2.01	
	A	41	ARG	O	B	161	ARG	HH22	2.34	
	A	43	GLN	HN	B	154	ASP	OD1	1.89	
	A	43	GLN	OE1	B	161	ARG	HH11	2.00	
9	A	43	GLN	HE2	B	47	ASP	OD2	1.74	
	A	33	ASP	OD1	B	128	LYS	HZ3	1.62	O
	A	33	ASP	OD2	B	135	ARG	HH11	1.55	O
	A	38	ASP	OD1	B	135	ARG	HE	1.83	O
10	A	38	ASP	OD2	B	135	ARG	HH22	1.70	O
	A	25	GLN	OE1	B	131	GLN	HE21	2.14	
	A	27	HIS	HE2	B	143	GLU	OE1	2.34	
	A	27	HIS	HE2	B	143	GLU	OE2	2.08	
	A	33	ASP	OD2	B	128	LYS	HZ2	1.56	O
	A	38	ASP	OD2	B	135	ARG	HE	2.10	O
	A	38	ASP	OD2	B	135	ARG	HH22	1.71	O
	A	43	GLN	HE2	B	47	ASP	OD1	1.83	

11	A	30	ASP	OD2	B	127	THR	HN	1.73	
	A	30	ASP	OD2	B	127	THR	HG1	1.66	
	A	33	ASP	OD1	B	128	LYS	HZ3	1.69	O
	A	38	ASP	OD1	B	135	ARG	HE	1.73	O
	A	38	ASP	OD2	B	135	ARG	HE	2.43	O
	A	38	ASP	OD2	B	135	ARG	HH22	1.74	O
	A	42	LYS	HZ1	B	154	ASP	OD2	1.64	O
	A	43	GLN	HE2	B	47	ASP	OD1	1.77	O
12	A	32	TYR	O	B	128	LYS	HZ1	2.03	
	A	33	ASP	OD1	B	135	ARG	HH11	1.99	O
	A	33	ASP	OD1	B	135	ARG	HH21	1.69	O
	A	33	ASP	OD2	B	128	LYS	HZ2	1.66	O
	A	38	ASP	OD1	B	135	ARG	HH22	1.96	O
	A	38	ASP	OD2	B	135	ARG	HE	1.81	O
	A	38	ASP	OD2	B	135	ARG	HH22	2.17	O
	A	42	LYS	HZ2	B	154	ASP	OD2	1.85	O
	A	43	GLN	HE2	B	47	ASP	OD1	1.64	
13	A	25	GLN	OE1	B	131	GLN	HE21	2.16	
	A	33	ASP	OD1	B	128	LYS	HZ3	2.09	O
	A	33	ASP	OD1	B	135	ARG	HH11	2.02	O
	A	33	ASP	OD2	B	135	ARG	HH11	2.33	O
	A	33	ASP	OD2	B	135	ARG	HH21	1.60	O
	A	38	ASP	OD2	B	135	ARG	HE	1.96	O
	A	38	ASP	OD2	B	135	ARG	HH22	1.70	O
14	A	25	GLN	HE2	B	131	GLN	OE1	2.22	
	A	31	GLU	OE2	B	128	LYS	HZ1	1.61	O
	A	33	ASP	OD2	B	128	LYS	HZ2	1.69	O
	A	38	ASP	OD1	B	135	ARG	HE	1.74	O
	A	38	ASP	OD2	B	135	ARG	HH22	1.66	O
	A	40	TYR	OH	B	131	GLN	HE21	1.88	
15	A	33	ASP	OD1	B	128	LYS	HZ3	1.69	O
	A	33	ASP	OD2	B	135	ARG	HH11	1.59	O
	A	33	ASP	OD2	B	135	ARG	HH21	2.48	O
	A	38	ASP	OD1	B	135	ARG	HE	1.71	O
	A	38	ASP	OD2	B	135	ARG	HH22	1.58	O
16	A	25	GLN	OE1	B	131	GLN	HE21	2.29	
	A	25	GLN	HE2	B	141	PHE	O	2.18	
	A	33	ASP	OD1	B	128	LYS	HZ3	1.65	O
	A	33	ASP	OD1	B	135	ARG	HH11	1.81	O
	A	33	ASP	OD2	B	135	ARG	HH11	2.40	O
	A	33	ASP	OD2	B	135	ARG	HH21	1.64	O
	A	38	ASP	OD2	B	135	ARG	HH22	1.55	O
17	A	1	SER	HN	B	47	ASP	OD1	1.87	
	A	25	GLN	HE2	B	141	PHE	O	1.78	

18	A	33	ASP	OD1	B	128	LYS	HZ3	1.65	O
	A	38	ASP	OD1	B	135	ARG	HE	1.95	O
	A	38	ASP	OD2	B	135	ARG	HE	2.08	O
	A	38	ASP	OD2	B	135	ARG	HH22	1.97	O
	A	42	LYS	HZ1	B	154	ASP	OD2	1.59	O
	A	43	GLN	OE1	B	161	ARG	HH12	2.04	
	A	43	GLN	HE2	B	47	ASP	OD1	2.26	
	A	43	GLN	HE2	B	47	ASP	OD2	1.94	
19	A	25	GLN	HE2	B	143	GLU	OE2	1.81	
	A	25	GLN	O	B	150	GLN	HE22	2.34	
	A	31	GLU	OE2	B	127	THR	HN	2.13	
	A	31	GLU	OE2	B	128	LYS	HN	1.92	O
	A	33	ASP	OD1	B	128	LYS	HZ3	1.68	O
	A	38	ASP	OD2	B	135	ARG	HE	2.13	O
	A	38	ASP	OD2	B	135	ARG	HH22	1.73	O
	A	41	ARG	HH2	B	162	GLU	OE2	1.95	O
20	A	1	SER	OG	B	181	SER	HN	2.48	
	A	1	SER	OG	B	181	SER	HG	1.75	
	A	3	GLU	OE2	B	177	LYS	HZ1	1.65	O
	A	25	GLN	OE1	B	131	GLN	HE22	2.47	
	A	25	GLN	HE2	B	143	GLU	OE2	1.74	
	A	33	ASP	OD1	B	128	LYS	HZ3	1.61	O
	A	38	ASP	OD2	B	135	ARG	HE	1.82	O
	A	38	ASP	OD2	B	135	ARG	HH22	2.05	O
21	A	49	GLU	OE2	B	183	THR	HG1	1.74	
	A	33	ASP	OD1	B	128	LYS	HZ3	1.63	O
	A	33	ASP	OD1	B	135	ARG	HH11	1.64	O
	A	33	ASP	OD2	B	135	ARG	HH11	2.48	O
	A	33	ASP	OD2	B	135	ARG	HH21	1.63	O
	A	38	ASP	OD1	B	135	ARG	HE	1.88	O
	A	38	ASP	OD2	B	135	ARG	HE	2.25	O
22	A	38	ASP	OD2	B	135	ARG	HH22	1.83	O

\*Cutoff distance to define a hydrogen bond is 2.5 Å.

# A hydrogen bond in an ion-pair interaction is indicated as "O"

**Table S5.** Statistics for the 20 lowest HADDOCK-score structures of the BI-2852-stabilized  $\beta$ - $\beta$  dimer of KRAS-G12D.

**BI-2852-stabilized  $\beta$ - $\beta$  dimer of KRAS-G12D**

<b>PRE-derived Distance Restraints</b>	
Number of PRE restraints ( $\pm 3.0 \text{ \AA}$ )	16
<b>Energy Statistics</b>	
HADDOCK score (a.u.)	$-62 \pm 6$
Van der Waals energy (kcal/mol)	$-37 \pm 9$
Electrostatic energy (kcal/mol)	$-85 \pm 31$
Desolvation energy (kcal/mol)	$-8 \pm 6$
Restraints violation energy (kcal/mol)	$0 \pm 0$

**Table S6.** Violation analysis of PRE-derived restraints of the BI-2852-bound KRAS-G12D versus the NMR-driven or crystal structure of the BI-2852-stabilized KRAS-G12D dimer.

NMR-driven Structure										
Chain	Residue Number	Atom Name*	Chain	Residue Number	Atom Name	Distance (Å)	$d_{eff}^*$	Average Distance (Å)	PRE Distance Restraint (Å)	Result <sup>#</sup>
A	1	CG	B	6	CD1	20.33	17.80	17.75	$19.15 \pm 3.00$	S
A	1	CG	B	6	CD2	19.66				
B	1	CG	A	6	CD1	20.18	17.70	14.20	$15.26^{\text{f}} \pm 3.00$	S
B	1	CG	A	6	CD2	19.58				
A	1	CG	B	36	CD1	13.20		19.59	$19.95 \pm 3.00$	S
B	1	CG	A	36	CD1	15.20				
A	1	CG	B	55	CD1	19.39		20.81	$22.90 \pm 3.00$	S
B	1	CG	A	55	CD1	19.78				
A	1	CG	B	79	CD1	23.71	20.69	19.23	$20.18 \pm 3.00$	S
A	1	CG	B	79	CD2	22.79				
B	1	OG	A	79	CD1	23.98	20.94	13.66	$15.52^{\text{f}} \pm 3.00$	S
B	1	OG	A	79	CD2	23.08				
A	1	CG	B	100	CD1	19.84		19.54	$22.58 \pm 3.00$	S
B	1	CG	A	100	CD1	18.61				
A	1	CG	B	103	CG1	15.79	14.63	19.54	$19.15 \pm 3.00$	S
A	1	CG	B	103	CG2	17.28				
B	1	CG	A	103	CG1	13.54	12.68	18.42	$19.95 \pm 3.00$	S
B	1	CG	A	103	CG2	15.30				
A	1	CG	B	159	CD1	22.78	19.54	14.76	$15.26^{\text{f}} \pm 3.00$	S
A	1	CG	B	159	CD2	21.27				
B	1	OG	A	159	CD1	22.54	19.53	19.54	$19.15 \pm 3.00$	S
B	1	OG	A	159	CD2	21.41				
Crystal Structure										
Chain	Residue Number	Atom Name*	Chain	Residue Number	Atom Name	Distance (Å)		Average Distance (Å)	PRE Distance Restraint (Å)	Result <sup>#</sup>
A	1	CG	B	6	CD1	18.97		18.61	$19.15 \pm 3.00$	S
A	1	CG	B	6	CD2	18.24				
B	1	CG	A	6	CD1	18.97		14.76	$15.26^{\text{f}} \pm 3.00$	S
B	1	CG	A	6	CD2	18.24				
A	1	CG	B	36	CD1	14.76		18.42	$19.95 \pm 3.00$	S
B	1	CG	A	36	CD1	14.76				
A	1	CG	B	55	CD1	18.42		19.54	$19.95 \pm 3.00$	S
B	1	CG	A	55	CD1	18.42				

A	1	CG	B	79	CD1	22.41		22.11	$22.90 \pm 3.00$	S
A	1	CG	B	79	CD2	21.81				
B	1	OG	A	79	CD1	22.41		18.58	$20.18 \pm 3.00$	S
B	1	OG	A	79	CD2	21.81				
A	1	CG	B	100	CD1	18.58		15.30	$15.52^{\text{f}} \pm 3.00$	S
B	1	CG	A	100	CD1	18.58				
A	1	CG	B	103	CG1	14.49		20.72	$22.58 \pm 3.00$	S
A	1	CG	B	103	CG2	16.11				
B	1	CG	A	103	CG1	14.49		20.72	$22.58 \pm 3.00$	S
B	1	CG	A	103	CG2	16.11				
A	1	CG	B	159	CD1	21.46		20.72	$22.58 \pm 3.00$	S
A	1	CG	B	159	CD2	19.97				
B	1	OG	A	159	CD1	21.46		20.72	$22.58 \pm 3.00$	S
B	1	OG	A	159	CD2	19.97				

\* In the crystal structure (PDB ID: 6GJ8) used in the HADDOCK calculation, the gamma-carbon atom (CG) of Met1 is substituted for the gamma-sulfur atom (SG) of Cys1.

# “S” and “V” represent satisfaction and violation, respectively, of experimental PRE distance restraints by the NMR-driven or crystal structure of the BI-2852-stabilized KRAS-G12D dimer.

<sup>f</sup>This distance was calculated based on the noise level of the paramagnetic spectrum as the corresponding peak was severely broadened beyond detection.

#### **4. References**

1. W. K. Gillette, D. Esposito, M. Abreu Blanco, P. Alexander, L. Bindu, C. Bittner, O. Chertov, P. H. Frank, C. Grose, J. E. Jones, Z. Meng, S. Perkins, Q. Van, R. Ghirlando, M. Fivash, D. V. Nissley, F. McCormick, M. Holderfield and A. G. Stephen, *Scientific reports*, 2015, **5**, 15916.
2. M. T. Mazhab-Jafari, C. B. Marshall, P. B. Stathopoulos, Y. Kobashigawa, V. Stambolic, L. E. Kay, F. Inagaki and M. Ikura, *Journal of the American Chemical Society*, 2013, **135**, 3367-3370.
3. M. T. Mazhab-Jafari, C. B. Marshall, M. J. Smith, G. M. Gasmi-Seabrook, P. B. Stathopoulos, F. Inagaki, L. E. Kay, B. G. Neel and M. Ikura, *Proceedings of the National Academy of Sciences of the United States of America*, 2015, **112**, 6625-6630.
4. F. Hagn, M. L. Nasr and G. Wagner, *Nature protocols*, 2018, **13**, 79-98.
5. V. Tugarinov, P. M. Hwang, J. E. Ollerenshaw and L. E. Kay, *Journal of the American Chemical Society*, 2003, **125**, 10420-10428.
6. F. Delaglio, S. Grzesiek, G. W. Vuister, G. Zhu, J. Pfeifer and A. Bax, *Journal of biomolecular NMR*, 1995, **6**, 277-293.
7. B. A. Johnson, *Methods in molecular biology*, 2004, **278**, 313-352.
8. J. L. Battiste and G. Wagner, *Biochemistry*, 2000, **39**, 5355-5365.
9. G. C. P. van Zundert, J. Rodrigues, M. Trellet, C. Schmitz, P. L. Kastritis, E. Karaca, A. S. J. Melquiond, M. van Dijk, S. J. de Vries and A. Bonvin, *Journal of molecular biology*, 2016, **428**, 720-725.
10. A. T. Brunger, *Nature protocols*, 2007, **2**, 2728-2733.
11. S. Jo, J. B. Lim, J. B. Klauda and W. Im, *Biophysical journal*, 2009, **97**, 50-58.